Examining the relative effects of nutrient loads and invasive *Dreissena* mussels on Lake Michigan's food web using an ecosystem model

April 2019

A project submitted in partial fulfillment of the requirements

for the degree of Master of Science (Natural Resources and

Environment) at the University of Michigan

Nicholas W. Boucher

Thesis Committee:
Dr. Hongyan Zhang, Chair
Dr. Edward Rutherford, Co-chair
Dr. Doran Mason

Table of Contents

Acknowledgements

I would like to thank my mentors on this project Dr. Hongyan Zhang, Dr. Ed Rutherford, and Dr. Doran Mason. This thesis would not have been possible without their thoughtful and honest feedback, their guidance throughout each stage of this project, and their patience. It has been an honor to have the opportunity to collaborate with three scientists as highly esteemed as Hongyan, Ed, and Doran.

This research was directly supported by funding from: The Great Lakes Fisheries Trust, The Great Lakes Restoration Initiative, and The Cooperative-Institute for Great Lakes Research, NOAA's Great Lakes Environmental Research Laboratory, and The University of Michigan School for Environment and Sustainability.

The Model used in this research was originally developed by CSIRO scientist Beth Fulton. I would like to thank both Beth and Bec Gorton for assistance with building, calibrating, and troubleshooting the Atlantis Model for Lake Michigan.

A number of people provided data or helped to generate model inputs. Haoguo Hu generated hydrodynamic inputs. Rick Barbiero shared zooplankton data from GLNPO Great Lakes monitoring program, Dr. Ashley Elgin provided observation values for dreissenid mussels. Dr. Bo Bunnell from USGS provided fish trawl data. Ryan Wehse from The Great Lakes Fishery commission provided fish stocking records.

I would also like to thank my parents (Bruce Boucher and Vicky Weill), my brothers (Bryant and Alexander Boucher), and my sisters in-law (Catherine and Missy Boucher) for their support throughout my time at SEAS.

List of Figures

List of Tables

Abstract

Lake Michigan has undergone ecosystem wide changes over the past century due to changing nutrient loads and an influx of invasive species. Zebra (*Dreissena polymorph*a) and Quagga mussels (*D. bugensis*; collectively Dreissenid mussels) have been a particularly impactful invasive species, and currently account for the majority of benthic biomass in Lake Michigan. Dreissenid mussel filtration, along with declining nutrient loads following the 1972 Great Lakes Water Quality Agreement, have reduced primary productivity and caused oligotrophication in Lake Michigan's offshore zone and a concurrent increase in nuisance algal blooms nearshore. However, the relative effects of these two factors on Lake Michigan's food web remain a key knowledge gap.

To quantify the relative effects of mussel grazing and nutrient loads on the Lake Michigan food web, I used the Lake Michigan Atlantis Model (LMAM) to predict biomass changes of Lake Michigan species under six model scenarios. The Atlantis model is a three-dimensional, spatially-explicit ecosystem model that takes into account water movement, seasonality, and food web interactions to dynamically predict biomass for functional groups at each trophic level over time. I calibrated the model using available agency food web data from 1994 to 2010, then ran 25 year simulations of 6 different scenarios including three nutrient loads (double baseline load, half baseline load, and baseline 1994 load) and two mussel scenarios (mussels present or absent). Model results indicated that mussel grazing has a much greater relative impact on the food web than changes in nutrient loads. Simulated mussel grazing on phytoplankton radiated up the food web to cause resource limitation for prey fish and piscivores. Effects on functional group biomass owing to changes in phosphorus loading were largely

masked by observed mussel effects. My findings contrast with other modeling studies that found nutrient loads also have a significant effect on productivity and biomass. These results suggest that management strategies that increase nutrient flow into Lake Michigan would have negligible positive effects on fish biomass.

Introduction

Invasive species and changing nutrient loads are major stressors to aquatic ecosystems worldwide. In Lake Michigan, there has been a steady decline in phosphorus concentrations, Lake Michigan's limiting nutrient, due to these two factors. Available nutrients in Lake Michigan first started to decline during the late 1970s and early 1980s following reductions in phosphorus inputs mandated by the Great Lakes Water Quality Agreement of 1972 between the United States and Canada (Dove and Chapra, 2015). The second inflection point of the decline in Lake Michigan's phosphorus concentration followed the invasion and expansion of *Dreissena* mussels in the 1990s and 2000s. Zebra Mussels, *Dreissena polymorpha,* became established in Lake Michigan in 1993 (Nalepa et al., 1998), while Quagga Mussels, *Dreissena rostriformis bugensis,* were first found in Lake Michigan in the late 1990s and had irrupted by 2004 (Nalepa et al., 2009). The profundal form of quagga mussels continues to expand its populations in waters deeper than 90 meters (Glyshaw et al., 2015). *Dreissenid mussels* are able to filter feed voraciously on phytoplankton, protozoa, and other seston even when water temperatures are low (Vanderploeg et al., 2002).

The decline in available phosphorus and the high mussel filtration have resulted in a decline in lake-wide productivity, and caused Lake Michigan's spring water clarity to increase by 110% between 1994 and 2008 (Vanderploeg et al., 2012). Dove and Chapra (2015) classified Lake Michigan's trophic status as 'ultra-oligotrophic', ranking it even less productive than Lake Superior. The oligotrophication of Lake Michigan has led to concerns that fish biomass may be limited by prey resources (Bunnell et al., 2014, 2018; Kao et al., 2018). The period following the *Dreissena* invasion has also been marked by

an increase in nearshore nuisance algae blooms, despite a lake wide decline in nutrient concentration (Tomlinson et al., 2010). Dreissenid filter feeding sequesters nutrients in near shore and benthic zones (Hecky et al., 2004; Turschak et al., 2014); the increased nutrient availability and water clarity caused by *Dreissena* filtration contribute to an increased incidence of nuisance blooms of the benthic algae *Cladophora glomerata* (Brooks et al., 2015; Bootsma et al., 2015). Furthermore, *Dreissena* filtration shifts available nutrients away from the offshore pelagic zone where alewife, bloater, and other important prey fish species feed. Both of these outcomes have profound implications for management of the lake as a shared valuable natural resource.

While the combined effects of reductions in nutrient concentrations and dreissenid mussel filtration have been well documented, there is not a consensus on their relative impacts. A 2018 report by the International Joint Commission listed the relative influence of mussel grazing versus nutrient load reductions as a key knowledge gap (Bunnell et al. 2018). Previous studies have examined this research question using a host of methodologies. Observational studies, like Bunnell et al.'s (2014) work examining evidence for top-down and bottom-up control, have provided a baseline understanding of food web dynamics in Lake Michigan and key species interactions. However, nutrient loading and mussel effects are confounding factors, and observational studies do not allow researchers to determine the relative influence of each factor separately. Additionally, owing to food web interactions, the effects of these changes may be indirect or too complex to observe with traditional methods.

A simulation approach is better suited for parsing the relative effects of multiple interactive factors. Kao et al. (2017) used Ecopath with Ecosim to investigate whole food

web effects of nutrients and *Dreissena,* but this approach does not include seasonal water movement, temperature fluctuations, or other considerations of Lake Michigan's physical environment, which are known to affect food web dynamics. Rowe et al. (2017) and Pilcher et al. (2017) both conducted studies using biophysical models that included water movement and seasonal variation within Lake Michigan's physical environment. However, Rowe et al. (2017) only considered these effects on primary production, while Pilcher et al. (2017) included lower trophic levels. Fish communities were not included in either of these studies.

This study is the first attempt to use an ecosystem model that simulates population dynamics and food web interactions at all of Lake Michigan's trophic levels and is driven by lake currents and water temperatures. This novel approach will build upon previous studies and provide further insight into how *Dreissena* mussel filtration and changing nutrient loads may independently and synergistically affect Lake Michigan's complex food web. I am particularly interested in examining how the presence of mussels affects the flow of biomass between trophic levels, and what implications these changes have for the management of the lake.

To investigate the relative effects of nutrient loading and *Dreissena* filtration, I applied the Atlantis Ecosystem Model (Fulton et al, 2003) to conduct a factorial analysis of nutrient and *Dreissena* mussel effects on the Lake Michigan food web. This approach allowed me to quantitatively parse the direct and/or indirect impacts of these two factors down to the species level of the food web and predict how future scenarios might affect food web biomass. There was no clear trend in phosphorus inputs into Lake Michigan between 1998 and 2010, but over the same time period there was an increase in

Dreissena biomass and a decline in zooplankton and prey fish biomass (Bunnell et al., 2014). The upward trend in *Dreissena* was coincident with a decline in offshore phosphorus concentrations, likely caused by dreissenid sequestration of phosphorus in the benthos and nearshore (Hecky et al. 2004, Dove and Chapra, 2015). Because a downward trend in lower trophic level biomass was observed during a time period when there was an upward trend in *Dreissena* biomass and no trend in phosphorus loads, I would expect *Dreissena* filtering to have a relatively higher impact on biomass than nutrient loading. I would also expect that on a longer time period than the 12 years observed in Bunnell et al.'s (2014) study, the resource limitation caused by mussel filtration would radiate up trophic levels and also affect piscivore biomass.

Methods

I used the Lake Michigan Atlantis Model (LMAM) to investigate the effects of nutrient loading and mussel biomass on Lake Michigan's food web. The Atlantis Ecosystem Model was developed by Beth Fulton and other scientists at the Commonwealth Scientific and Industrial Research Organization (CSIRO) in Australia. The Atlantis Model includes physical, chemical, and ecological processes in a three dimensional and spatially explicit model domain (Fulton, 2001; Fulton et al., 2003; Fulton et al., 2004a, Fulton et al., 2004b; Fulton et al., 2004c). This model was configured and implemented for use in the Great Lakes Region by Drs. Hongyan Zhang, Ed Rutherford, and Doran Mason at the National Oceanographic and Atmospheric Administration's Great Lakes Environmental Research Laboratory (NOAA-GLERL). The Atlantis model includes three sub-models for fisheries, ecology, and hydrodynamics; the configuration used in this study focused on hydrodynamics and ecology.

Model domain and design

In the Lake Michigan Atlantis Model (LMAM), the spatial domain of Lake Michigan is divided into 35 irregular polygons based on bathymetry, fisheries management units, and state boundaries. Polygons separated by bathymetry are divided on the 30 meter and 110 meter isoclines (Figure 1). Nutrients are added to the system at sixteen of the nearshore polygons to represent major point sources of nutrient loading into the lake. Each polygon is separated into between 1 and 6 vertical layers depending on overall depth and includes an additional sediment layer (Figure 2).

Physical model

The hydrodynamic sub-model for LMAM tracks water movement throughout the model domain as well as the movement of nutrients and plankton. The driving force for this sub-model is output from the Lake Michigan Finite Volume Community Ocean Model (FVCOM. Chen et al. 2006). Nutrient inputs are advected throughout the lake by currents defined from FVCOM's hydrodynamic simulations. For this study, FVCOM output from 1998 is the driving force behind LMAM's hydrodynamic inputs.

Nutrient inputs

Nutrient loads from 1994-2008 were provided by Dr. David Dolan (University of Wisconsin, Green Bay, personal communication). Data from Muskegon River have both phosphorus and nitrogen loads, while other rivers only have phosphorus loads. Nitrogen loads (NH3, NO2+NO3, and DON) for other rivers were calculated based on the monthly ratios between TDP and nitrogen forms that derived from loading data of the Muskegon River, i.e. assuming the ratios are the same across all tributaries to the Lake Michigan at a given month.

Biological model

Within LMAM, 35 functional groups were parameterized and aggregated based on species, trophic level, and life history (Table 1). These functional groups encompassed a simplified version of the Lake Michigan food web from detritus and primary producers

to piscivorous fish. At lower trophic levels, functional groups were modeled as biomass pools. Vertebrates are all fishes and were separated into year classes.

Calibration

The Atlantis model was previously calibrated with a focus on the upper food web and fish biomass trends on a lake wide scale using trawl data (Zhang et al., in prep). Diet compositions were taken from a previous modeling study of the Lake Michigan food web using Ecopath with Ecosim (Rutherford et al. in prep). Additional data sources are included in the appendix.

To make LMAM suitable for this study, I focused most of my calibration efforts on *Dreissena.* To set biomass, I used dreissenid biomass grouped by depth (Elgin, pers. comm.). I set starting biomass of Dreissena in each of Atlantis's boxes to the observed biomass at that box's depth. Using experimental data from a dreissenid feeding study, I set the clearance rate for dreissenid mussels to 0.004017 m^3 /individual/day (Vanderploeg et al. 2010).

Cladophora glomerata was calibrated using parameters from the Great Lakes *Cladophora* model developed by Canale and Auer (1982), and parameterized for Lake Michigan by Tomlinson et al. (2010). This model provided us with Lake Michigan specific parameters for *Cladophora* growth, phosphorus uptake, phosphorus content per mg dry weight, and half saturation constant for phosphorus (Tomlinson et al. 2010). The photic zone depth for *Cladophora* growth was set at $\leq$ 55 meters.

I plotted relative biomass for LMAM output and lake-wide observation data for 16 of LMAM functional groups to assess whether LMAM was accurately predicting trends in biomass. To quantitatively assess model skill, I calculated root mean square deviation between modeled biomass output and observed biomass. For *Dreissena* I

compared observed biomass to absolute biomass output because accurate calibration of dreissenid mussels is key to understanding their effects on the Lake Michigan Food web. For cladophora there were no time series observation data available, so I conducted a qualitative skill assessment.

Scenario Simulations

After calibrating the LMAM, I simulated food web responses to nutrient loads and *Dreissena* by conducting a 3x2 factorial experiment with 3 levels of nutrient treatment and mussel presence/absence scenarios. To minimize inter-annual variation in biomass owing to other factors, I used data from one year (1994) constant input for fish stocking, hydrodynamics, and temperature throughout each model run. The nutrient treatment levels were low, baseline, and high. Baseline nutrient loads were the reported values from 1994 with the low nutrient treatment set as half of the baseline loads (0.5*1994 loads) and high nutrient treatment as double the baseline loads (2*1994 loads). For mussel presence treatments, I set starting mussel biomass to 1998 observation levels. For mussel absence treatments I removed mussels from the model completely. In each of the six scenarios I conducted a 50 year model run allowing for 25 years of model burn in and 25 years of output for analysis. After conducting the six treatment scenarios, I used relative biomass outputs to generate box and whisker plots of each scenario. I also fitted LMAM output data to a linear model and conducted a factorial ANOVA on biomass outputs for each functional group over each of the six scenarios. To provide more insight into changes in biomass across scenarios, I averaged instantaneous diet composition for the last 25 years of the model run for select model groups. Invertebrate consumption is

reported as mg N s^{-1}, and vertebrate consumption is reported as number of prey/second. Atlantis does not output the age structure or size of prey fish consumed by piscivores, so I calculated changes in average individual biomass and number of prey fish consumed at the end of the model simulation between mussels present and mussels absent scenarios.

Results

Model Skill Assessment

Plotting relative biomass of model output and observations together allowed me to determine that modeled dynamics of our functional groups was reasonable. Alewife model output followed similar trends to the observation values, however modeled biomass was significantly higher in the period from 2004 to 2008 (Figure 3). Model predictions of bloater biomass were significantly higher for the first 10 years of the model run (1994-2004). Once biomass stabilized (2004-2010) output matched observations well (Figure 4). Modeled relative biomass of Rainbow Smelt closely followed observations throughout the calibration run (Figure 5). Observed relative biomass of Deepwater Sculpin increased from 1994 to a peak in 1997 followed by a gradual decline for the remainder of the calibration period. Deepwater Sculpin relative biomass output followed this same pattern, however the peak in 1997 was higher than observed biomass (Figure 6). There were only four observation points during our calibration period for Round Goby. Observed relative biomass for Round Goby nearly doubled between 2003 and 2004 followed by a more gradual increase until the last available observation point in 2007. Model output for Round Goby biomass decreased between 2003 and 2004, however there is a similar increase in the period between 2004 and 2007 (Figure 7). Lake Whitefish modeled output was consistently low and stable throughout the calibration period while observations showed a slight increase from 1994 to 1999 and a slight decrease from 2005 to 2010 (Figure 8). Steelhead, Coho Salmon, and Chinook Salmon biomass output followed the same overall trend as observation data, however modeled output was lower than observed biomass throughout the calibration period for all three of

these groups (Figure 9; Figure 10; Figure 11). Model output of Lake Trout relative biomass was significantly higher than observed relative biomass between 1999 and 2006, but once biomass stabilized model predictions and observations were the same general magnitude (Figure 12). Bythotrephes and *Diporeia* model output both followed observed relative biomass closely throughout the calibration period (Figure 13; Figure 14). Model predictions for Copepod and Chironomid biomass were both lower than observed relative biomass during the calibration period (Figure 15; Figure 16). Mysis biomass output was higher than observed relative biomass for all five observation points that were available (Figure 17).

Because of the importance of *Dreissena* filtration on this study, I compared absolute biomass of the output to absolute biomass of available observations in wet weight. Modeled biomass increased much more quickly than observed biomass between 1994 and 2005 leveling off at approximately 150 metric tonnes. However, observed biomass increased dramatically between 2005 and 2010 reaching a peak of 310 metric tonnes in 2010 (Figure 18). RMSD for all groups that had observation data available was acceptable with the RMSD for *Dreissena* being the highest because I compared absolute biomass rather than relative biomass (Table 2).

Prey Fish

The modeled changes in prey fish biomass between mussels present and mussels absent scenarios were more significant than changes between nutrient scenarios across most of the eight prey fish groups (Figure 18). Alewife, Bloater, Slimy Sculpin, and Deepwater Sculpin had lower biomass with mussels present compared to mussels absent scenarios. The biomass of these four prey fish groups were more variable in the mussels

present scenarios compared to mussels absent. Lake Whitefish and Round Goby were the only two prey fish groups that had higher relative biomass with mussels present compared to mussels absent. Biomass of Yellow Perch and Rainbow Smelt biomass did not change significantly across any of the six scenarios. For Deepwater Sculpin, there was a statistically significant interaction effect between mussels and nutrients ($P < 0.05$) when comparing the low nutrient scenario to the high nutrient scenario, but not when comparing the low scenario to the baseline nutrient scenario (Table 3).

Alewife consumed more prey biomass in the mussels absent scenarios than in the mussels present scenario. With mussels present, Alewife consumed primarily *Mysis* with some rotifers, copepods, and small amounts of other invertebrates (Figure 19). When mussels were absent, Alewife consumed a higher biomass of rotifers and *Diporeia*, less of Mysis, and about the same amount of other invertebrates. Like Alewife, Bloater consumed more under the mussels absent scenarios than the mussels present scenarios (Figure 20). In all six scenarios, Bloater consumed primarily *Diporeia*, protozoans, and Mysis, with higher consumption of protozoans and Diporeia with mussels absent, but less Mysis. Slimy Sculpin biomass was too low to calculate diet composition in the mussels present scenarios (Figure 21). In the mussels absent scenarios, Slimy Sculpin consumed the least in the low nutrient scenario, and the most in the high nutrient scenario. Across these three scenarios, Slimy Sculpin diet was dominated by oligochaetes with some Diporeia and Mysis. Deepwater Sculpin consumed > eight fold more biomass in the mussels absent scenarios compared to the mussels present scenarios (Figure 22). Deepwater sculpin diets were dominated by oligochaetes with small amounts of Diporeia and Mysis. Round Goby consumed more in the mussels present scenarios than the

mussels absent scenarios with not much change based on nutrients (Figure 23). In the mussels present scenarios, *Dreissena* comprised the largest portion of Round Goby diets. In the mussels absent scenarios, Round Goby consumed mostly oligochaetes and Diporeia with some amphipods. Lake Whitefish consumed almost only Round Goby, and they consumed slightly more in the mussels absent scenarios with their highest consumption in the high nutrients mussels absent scenario (Figure 24). The invertebrate portion of Lake Whitefish diet is dominated by *Dreissena* in the mussels on scenarios with some *Diporeia* and Mysis (Figure 25). With mussels off, Lake Whitefish consume much fewer invertebrates with this portion of their diet made up almost entirely by Mysis and *Diporeia.* Yellow Perch consumed a greater number of vertebrates in the mussels present scenarios than in the mussels absent scenarios (Figure 26). In the low, baseline, and high nutrient with mussels present scenarios, Yellow Perch consumed about 1.6 diet items per second on average while they consumed about 1.4 diet items per second in the baseline and high mussels absent scenarios and about 1.2 in the low nutrient mussels absent scenarios. Across all 6 scenarios, Yellow Perch vertebrate diet primarily consisted of Alewife and Rainbow Smelt. Yellow perch consumed slightly more invertebrates with mussels absent compared to mussels present with not much change in their diet composition (Figure 27). Rainbow Smelt diets mostly consisted of Alewife and other Rainbow Smelt across all 6 scenarios (Figure 28). Rainbow Smelt consumed slightly more with mussels absent than mussels present, and consumed the least in the low nutrient scenarios and most in the high nutrient scenarios. Rainbow Smelt consumption of invertebrates increased with mussels absent and did not show much change across nutrient loading scenarios (Figure 29).

When mussels were removed from model scenarios, average size of six of the eight prey fish species across age classes increased with Lake Whitefish and Round Goby being the only two species that decreased in average size when mussels were absent (Figure 30).

Piscivores

As was the case for planktivorous prey fish groups, biomass of all four piscivore groups responded more to the mussel presence/absence scenarios than to changes in nutrient concentration (Figure 31). Lake Trout and Steelhead biomass was greater with mussels absent than with mussels present. Biomass of Chinook and Coho Salmon did not differ significantly (Figure 31). Variance in biomass of all four piscivore groups also was greater with mussels absent than mussels present. For lake trout biomass, there was a significant interaction effect between mussels and nutrients (Table 3). Lake trout biomass was higher at low compared to high nutrient scenarios, but did not differ between the low and baseline nutrient scenarios.

Chinook diets consisted primarily of Alewife and Bloater with some Rainbow Smelt (Figure 32). Chinook had a slightly higher consumption rate on average in the mussels present scenarios that increased with increase nutrient loads. With mussels absent, Chinook Salmon consumption was lower in the low and baseline nutrient scenarios, and slightly higher in the high nutrient scenario. Coho Salmon diets followed similar trends to Chinook Salmon (Figure 33). They consumed primarily Alewife and Bloater with some Rainbow Smelt. Coho incorporated Deepwater Sculpin into their diets in the mussels absent scenarios. Lake Trout consumed almost three times more in the mussels absent scenarios than the mussels present scenarios, with the highest

consumption rate under the baseline nutrient (Figure 34). In the mussels present scenarios, Lake Trout consumed primarily Alewife and Bloater, but with mussels absent Lake Trout diet shifted to consist mostly of Deepwater Sculpin with some Alewife, Bloater, and Slimy Sculpin. Across all six scenarios, Steelhead consumed primarily Rainbow Smelt and Alewife (Figure 35). Steelhead consumption did not change much with mussels absent scenarios vs present scenarios. However, in the mussels absent scenarios, steelhead consumed the least in the low nutrient scenario and the most in the high nutrient scenario.

Pelagic Lower Food Web

Rotifer biomass was significantly higher in scenarios when mussels were absent than with mussels present (Figure 36). Rotifer biomass also was significantly higher with increases in nutrient loads. Mysis and protozoan biomass were both significantly higher with mussels present in the model. Bythotrephes biomass was higher with mussels present than with mussels absent, but did not vary with changes in nutrients. Copepod biomass varied across nutrient and mussel scenarios, but had no significant trends. Cladoceran biomass did not vary significantly with either mussel or nutrient scenarios.

Copepods consumed primarily protozoans and diatoms, and they consumed more in the mussels absent scenarios than with mussels present. Copepod diet did not differ with nutrients under a mussels absent scenario, but with mussels present copepods consumed the most under the high nutrient treatment and the least under the low nutrient treatment (Figure 37). Cladocerans consumed slightly more in the mussels present scenarios than the mussels absent scenarios with their diets primarily consisting of

protozoans and diatoms (Figure 38). Bythotrephes diet consisted mostly of cladocerans with some rotifers and copepods, with slightly higher consumption in the mussels absent scenarios than the mussels present scenarios (Figure 39). Across all six scenarios, Mysis consumed mostly copepods, protozoans, and cladocerans as well as some diatoms (Figure 40). Mysis consumed about twice as much in the mussels absent scenarios as the mussels present scenarios. In the mussels off scenarios they consumed the most in the high nutrient scenario and the least in the low nutrient scenario, while in the mussels absent scenarios they consumed the most in the baseline nutrient scenario and the least in the high nutrient scenario. Rotifers consumed primarily diatoms and protozoans (Figure 41). Rotifers consumed much more in the mussels absent scenarios than in the mussels present scenarios, and they consumed slightly more in the high nutrient scenarios than in the low nutrient scenarios. Protozoan diets were primarily detritus and picoplankton (Figure 42). Protozoans showed similar trends in their diets to rotifers; they consumed more in mussels absent scenarios compared to mussels present scenarios.

Bacteria

Biomass of pelagic and benthic bacteria both were significantly higher in scenarios with mussels absent than mussels present. However, benthic bacteria biomass was much higher with mussels absent (Figure 43). Benthic bacteria biomass varied significantly with nutrient load scenarios when mussels were absent, but not with mussels present. Pelagic bacteria biomass was not significantly affected by nutrients (Table 3). Biomass of benthic bacteria was affected by the interaction between nutrients and mussels.

Benthos

Amphipods, Diporeia, and Oligochaetes all decreased significantly with mussels present compared to mussels absent (Figure 44). Of these three functional groups, Oligochaetes decreased the most while Amphipods decreased the least. Amphipods did not show any statistically significant trends in relation to nutrient loads. Diporeia biomass increased 0.4 percent from low to baseline nutrient scenarios and 0.9% from low to high nutrient scenarios while oligochaetes increase 11.1% and 27.2% across the same scenarios. Biomass of all three of these groups were affected by the interaction between mussels and nutrient loads. Chironomid biomass showed opposite trends in mussels present scenarios versus mussels absent scenarios. Under mussels present scenarios, Chironomid biomass decreased with increasing nutrient loads. Under mussels absent scenarios, Chironomid biomass increased when nutrient loads increased.

For Amphipods, Diporeia, and Oligochaetes, total consumption matched trends in their biomass (Figure 45; Figure 46; Figure 47). Each of these groups consumed more in the mussels absent scenarios than the mussels present scenarios. Within the mussel scenarios, Amphipods, Diporeia, and Oligochaetes consume slightly more in the high nutrient scenarios than in the low nutrient scenarios. All three groups consumed primarily detritus while Diporeia included Oligochaetes in their diet in addition to detritus. Chironomids consumed more in the mussels absent scenarios than the mussels present scenarios (Figure 48). Chironomid diet consisted mainly of detritus.

Primary producers

Blue Green Algae experienced a relatively small increase (<5 %) when mussels were absent. Blue Green Algae biomass was affected by the interaction between mussels and nutrients. Macrophyte biomass increased by 10% with mussels absent. Picoplankton and Diatoms did not vary significantly across either mussel or nutrient model scenarios (Figure 49).

Discussion

The results of this study supported my hypothesis that *Dreissena* mussels may have a much greater impact than nutrient loads on biomass of different trophic groups. The results also support my hypotheses that *Dreissena* filtration would cause resource limitation for zooplankton, prey fish and piscivores.

Prey fish

LMAM output indicated that presence or absence of mussels had a greater effect on the biomass of food available to prey fish than nutrient scenarios. The negative relationship between *Dreissena* biomass and biomass of Alewife, Bloater, Slimy Sculpin, and Deepwater Sculpin suggests *Dreissena* mussels may have a limiting effect on biomass of these prey fish. The negative relationship between Alewife biomass and mussels was coincident with changes in Alewife diet composition suggesting that *Dreissena* are causing resource limitation for Alewife. Alewife consumption was lower with mussels present and dominated by Mysis; with mussels absent, Alewife consumption was higher and included a greater proportion of rotifers as well as *Diporeia*.These results are consistent with biomass observations that suggest Alewife are resource limited owing to the Dreissenid mussel invasion (Vanderploeg et al., 2012). Our findings also concur with an Ecopath with Ecosim study that found dreissenid mussel filtering is limiting alewife biomass (Kao et al., 2017).

Benthivores, Lake Whitefish and Round Gobies, had a positive relationship with mussels. *Dreissena* are the largest component of Round Goby diet in the mussels present scenarios. However, with mussels absent, Round Goby consumption was significantly

lower and their diet was dominated by Oligochaetes and *Diporeia* (Supplemental materials, Round Goby Diet). Modeled diet of Lake Whitefish was dominated by Round Goby (Supplemental materials, Lake Whitefish Diet) which explains why these two groups largely followed the same trends in biomass. This is consistent with observations of their population dynamics following the *Dreissena* invasion (Madenjian et al., 2015). Rainbow Smelt did not show any statistically significant relationship across mussel or nutrient loading scenarios in contrast to observations that they declined significantly following the *Dreissena* invasion (Bunnell et al., 2014). Yellow Perch, Steelhead, and Coho Salmon all include Rainbow Smelt as a large proportion of their diets. Thus, top down effects of this predation may be preventing Rainbow Smelt from showing any clear trends due to mussels or nutrient loads across the six scenarios.

Piscivores

Piscivore consumption of prey fish did not appear to change much for the six treatment scenarios. However, the Atlantis model reports vertebrate consumption in number per second rather than biomass per second which may obscure the actual amount consumed. Analysis of average prey fish size for each simulation scenario showed that all prey fish groups except for Lake Whitefish and Round Goby were significantly larger when mussels were removed from the system,which follows observations that prey fish condition declined in Lake Michigan after the dreissenid irruption (Bunnell et al., 2014). This result explains why piscivore consumption was relatively unchanged across all six model scenarios—even though their biomass fluctuated significantly ($p < 0.05$) across the scenarios.

Primary producers

Rowe et al. (2017) and Pilcher et al. (2017) both found that during periods when the water column is well mixed, mussels have a greater effect on primary productivity than do changes in nutrient loads. The LMAM output shows evidence of mussel effects at higher trophic levels, but did not show a strong interaction effect of mussels and nutrients for picoplankton, diatoms, or blue-green algae. This discrepancy may be caused by the additional trophic levels included in LMAM but not in the Rowe et al. (2017) or Pilcher et al. (2017) biophysical models. Increased consumption of primary producers may have kept biomass at similar levels despite increased productivity.

Additionally, the LMAM output indicated that the presence of mussels had a strong negative effect on *Cladophora.* Based on the effects described by Hecky et al. (2004) and confirmed by Auer et al. (2010), Madenjian et al (2014), and others, one would expect the presence of mussels to increase the light and nutrients available to *Cladophora* and in turn have a positive effect on *Cladophora* biomass in LMAM. This opposite effect might be explained by a model bias; in the Atlantis model, mussel excretion is added back into the water column rather than into the sediment layer. Adding nutrients to the water column rather than the sediment layer allows uptake by primary producers other than just *Cladophora* and also contributes to shading; these effects may have counteracted any additional growth of *Cladophora* one would expect to see.

Zooplankton

Mysis biomass declined significantly when *Dreissena* were removed from LMAM. This is likely due to predation effects from planktivorous fish. Alewife and Bloater are two of Mysis' main predators (Crowder and Binkowski, 1983), and they both experienced a decline in biomass when *Dreissena* were included in model scenarios. Copepod biomass was not affected by mussel presence, possibly because in LMAM, Calanoid copepods and Cyclopoid copepods were included in one copepod functional group. Observations show that Calanoid copepods remained stable during the *Dreissena* invasion while cyclopoid copepods decreased over the same time period (Madenjian et al., 2015). Furthermore, Diaptomid copepods are herbivorous while Calanoid and Cyclopoid copepods are carnivorous (Vanderploeg et al., 2012). Aggregating different copepod species into one functional group created a group with a broad and flexible diet that may have allowed them to maintain stable biomass under mussel scenarios.

The decline in *Bythotrephes* biomass declined significantly with mussels present in LMAM, likely caused by resource limitation. *Bythotrephes* consumption was significantly lower when mussels were present, especially consumption of rotifers and cladocerans (Supplementary material; *Bythotrephes* diets). This decline contrasts with empirical observations by Engevold et al. (2015) who found no significant decline in biomass of *Bythotrephes longimanus* between the time periods before and after *Dreissena spp.* invasion. Water clarity, which increased from dreissenid filtering, may improve *Bythotrephes* visual predation ability and consequently increase Bythotrephes biomass, but light does not affect predation in LMAM

Benthos

Diporeia biomass was significantly lower when mussels were included in the LMAM. This follows observations summarized by Madenjian et al (2015) which concluded that *Diporeia* decline was caused by the invasion of *Quagga* mussels between 2000 and 2010. The source of the Diporeia spp. decline in LMAM can be attributed to resource limitation. *Diporeia* consumption of detritus increased significantly in mussels off scenarios which increased their overall consumption despite declines in their consumption of oligochaetes.The mechanism for the decline of *Diporeia* following the *Dreissena* invasion is not well understood. Results from LMAM scenarios help to support the hypothesis that resource limitation may at least partially explain the *Diporeia* decline (Nalepa et al., 2006); however, LMAM is not equipped to examine alternative hypotheses that *Diporeia* were negatively affected by viruses that *Dreissena* mussels introduced (Cave and Strychar, 2014; Hewson et al., 2013)

Model Biases

Discrepancies between observed effects of mussels and nutrients and model output present in LMAM may be due to biases in model configuration. Potential model biases are illustrated by functional groups with a high residual mean square deviation when comparing calibration runs to observation data. For example, despite efforts to calibrate *Dreissena* to closely match observations, I was unable to achieve the same absolute biomass as those observed. However, the scenarios described in this model configuration still showed a significant mussel effect on functional group biomass and consumption.

Another potential model bias resulted from the stock-recruit algorithm in LMAM. The recruitment function for *Dreissena* in LMAM simply adds gained biomass into the system based on the growth of existing mussel biomass present in each box; this direct recruitment function eliminates mussel veligers from consideration. Mussel veligers are now commonly consumed by larval fish (Withers et al., 2015, Eppehimer et al. in press). Exclusion of veligers in the food web may cause the negative relationship between mussels and prey fish to be more pronounced than in reality. Withers et al.'s (2015) findings suggest that mussel veligers allow biomass to flow from mussel populations to prey fish populations whereas in LMAM, Round Goby and Lake Whitefish are the only two functional groups that can consume mussels.

Management Implications

Findings from this factorial analysis indicate that ecosystem engineering by *Dreissena spp.* is causing resource limitation for prey fish and piscivores. Some studies suggest possibly relaxing limits on nutrient loads to prevent harmful impacts on upper trophic levels (Kao et al., 2017). However, my findings suggest that even doubling nutrient loads flowing into Lake Michigan would not have a significant positive impact on prey fish or piscivore biomass. Moreover, the shunting effect that *Dreissena* mussels have on the phosphorus cycle might cause harmful effects in the nearshore zone such as localized eutrophication, hypoxia, and nuisance *Cladophora* blooms.

Future Work

While this application of LMAM does include some of Atlantis's underlying three dimensional and spatially explicit capabilities, further calibration and analysis of spatially explicit model environments would allow future researchers to take advantage of Atlantis model's full potential. LMAM is currently calibrated to an acceptable level on a lakewide scale, but many functional groups were not spatially calibrated at this time. Improving seasonal spatial calibration of fish species would allow prediction of fish biomass in nearshore versus offshore areas as well as for the eastern and western sides of the lake. This would permit investigation of how ecological changes at the lake-wide scale would affect the lake's smaller management units and how lake-wide management would affect food webs in different lake areas. Additionally, calibrating zooplankton distribution in the water column could potentially further elucidate the role of diel vertical migration in interactions between the lower food web, planktivorous fish, and piscivores.

Future work with the LMAM also could include simulating the effects of other factors that might have a synergistic or antagonistic interaction with nutrient loads and mussels. One particularly timely and relevant factor could be the effect of climate warming on nutrient cycling throughout the lake which Atlantis is well equipped to investigate. Fulton (2011) used the Atlantis model to investigate the effects of climate change on the food web off the coast of Southeast Australia. In Lake Michigan, a warming climate can be expected to cause both earlier onset of stratification as well as a longer stratification period (Brooks and Zastrow, 2002; McCormick, 1990). Recent modeling studies (Rowe et al., 2017, Pilcher et al., 2017) indicated that nutrient loads would have a greater effect on lake productivity during stratified periods when the upper water column is separated from mussel grazing. Studies using LMAM could incorporate

hydrodynamic files with deeper thermoclines and longer stratification periods to investigate potential effects caused by climate change. Additionally, climate change is predicted to decrease amount and duration of ice cover, increase winter and spring precipitation, and cause a decline in precipitation during summer by as much as 50 % drier (Hayhoe et al., 2010). LMAM could be used to investigate the effects of climate change on nutrient loads with higher pulses during the winter and spring to simulate increased rainfall during that time period.

References

Brooks, A. S. & Zastrow, J. C. The Potential Influence of Climate Change on Offshore Primary Production in Lake Michigan. *J. Great Lakes Res.* 28, 597–607 (2002).

Bunnell, D.B., Carrick, H.J., Madenjian, C.P., Rutherford, E.S., Vanderploeg, H.A., Barbiero, R.P., Hinchey-Malloy, E., Pothoven, S.A., Riseng, C.M., Claramunt, R.M., and eight others. 2018. Are changes in lower trophic levels limiting prey-fish biomass and production in Lake Michigan? Great Lakes Fishery Commission Miscellaneous Publication 2018-01.

Bunnell, D. B. *et al.* Are Changes in Lower Trophic Levels Limiting Prey-Fish Biomass and Production in Lake Michigan ? *Gt. Lakes Fish. Comm. Misc. Publ.* 2018–1, 41 (2018).

Bunnell, D. B., Madenjian, C. P., Holuszko, J. D., Adams, J. V. & French, J. R. P. Expansion of Dreissena into offshore waters of Lake Michigan and potential impacts on fish populations. *J. Great Lakes Res.* 35, 74–80 (2009).

Bunnell, D. B. *et al.* Changing ecosystem dynamics in the Laurentian Great Lakes: Bottom-up and top-down regulation. *Bioscience* 64, 26–39 (2014).

Cave, C.S., K.B. Strychar. 2014, Decline of *Diporeia* in Lake Michigan: Was disease associated with invasive species the primary factor? Int. J. Biol. 7:93-99

Hewson, I., J.B. Eaglesham, T.O. Hook, B.A. LaBarre, M.A. Sepulveda, P.D. Thompson, J.M. Watkins, L.G. Rudstam. 2013. Investigation of viruses in *Diporeia spp.* from the Laurentian Great Lakes and Owasco Lake as potential stressors of declining populations. Journal of Great Lakes Research. 39:499-506

Collingsworth, P. D., Bunnell, D. B., Madenjian, C. P. & Riley, S. C. Comparative Recruitment Dynamics of Alewife and Bloater in Lakes Michigan and Huron. *Trans. Am. Fish. Soc.* 143, 294–309 (2014).

Chen, C., Beardsley, R. C., and Cowles, G. (2006), An unstructured grid, finite-volume coastal ocean model: FVCOM user manual, manual, 315 pp., Sch. for Mar. Sci. and Technol., Univ. of Mass. Dartmouth, New Bedford, Mass.

Engevold, P. M., Young, E. B., Sandgren, C. D. & Berges, J. A. Pressure from top and bottom: Lower food web responses to changes in nutrient cycling and invasive species in western Lake Michigan. *J. Great Lakes Res.* 41, 86–94 (2015).

Fahnenstiel, G. *et al.* Recent changes in primary production and phytoplankton in the offshore region of southeastern Lake Michigan. *J. Great Lakes Res.* 36, 20–29 (2010).

Fulton, E. A. 2001. The effects of model structure and complexity ont eh behavior and performance of marine ecosystem models. Ph.D. dissertation, University of Tasmania, Hobart, Tasmania, Australia.

Fulton, E. A., J. S. Parslow, A. D. M. Smith, and C. R. Johnson. 2004a. Biogeochemical marine ecosystem models II: the effect of physiological detail on model performance. Ecological Modelling **173**:371-406.

Fulton, E. A., A. D. M. Smith, and C. R. Johnson. 2003. Mortality and predation in ecosystem models: is it important how these are expressed? Ecological Modelling **169**:157-178.

Fulton, E. A., A. D. M. Smith, and C. R. Johnson. 2004b. Biogeochemical marine ecosystem models I: IGBEM - a model of marine bay ecosystems. Ecological Modelling **174**:267-307.

Fulton, E. A., A. D. M. Smith, and C. R. Johnson. 2004c. Effects of spatial resolution on the performance and interpretation of marine ecosystem models. Ecological Modelling **176**:27-42.

Jude, D. J. *et al.* Trends in *Mysis diluviana* abundance in the Great Lakes, 2006–2016. *J. Great Lakes Res.* 44, 590–599 (2018).

Kao, Y.-C., Adlerstein, S. & Rutherford, E. The relative impacts of nutrient loads and invasive species on a Great Lakes food web: An Ecopath with Ecosim analysis. *J. Great Lakes Res.* 40, 35–52 (2014).

Kao, Y. C., Rogers, M. W. & Bunnell, D. B. Evaluating Stocking Efficacy in an Ecosystem Undergoing Oligotrophication. *Ecosystems* 1–19 (2017). doi: 10.1007/s10021-017-0173-5

Kerfoot, W. C. *et al.* Approaching storm: Disappearing winter bloom in Lake Michigan. *J. Great Lakes Res.* 36, 30–41 (2010).

Madenjian, C. P., Holuszko, J. D. & Desorcie, T. J. Growth and Condition of Alewives in Lake Michigan, 1984–2001. *Trans. Am. Fish. Soc.* 132, 1104–1116 (2003).

Madenjian, C. P. *et al.* Changes in the Lake Michigan food web following dreissenid mussel invasions: A synthesis. *J. Great Lakes Res.* 41, 217–231 (2015).

Maranger, R., S. Jones, and J. Cotner. 2018. Stoichiometry of carbon, nitrogen, and phosphorus through the freshwater pipe. *Limnology and Oceanography Letters*. 3: 89-101

McCormick, M. J. Potential Changes in Thermal Structure and Cycle of Lake Michigan Due to Global Warming. *Trans. Am. Fish. Soc.* 119, 183–194 (1990).

Nalepa, T., Fanslow, D. L. & Lang, G. A. Transformation of the offshore benthic community in Lake Michigan: recent shift from the native amphipod Diporeia spp. to the invasive mussel *Dreissena rostriformis bugensis*. *Freshw. Biol.* **54,** 466–479 (2009).

Nalepa, T. F. *et al.* Continued disappearance of the benthic amphipod *Diporeia* spp. in Lake Michigan: is there evidence for food limitation? *Can. J. Fish. Aquat. Sci.* **63,** 872–890 (2006).

Pilcher, D. J., McKinley, G. A., Kralj, J., Bootsma, H. A. & Reavie, E. D. Modeled sensitivity of Lake Michigan productivity and zooplankton to changing nutrient concentrations and quagga mussels. *J. Geophys. Res. Biogeosciences* 122, 2017–2032 (2017).

Pothoven, S. A., Nalepa, T. F., Schneeberger, P. J. & Brandt, S. B. Changes in Diet and Body Condition of Lake Whitefish in Southern Lake Michigan Associated with Changes in Benthos. *North Am. J. Fish. Manag.* 21, 876–883 (2001).

Prater, C. *et al.* Variation in particulate C:N:P stoichiometry across the Lake Erie watershed from tributaries to its outflow. *Limnol. Oceanogr.* **62,** S194–S206 (2017).

Rogers, M. W., Bunnell, D. B., Madenjian, C. P. & Warner, D. M. Lake Michigan offshore ecosystem structure and food web changes from 1987 to 2008. *Can. J. Fish. Aquat. Sci.* **71,** 1072–1086 (2014).

Simpson, N. T., Honsey, A., Rutherford, E. S. & Höök, T. O. Spatial shifts in salmonine harvest, harvest rate, and effort by charter boat anglers in Lake Michigan, 1992–2012. *J. Great Lakes Res.* 42, 1109–1117 (2016).

Stewart, T. J. & Sprules, W. G. Carbon-based balanced trophic structure and flows in the offshore Lake Ontario food web before (1987-1991) and after (2001-2005) invasion-induced ecosystem change. *Ecol. Modell.* 222, 692–708 (2011).

Tomlinson, L. M., Auer, M. T., Bootsma, H. A. & Owens, E. M. The Great Lakes Cladophora Model: Development, testing, and application to Lake Michigan. *J. Great Lakes Res.* **36,** 287–297 (2010).

Vanderploeg, H. A. *et al.* Seasonal zooplankton dynamics in Lake Michigan: Disentangling impacts of resource limitation, ecosystem engineering, and predation during a critical ecosystem transition. *J. Great Lakes Res.* 38, 336–352 (2012).

Report, F., International, T. & Commission, J. Understanding Declining Offshore Productivity in the Great Lakes. (2018).

Rowe, M. D. *et al.* Influence of invasive quagga mussels, phosphorus loads, and climate on spatial and temporal patterns of productivity in Lake Michigan: A biophysical modeling study. *Limnol. Oceanogr.* 62, 2629–2649 (2017).

Wehse, R., Hansen, M. J., Treska, T. J., Holey, M. E. & Office, G. B. F. and W. C. *Summary of 2016 Lake Trout and Salmonid Stocking in Lake Michigan*. (2017).

Wells, L. Effects of Alewife predation on Zooplankton populations in Lake Michigan. *Limnol. Oceanogr.* 15, 556–565 (1970).

Withers, J. L., Sesterhenn, T. M., Foley, C. J. & Troy, C. D. Diets and growth potential of early stage larval yellow perch and alewife in a nearshore region of southeastern Lake Michigan. *J. Great Lakes Res.* 41, 197–209 (2015).

Tables

Table 1. Functional groups parameterized for LMAM, the codes used to represent them in LMAM output, and their scientific name (if applicable).

Code	Name	Long Name	Scientific Name
ALE	Alewife	Alewife	*Alosa pseudoharengus*
BLT	Bloater	Bloater	*Coregonus hoyii*
SSP	Sculpin_S	Slimy Sculpin	*Myoxocephalus thompsonii*
DSP	Sculpin_D	Deepwater Sculpin	
LWF	Whitefish	Lake Whitefish	*Coregonus clupeaformis*
RDG	Goby	Round Goby	*Neogobius melanostomus*
YPH	Perch	Yellow Perch	*Perca flavescens*
WAE	Walleye	Walleye	*Sander vitreus*
RSM	Smelt	Rainbow Smelt	*Osmerus mordax*
SLP	Lamprey	Sea Lamprey	*Petromyzon marinus*
CHK	Chinook	Chinook Salmon	*Oncorhynchus tshawytscha*
CHO	Coho	Coho Salmon	*Oncorhynchus kisutch*
STH	Steelhead	Steelhead Trout	*Oncorhynchus mykiss*
LKT	Lake_Trout	Lake Trout	*Salvelinus namaycush*
BBT	Burbot	Burbot	*Lota*
SLC	Silver_C	Silver Carp	*Hypophthalmichthys molitrix*
BHC	Bighead_C	Bighead Carp	*Hypophthalmichthys nobilis*
COP	Copepods	Copepods	-
CLA	Cladocerans	Herbivorous Cladocerans	-
BYT	Bythotrephes	Bythotrephes	-
MYS	Mysis	Mysis	-
ROT	Rotifers	Rotifers	-
PRO	Protozoa	Protozoa	-
PB	Pelag_Bact	Pelagic Bacteria	-
BB	Sed_Bact	Sediment Bacteria	-
AMP	Amphipods	Amphipods	-
DRE	Dreissenids	Dreissenid Mussels	*Dreissena spp*
CHI	Chironomids	Chironomids	-
DIP	Diporeia	Diporeia	-
OLI	Oligochaetes	Oligochaetes	-

GRN	Greens	Green Algae
PIC	Picoplankton	Picoplankton
BLU	Blue_Greens	Blue Green Algae
DIA	Diatom	Diatoms
MA	Macroalgae	Benthic Macroalgae
DL	Lab_Det	Labile Detritus
DR	Ref_Det	Refractory Detritus

Table 2. RMSD Values for each LMAM functional group that had observation data available. RMSD is calculated from relative biomass for all groups except Dreissena which are calculated from absolute biomass.

Species	**RMSD**
Copepods	4.40
Bythotrephes	0.21
Mysis	2.50
Diporeia	0.16
Chironomids	6.93
Dreissena	92.37*
Alewife	5.58
Bloater	2.40
Rainbow Smelt	0.38
Deepwater Sculpin	0.82
Round Goby	1.20
Steelhead	0.82
Lake Whitefish	1.76
Lake Trout	1.62
Coho Salmon	0.86
Chinook Salmon	1.24

Table 3. Summary of Atlantis results based on linear models (bolded values are considered statistically significant at the P<0.05 level).

Group	Mussels Coefficient	Nutrients A:B Coefficient	Nutrients A:C Coefficient	Nutrients B:Mussels Coefficient	Nutrients C:Mussels Coefficient
ALE	**-0.771**	0.101	0.131		
BLT	**-0.198**	0.0005	0.004		
SSP	**-1.227**	**0.053**	0.148		
DSP	**-3.874**	0.036	0.019	-0.118	**1.69**
LWF	**0.019**	9.5E-05	**0.001**		
RDG	**1.319**	0.003	0.045		
YPH	**-0.36**	-0.047	0.11		
RSM	0.014	0.004	0.003		
SLP	-0.020	0.0002	-0.0006		
CHK	**-0.018**	**0.005**	**0.012**		
CHO	**-0.05**	0.007	.0008		
STH	**-0.101**	**0.007**	**0.011**		
LKT	**-0.472**	0.003	0.002	-0.013	**-0.2**
COP	0.005	**-0.027**	0.0008		
CLA	-0.0005	0.008	0.013		
BYT	**-0.55**	-0.034	0.048		
MYS	**0.551**	-0.007	0.001		
ROT	**- 8.1**	0.083	**0.51**	**0.89**	**1.47**
PRO	**0.37**	0.06	-0.09		
PB	**-0.03**	-0.002	0.0006		
BB	**-5.66**	0.003	0.02	**-1.19**	**-2.7**
AMP	**-0.015**	6.8E-05	1.9E-04	**-0.24**	**-0.96**
CHI	**0.03**	-0.006	**-0.013**	**0.0107**	**0.052**
DIP	**-0.33**	**0.004**	**0.01**	**0.011**	**0.03**
OLI	**- 8.3**	**0.11**	**0.27**	**0.118**	**-0.19**
PIC	-0.06	-0.03	-0.04		
BLU	**0.048**	**-0.041**	0.018	**0.08**	**0.24**
DIA	0.001	-0.01	0.004		
MA	**-9.9**	0.49	0.31		

Table 4. Initial population biomass, growth rates, and consumption rates for fish species in LMAM were from the Lake Michigan Ecopath with Ecosim model (Rutherford, Zhang, and Mason et al. unpublished data).

Group codes	Groups/species	Biomass (g/m^2)	Growth rates (P/B, per year)	Consumption rates (Q/B, per year)
		0.598164	3.59	31.8
ALE	Alewife YOY			
		1.55	1.6	12.43
	Alewife YAO			
BLT	Bloater YOY	0.055827	0.944	36.82039
	Bloater YAO	3.9	0.69	9.2
		0.167	1.51	7.53
SSP	Slimy Sculpin			
		0.748	1.13	6.327
DSP	Deepwater Sculpin			
LWF	Lake Whitefish YOY	0.025674	0.944	23.41389
	Lake Whitefish Juvenile	0.700357	0.69	8.244582
	Lake Whitefish Adults	0.48	0.7625	5.08
		0.01	0.71	4.7
RDG	Round Goby			
YPH	Yellow Perch YOY	0.003809	2.66	7.336398
	Yellow Perch Juvenile	0.010279	1.637	4.074439
	Yellow Perch Adults	0.03	0.8	2.207
		0.0127	0.214	1.373
WAE	Walleye			
RSM	Rainbow Smelt YOY	0.044501	2.26	10.03159
	Rainbow Smelt Adults	0.864	0.529	3.678
		0.000226	0.42	130
SLP	Sea Lamprey			
		0.011228	0.931	13.21298
CHK	Chinook Salmon year 0			
	Chinook Salmon year 1	0.048398	1.125	7.66106
	Chinook Salmon year 2	0.04128	1.2	5.59
	Chinook Salmon year 3	0.02037	1.2	4.755089
	Chinook Salmon year 4	0.005161	2.558	4.376491
		0.012	0.74	6.38
CHO	Coho Salmon year 1-2			
STH	Steelhead Trout year 1	0.01549	0.518	4.307736
	Steelhead Trout year 2-5	0.077	0.305	2.9043
	Steelhead Trout year 5+	0.017145	1.48	2.530676
		0.093	0.653	3
LKT	Lake Trout			
		0.359	0.25	4.4568
BBT	Burbot			
		5.63	4.9	22.3
COP	Copepods			
		1.472	18.04	64.42857
CLA	Herbivorous Cladocerans			
BYT	Bythotrephes	0.0528	26.18	96.96296

MYS	Mysis	2.04	4.6	13.7
ROT	Rotifers	0.568	44.9	187.0833
PRO	Protozoa	8.42942	108.7	317.6
PB	Pelagic Bacteria	17.73281	248	473
DRE	Dreissenid Mussels	2.26	3	11.86
CHI	Chironomids	0.632	7	37.03704
DIP	Diporeia	14.44	5.86	91.5
OLI	Oligochaetes	9.95	4.425	23.4127
GRN	phytoplankton	23.95705	200	-
PIC	Picoplankton	10.43393	343.8	-

Table 5: Parameters of fish age and length. Values from parameters of a and b for the length (mm) -weight (g) relationship were from Schneider et al. (2000). Weight (W) is calculated from length (L) as $\log_{10} W = a+b (\log_{10} L)$. The data sources for modeled maximum age classes were specified for each fish species.

Code	a	b	Max. age in the model	
			Year	Data sources
ALE	-5.28911	3.0637	6	(Tsehaye et al. 2014)
BLT	-5.42905	3.111	9	(Bunnell et al. 2006)
SSP	-5.29903	3.25202	7	
DSP	-5.29903	3.25202	7	
LWF	-5.79403	3.29176	15	(Pothoven et al. 2001)
RDG	-5.40464	3.2674	7	
YPH	-5.33475	3.17285	10	(Wilberg et al. 2005)
WAE	-5.14176	3.03606	12	(Hanchin et al. 2007)
RSM	-5.12117	2.96408	5	(Tsehaye et al. 2014)
SLP	-2.8623	1.9651	3	(Dawson et al. 2009)
CHK	-5.31348	3.113913	5	(Rogers et al. 2014)
CHO	-6.169	3.427	3	(Honeyfield et al. 2008)
STH	-5.1477	3.05253	8	(Rand et al. 1993)
LKT	-5.519	3.17882	16	(Madenjian et al. 1998)
BBT	-5.21478	3.03888	12	(Rudstam et al. 1995)

Table 6: Parameter values for fish recruitment models. The Beverton-Holt (BH) recruitment model predicts recruits (Rc) = $(Sp \cdot \alpha)/(Biom+\beta)$. The Ricker (R) recruitment model predicts $Rc=Biom \cdot e^{(\alpha \cdot (1-Biom/\beta))}$, where Biom is population biomass, and Sp is spawning biomass, and α and β are empirically estimated regression coefficients.

Fish	α	β	recruitment	Data sources
ALE	0.173911	3.22E-12	R	USGS bottom trawl YOY and YAO data
BLT	0.003076	1.38E-12	R	USGS bottom trawl YOY and YAO data
SSP	1.30E+13	2.925E+09	BH	(Madenjian et al. 2005)
DSP	3.58E+13	2.925E+11	BH	(Madenjian et al. 2005)
LWF	2.03E+08	4.68E+10	BH	(Caroffino and Lenart)
RDG	8.5E+12	2.925E+09	BH	This study
YPH	0.054646	9.97E-12	R	(Wilberg et al. 2005)
WAE	5E+7	1.20E+11	BH	This study
RSM	0.488168	2.09E-11	R	USGS bottom trawl YOY and YAO data
CHK	2323690	1.16E+09	BH	E. Rutherford (1997)
CHO	2.42E-05	5.15E-11	R	E. Rutherford (1997)
STH	0.000344	2.67E-10	R	E. Rutherford (1997)
LKT	-	-	-	All stocked

Figures

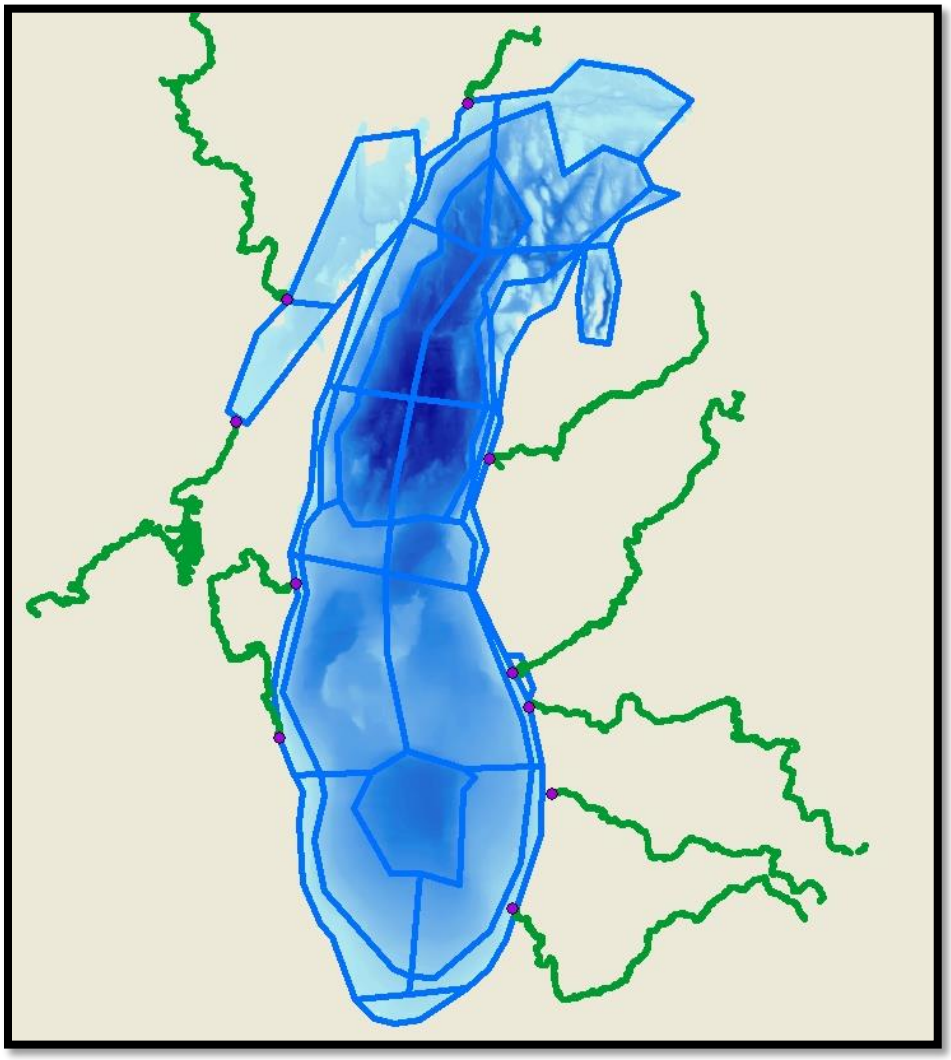

Figure 1. Habitat boxes defined in the Lake Michigan Atlantis Model with green lines representing major tributaries for nutrient loading.

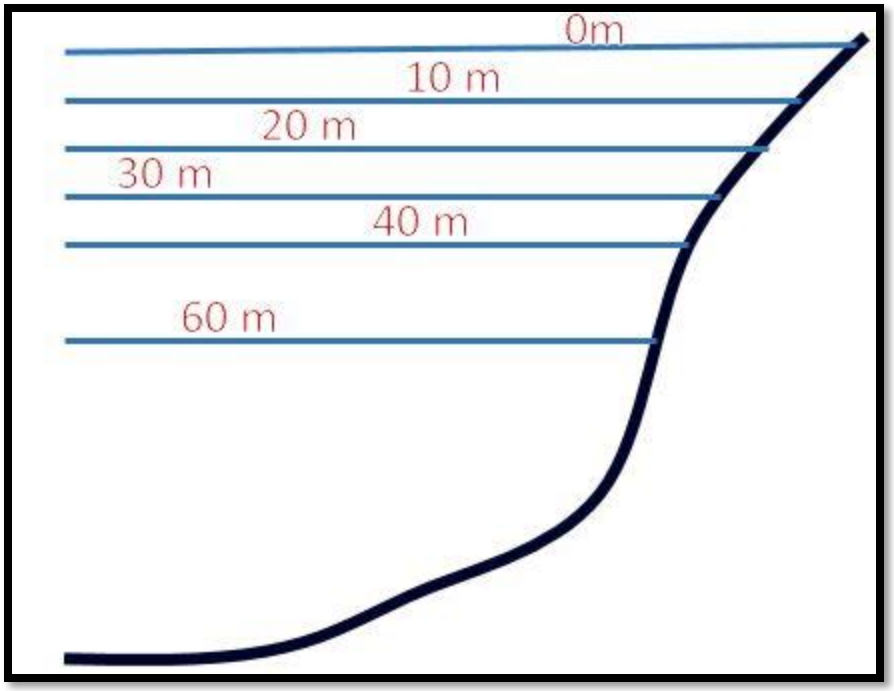

Figure 2. Vertical resolution of the Lake Michigan Atlantis model. Each habitat box is divided into between 1 and 6 depth layers based on bathymetry.

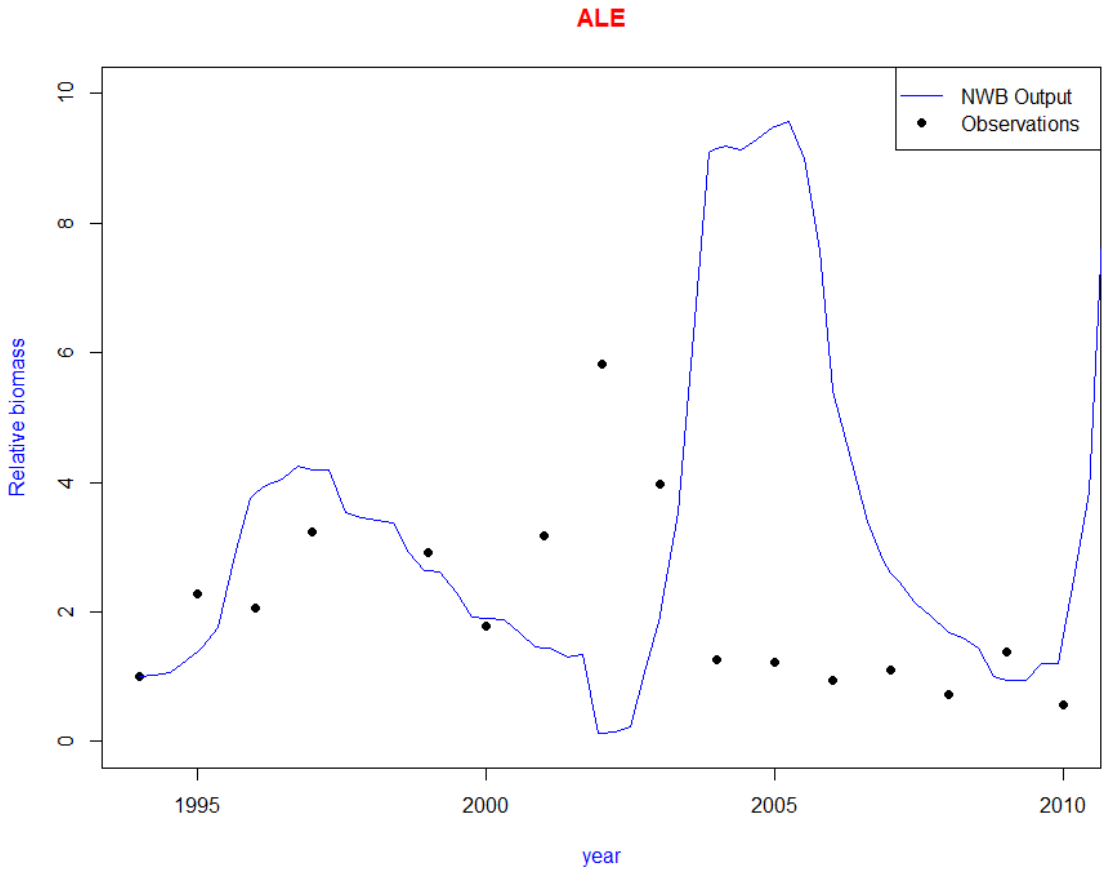

Figure 3. Relative biomass of Alewife output (line) compared with observation values (points). RMSD can be found in table 2.

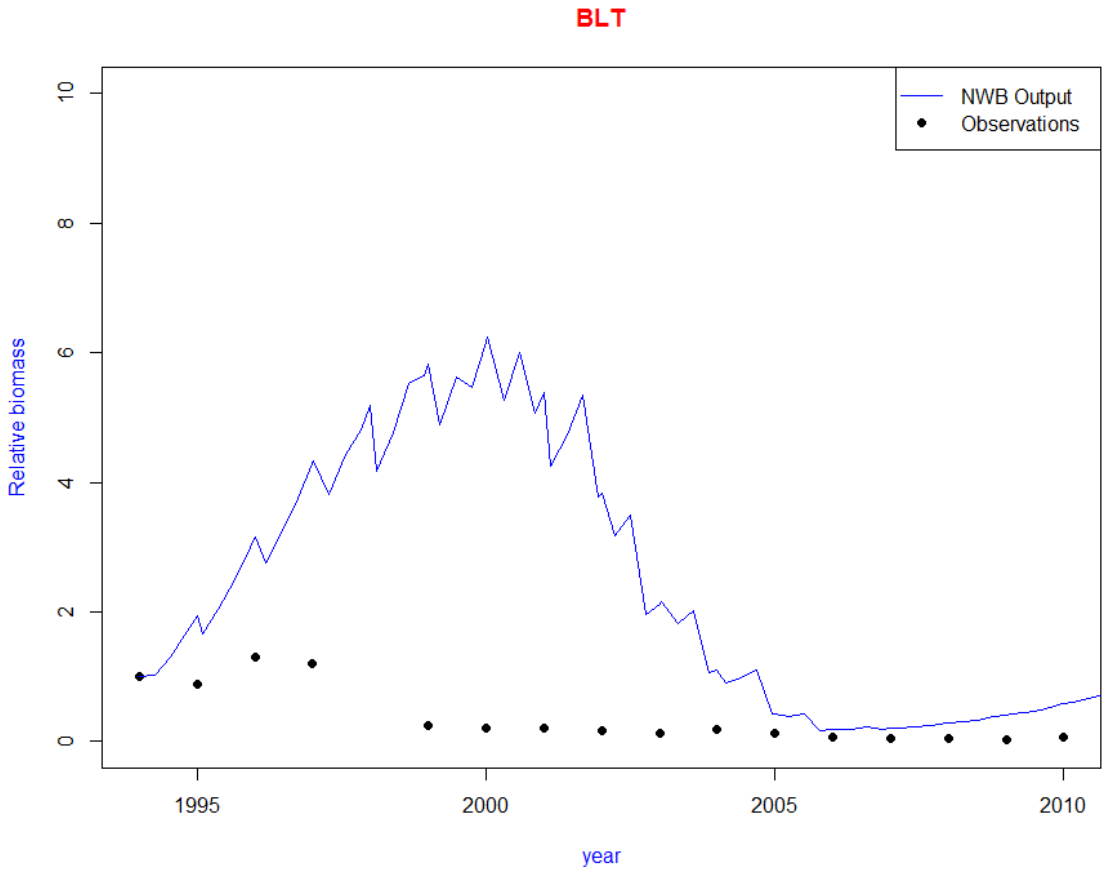

Figure 4. Relative biomass of Bloater output (line) compared with observation values (points). RMSD can be found in table 2.

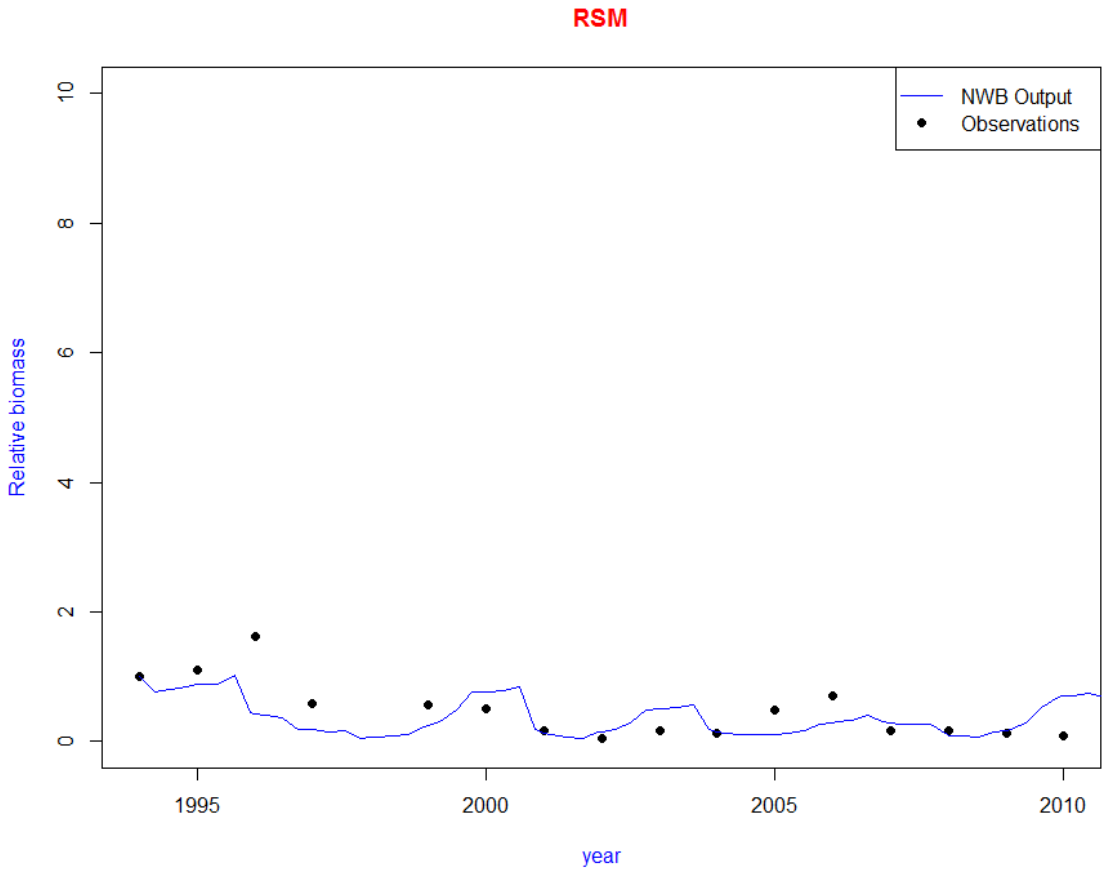

Figure 5. Relative biomass of Rainbow Smelt output (line) compared with observation values (points). RMSD can be found in table 2.

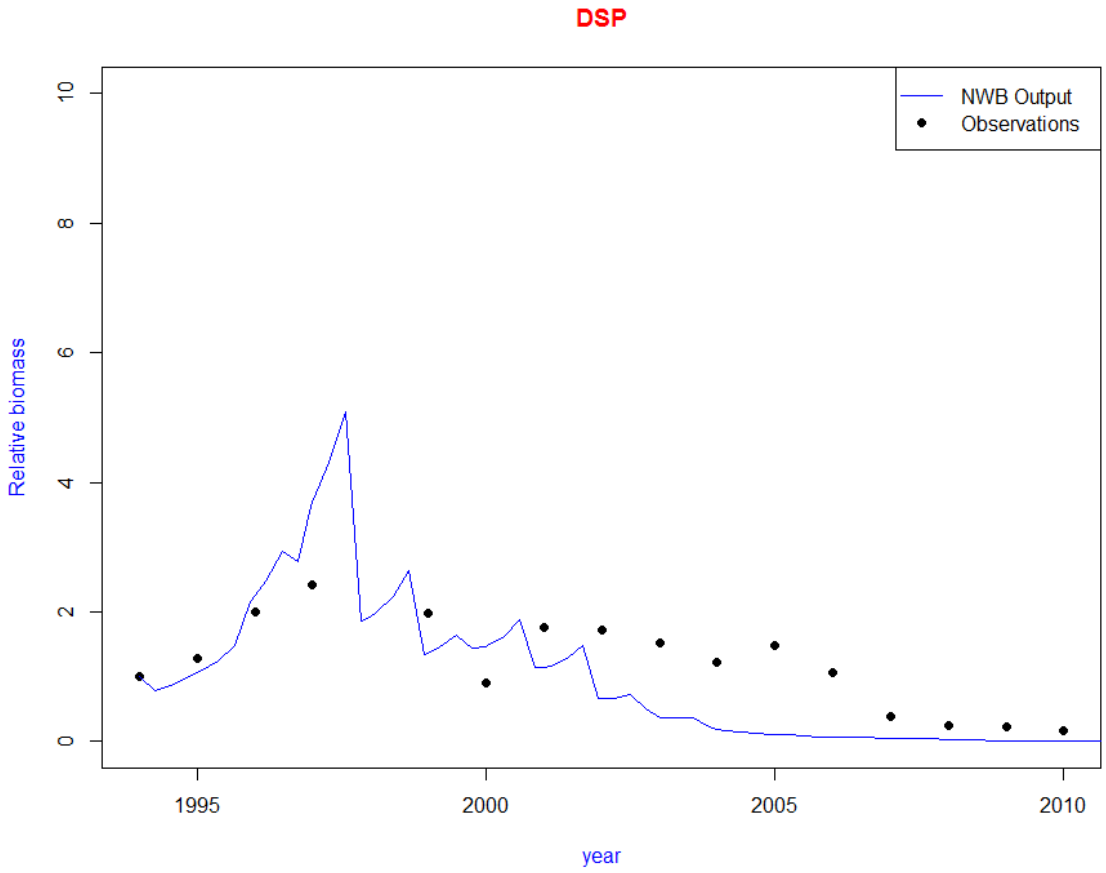

Figure 6. Relative biomass of Deep Water Sculpin output (line) compared with observation values (points). RMSD can be found in table 2.

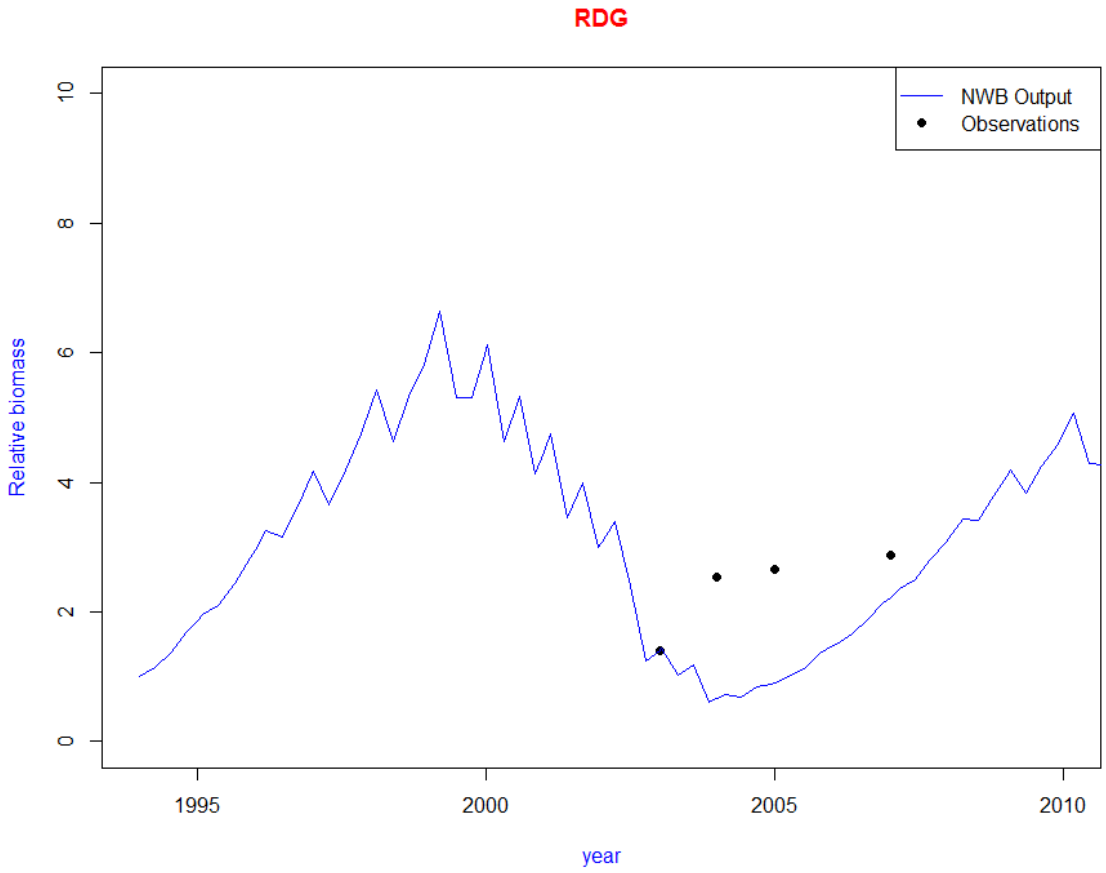

Figure 7. Relative biomass of Round Goby output (line) compared with observation values (points). RMSD can be found in table 2.

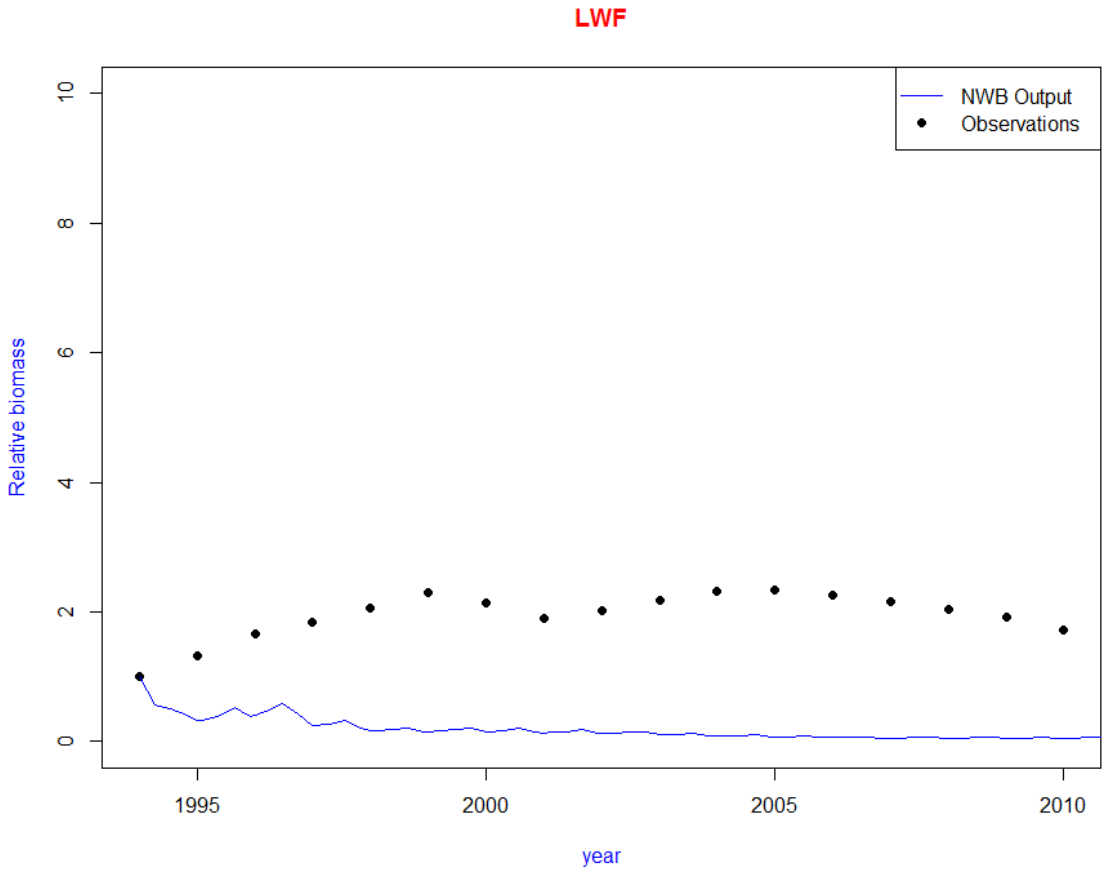

Figure 8. Relative biomass of Lake Whitefish output (line) compared with observation values (points). RMSD can be found in table 2.

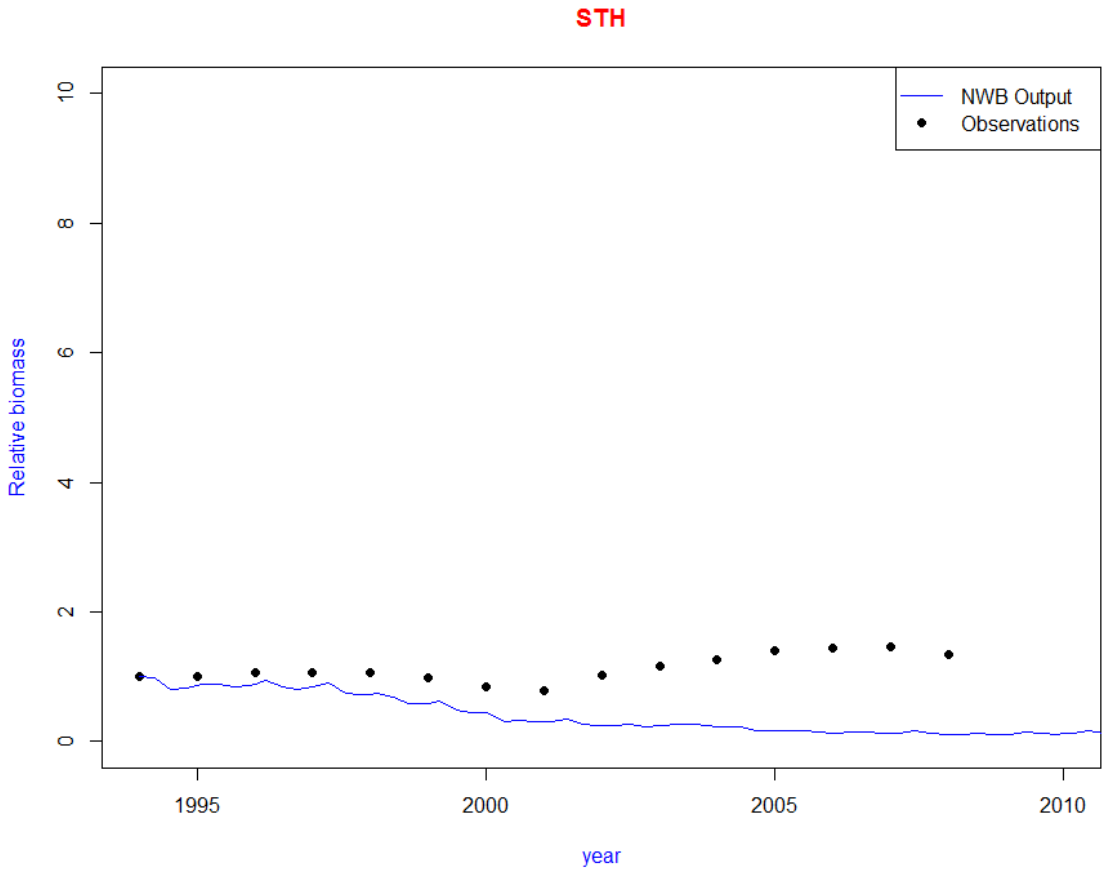

Figure 9. Relative biomass of Steelhead output (line) compared with observation values (points). RMSD can be found in table 2.

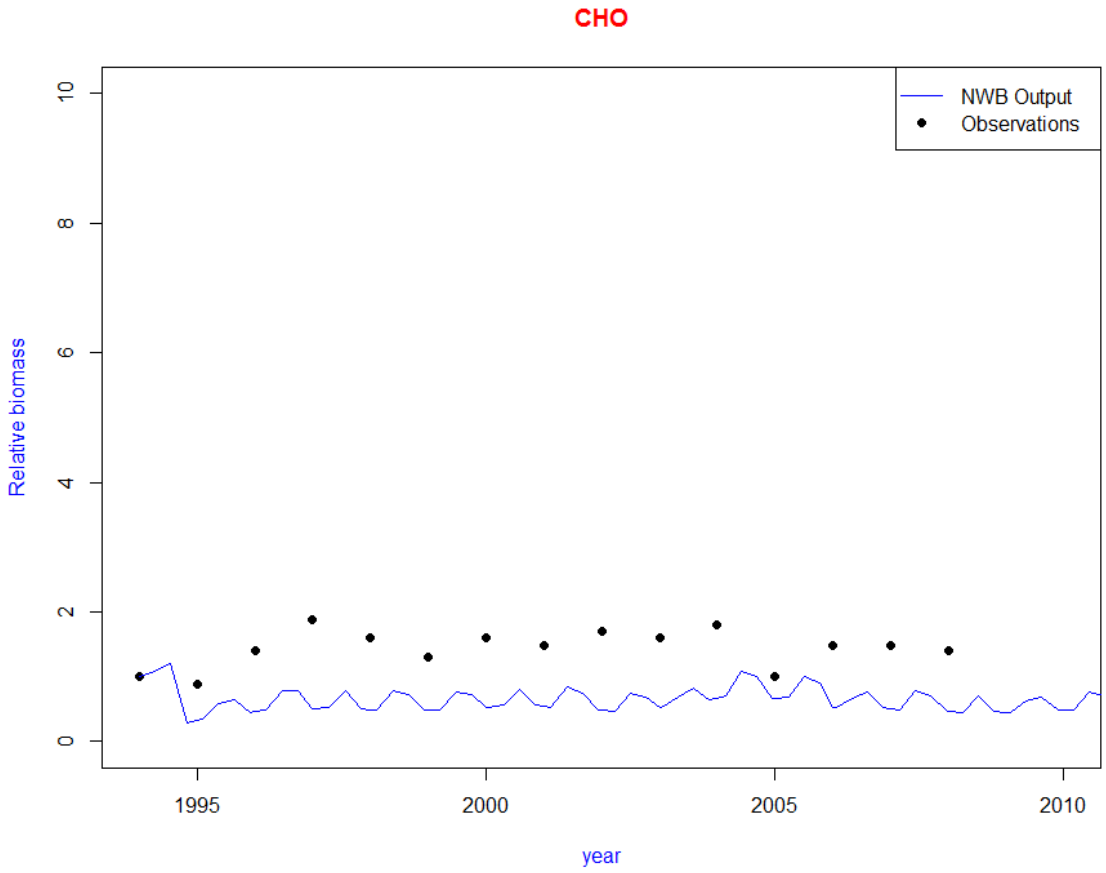

Figure 10. Relative biomass of Coho Salmon output (line) compared with observation values (points). RMSD can be found in table 2.

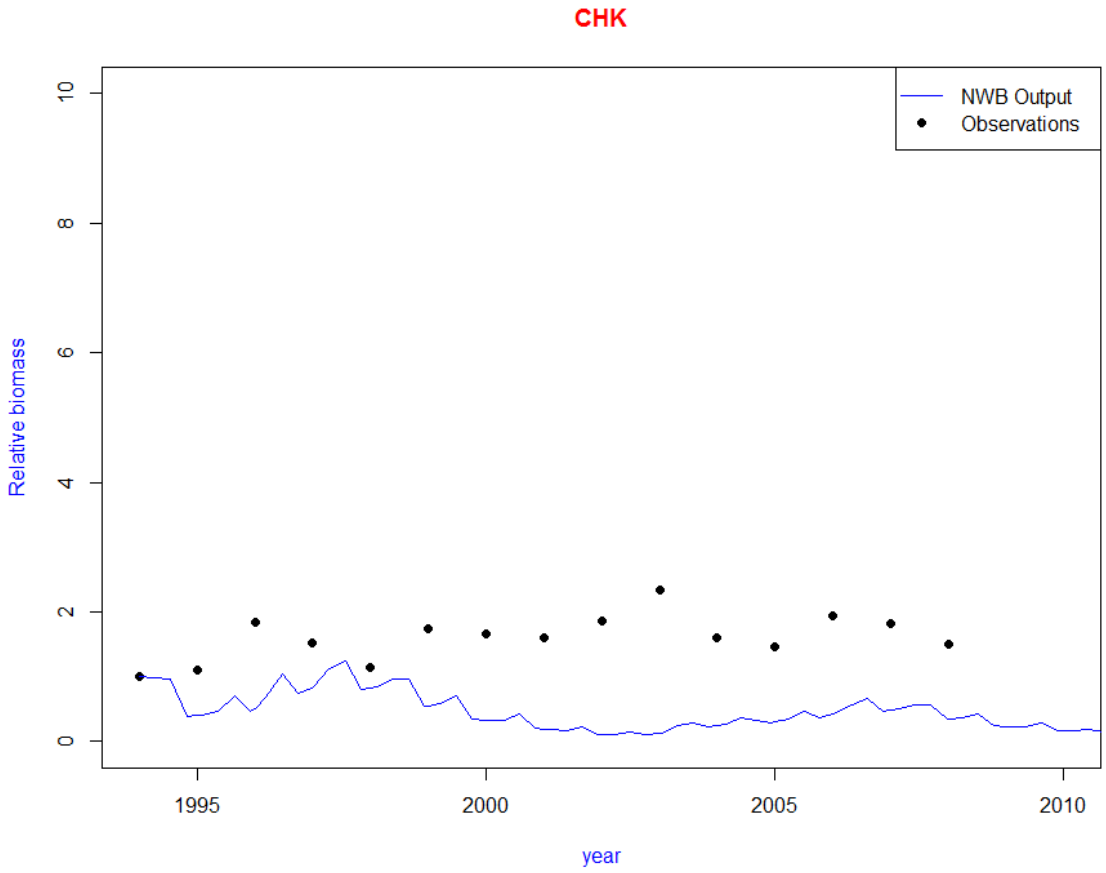

Figure 11. Relative biomass of Chinook Salmon output (line) compared with observation values (points). RMSD can be found in table 2.

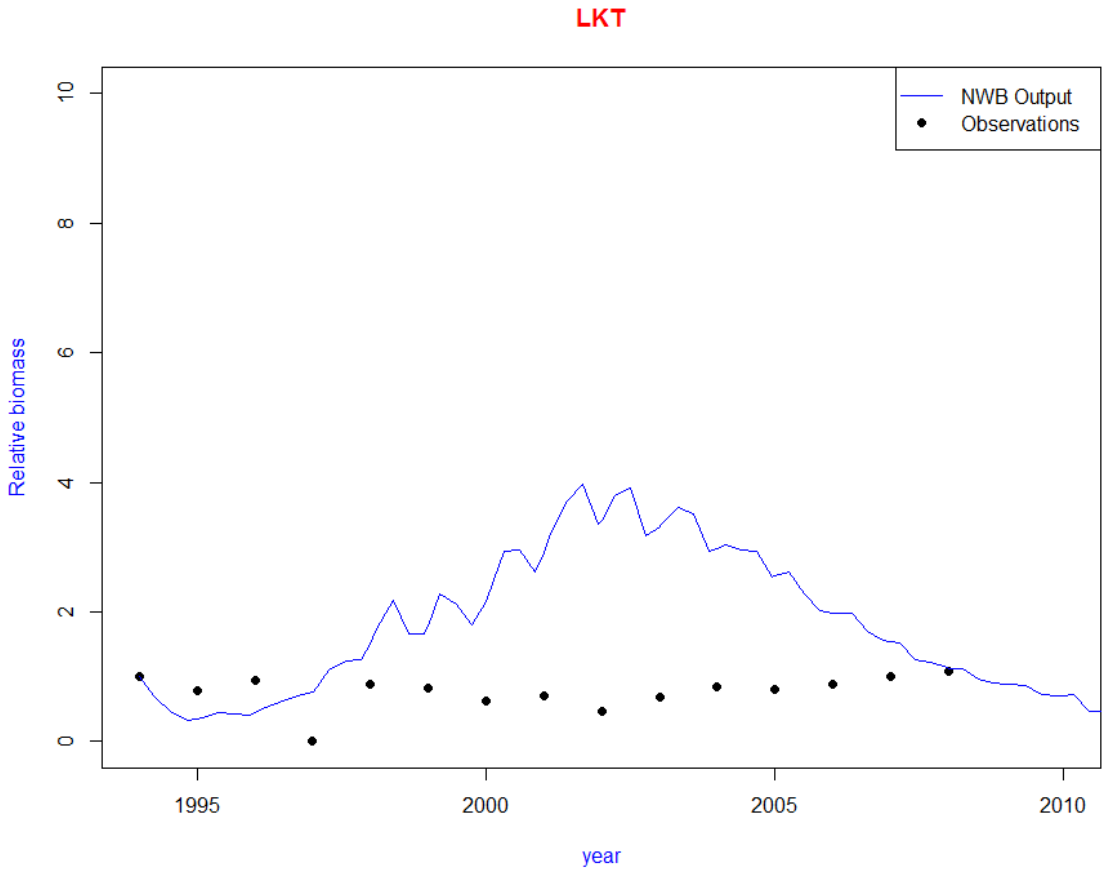

Figure 12. Relative biomass of Lake Trout output (line) compared with observation values (points). RMSD can be found in table 2.

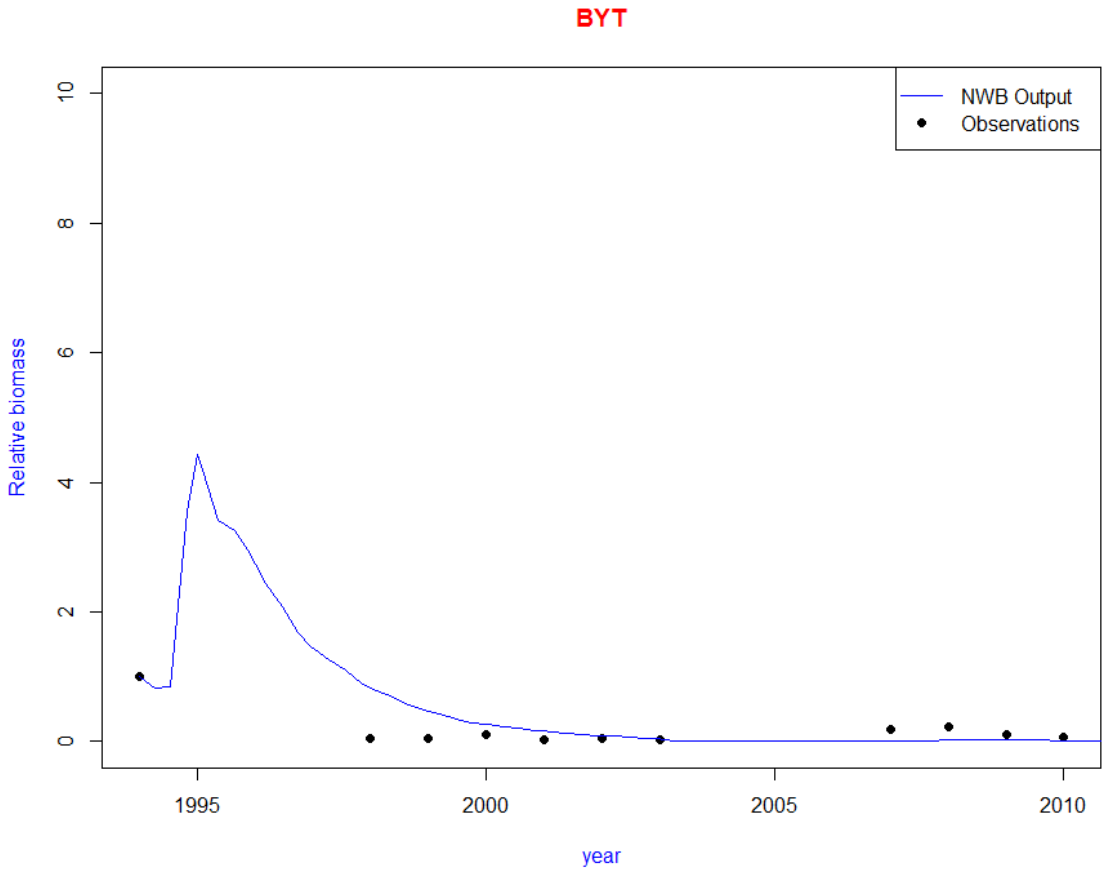

Figure 13. Relative biomass of Bythotrephes output (line) compared with observation values (points). RMSD can be found in table 2.

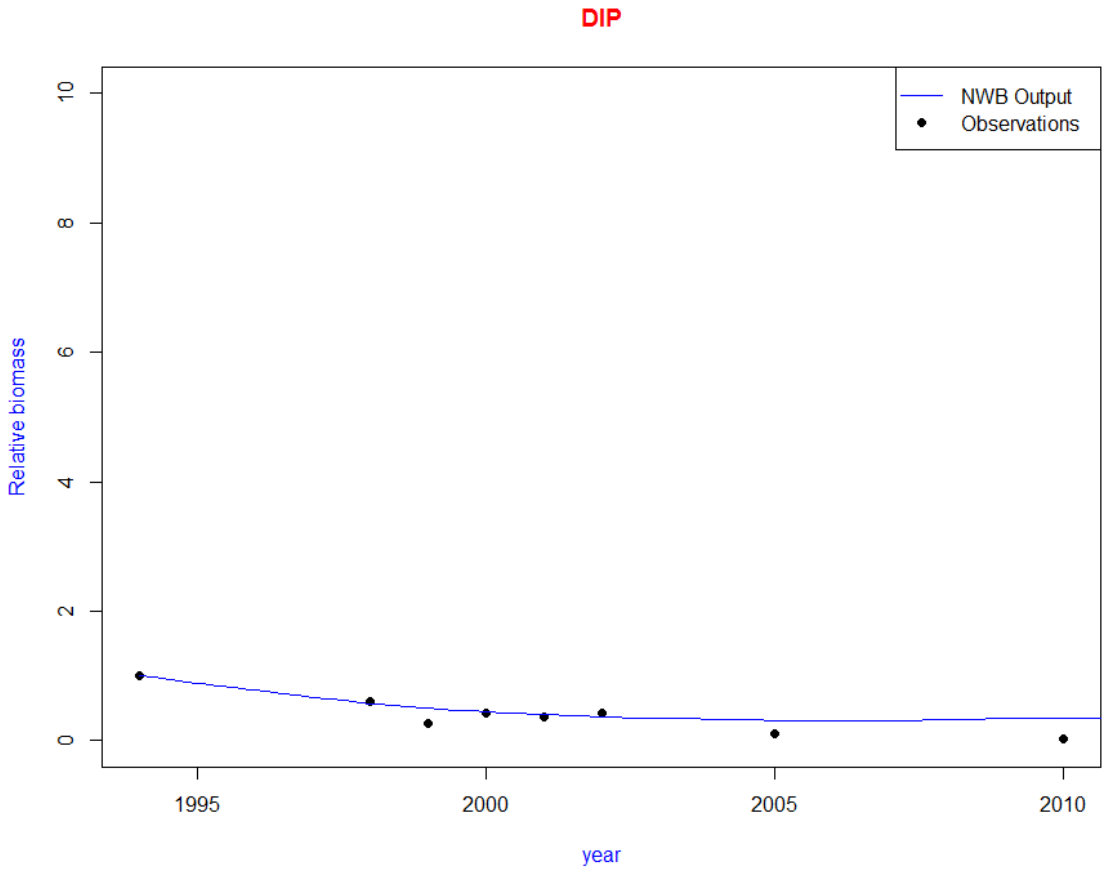

Figure 14. Relative biomass of Diporeia output (line) compared with observation values (points). RMSD can be found in table 2.

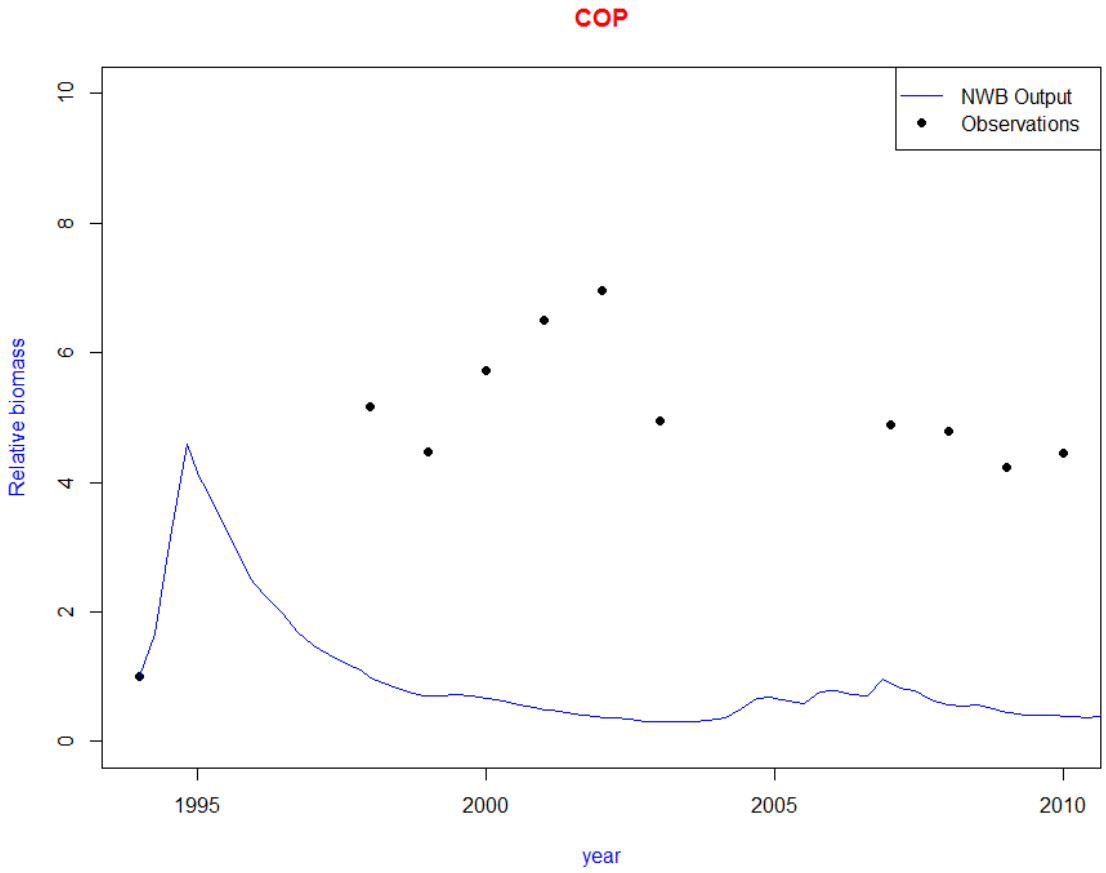

Figure 15. Relative biomass of Copepod output (line) compared with observation values (points). RMSD can be found in table 2.

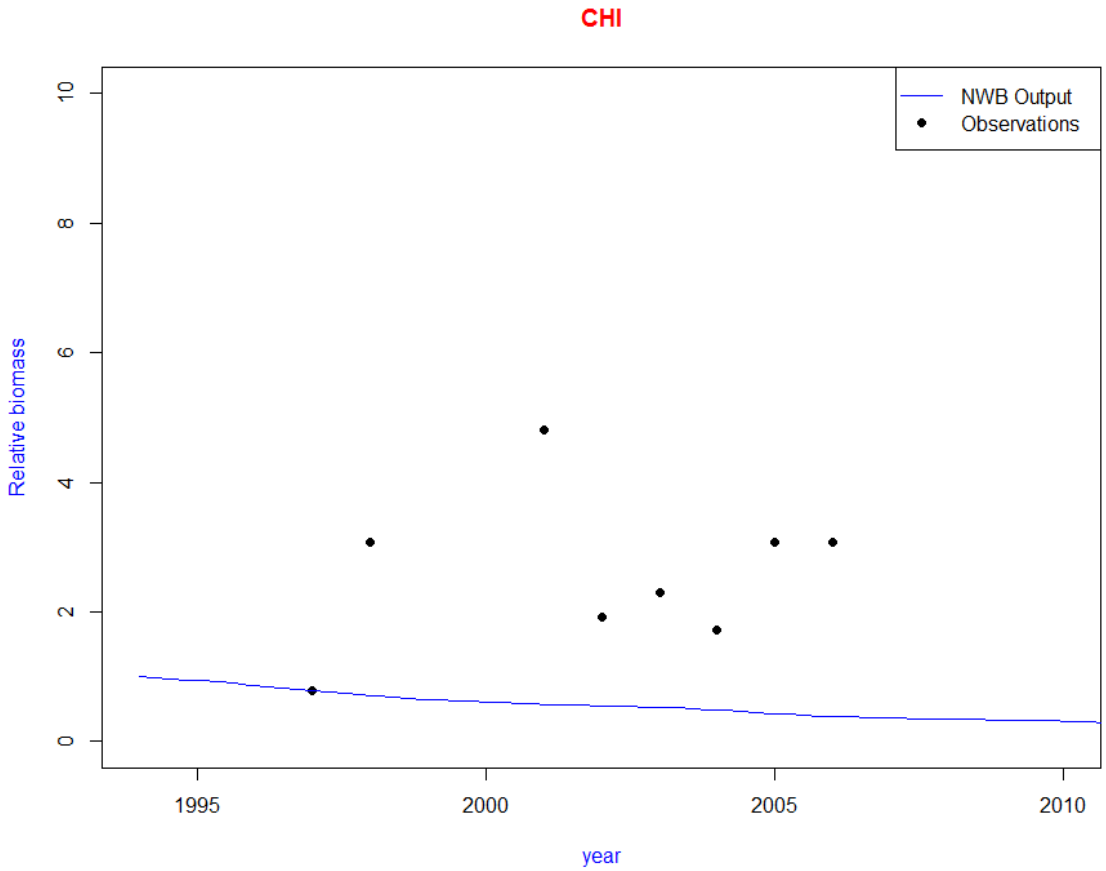

Figure 16. Relative biomass of Chironomid output (line) compared with observation values (points). RMSD can be found in table 2.

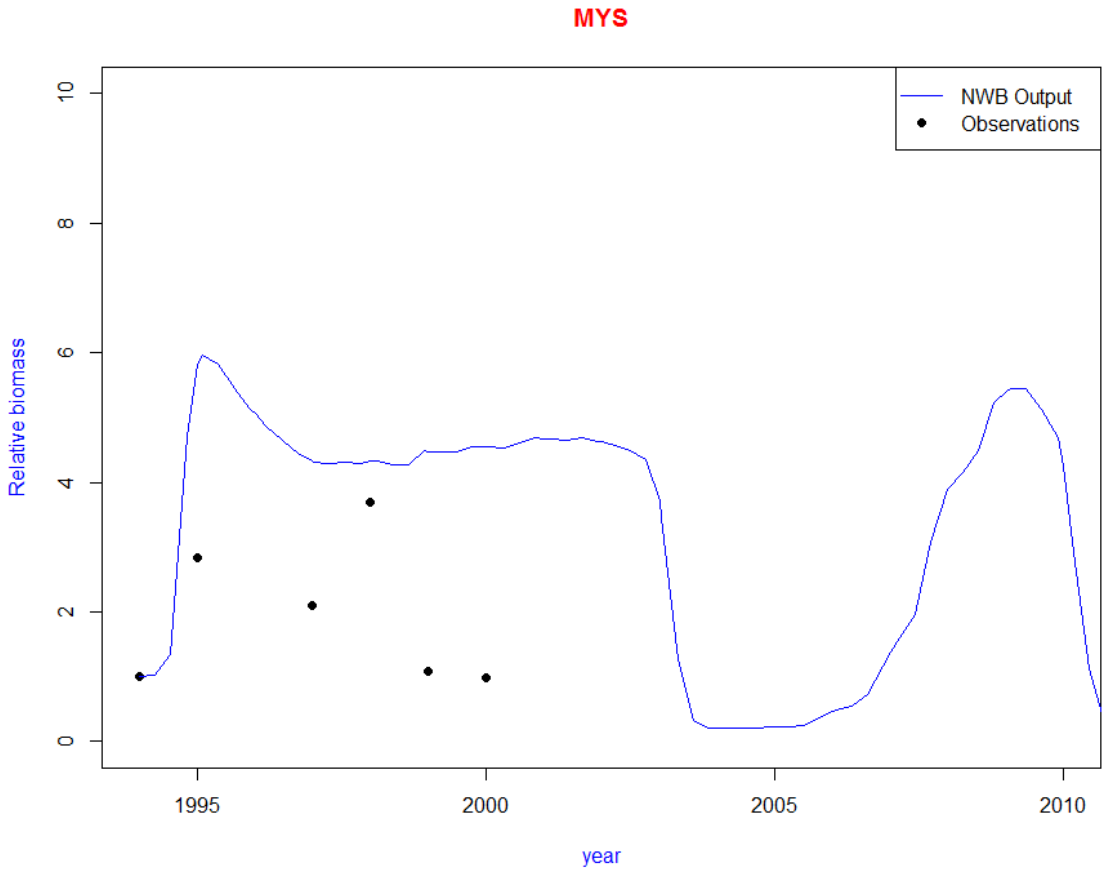

Figure 17. Relative biomass of Mysis output (line) compared with observation values (points). RMSD can be found in table 2.

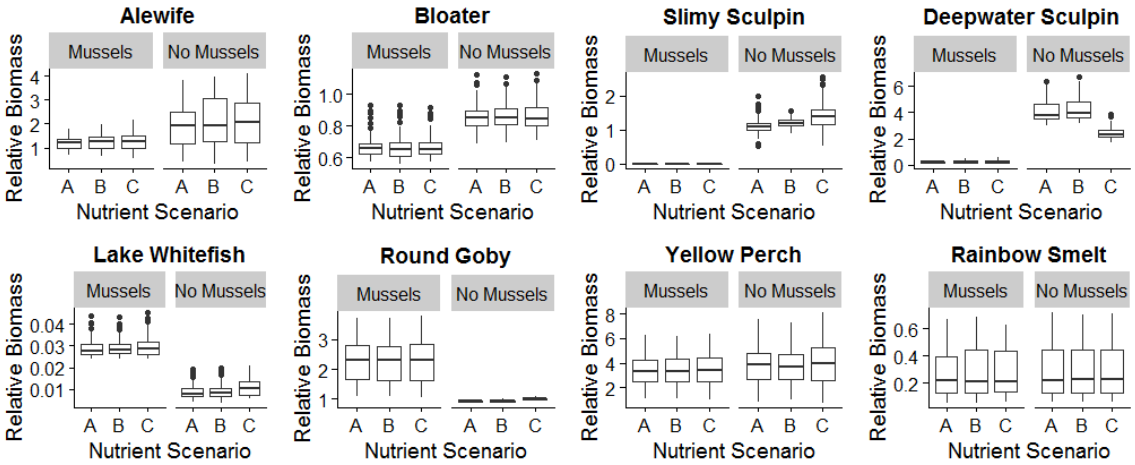

Figure 18. LMAM prediction of prey fish biomass under scenarios of dreissena mussel presence/absence and varying nutrient loading scenarios. A is low nutrient levels (0.5*1994 loads), B is baseline nutrient levels (1994 loads), C is high nutrient levels (2* 1994 loads).

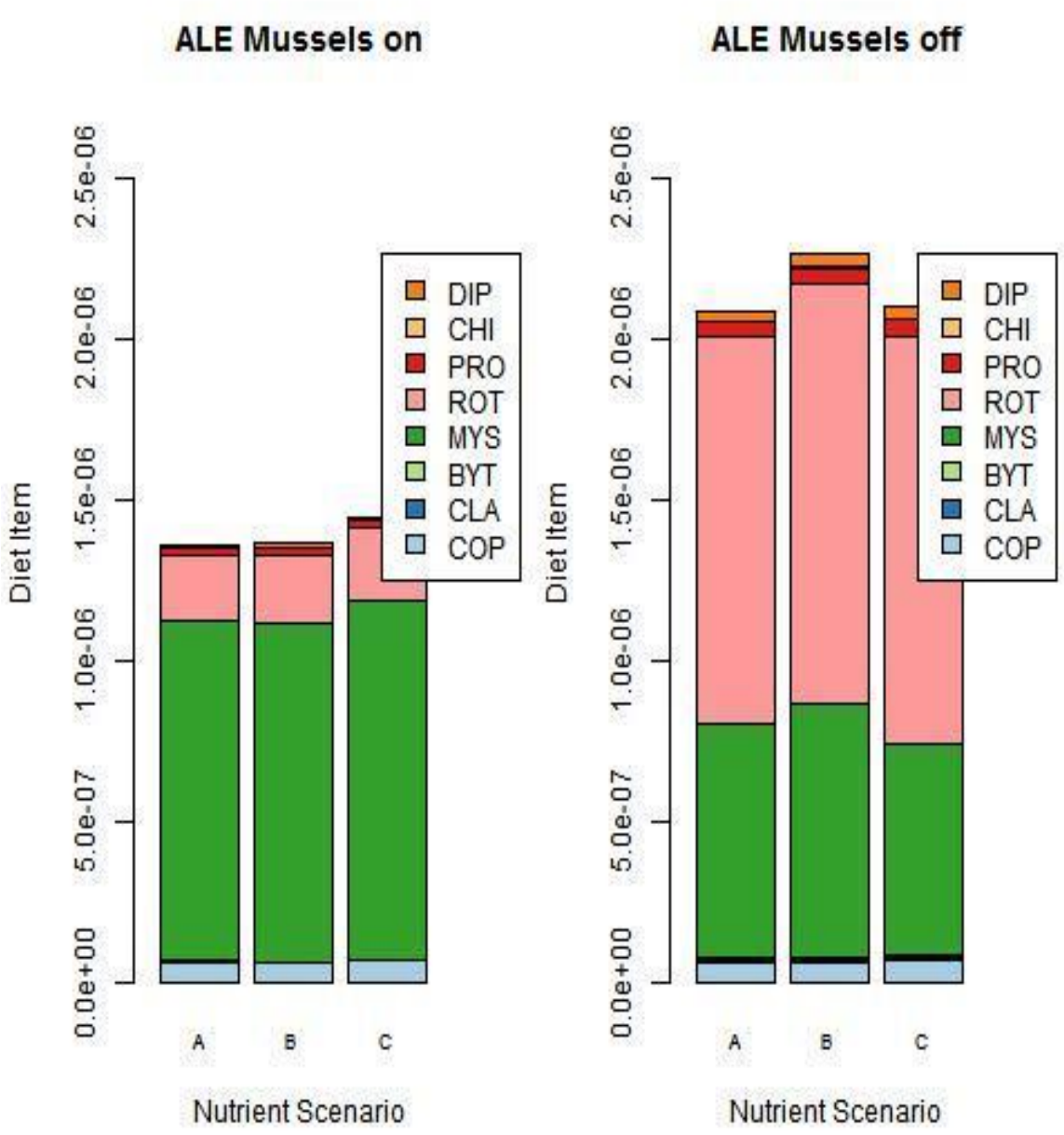

Figure 19. Alewife diet composition in mg N/m^3 s^{-1} averaged for the last 25 years of each 50 year run. A, B, and C are low, baseline, and high nutrient scenarios, respectively. Mussels present scenarios are displayed on the left. Mussels absent scenarios are displayed on the right. See Table 1 for species codes.

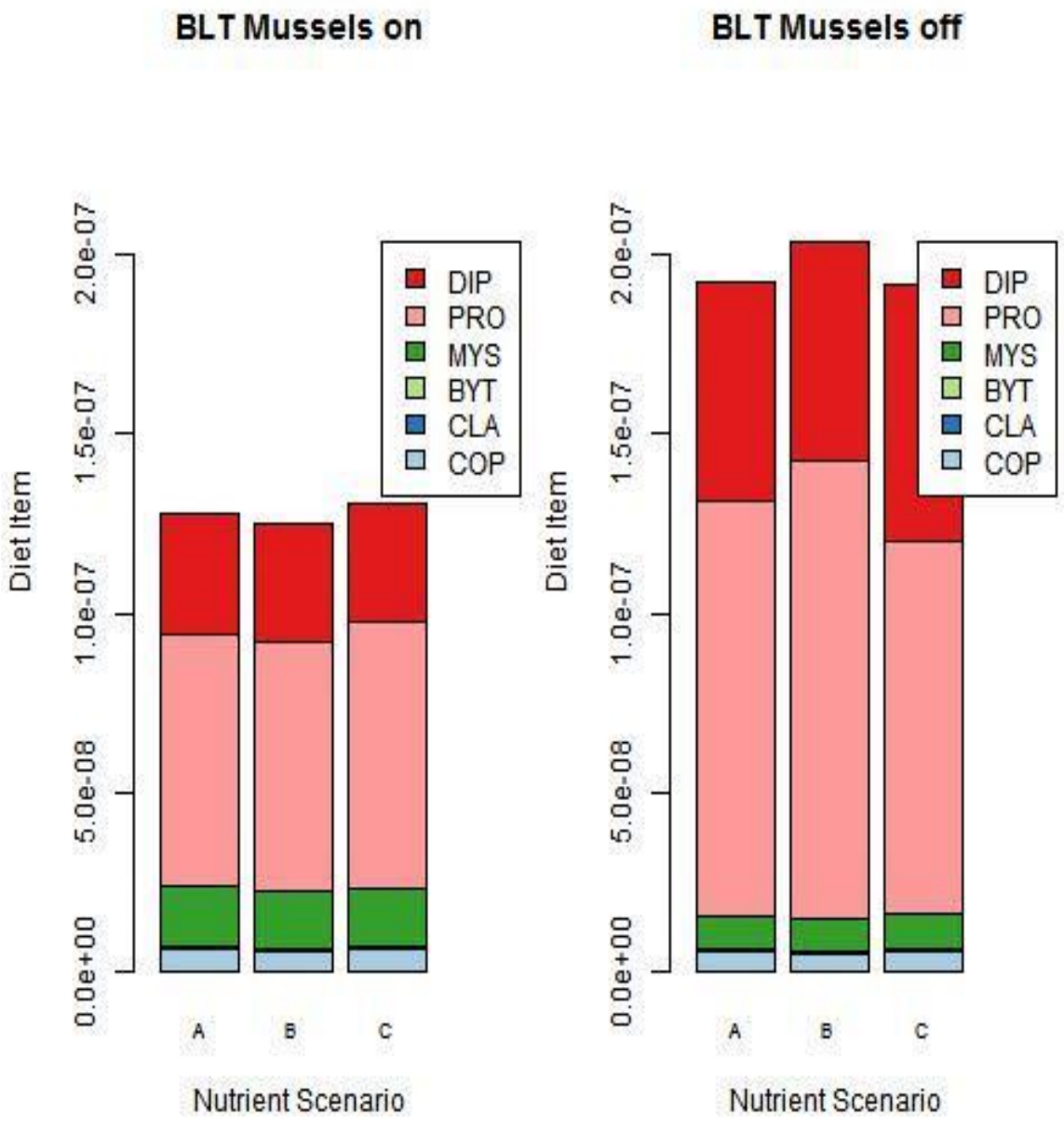

Figure 20. Bloater diet composition in mg N/m^3 s^{-1} averaged for the last 25 years of each 50 year run. A, B, and C are low, baseline, and high nutrient scenarios, respectively. Mussels present scenarios are displayed on the left. Mussels absent scenarios are displayed on the right. See Table 1 for species codes.

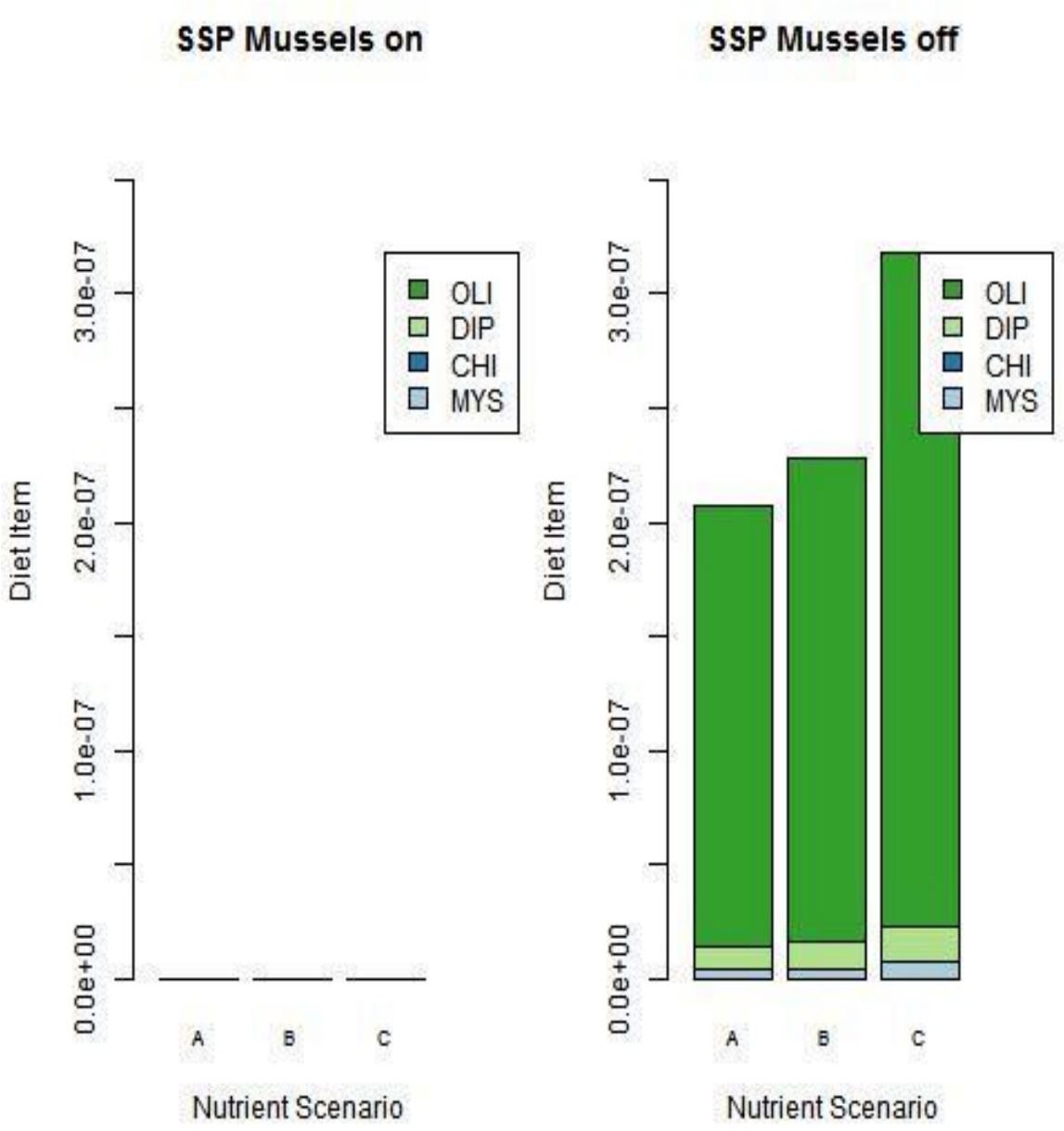

Figure 21. Slimy Sculpin diet composition in mg N/m^3 s^{-1} averaged for the last 25 years of each 50 year run. A, B, and C are low, baseline, and high nutrient scenarios, respectively. Mussels present scenarios are displayed on the left. Mussels absent scenarios are displayed on the right. See Table 1 for species codes.

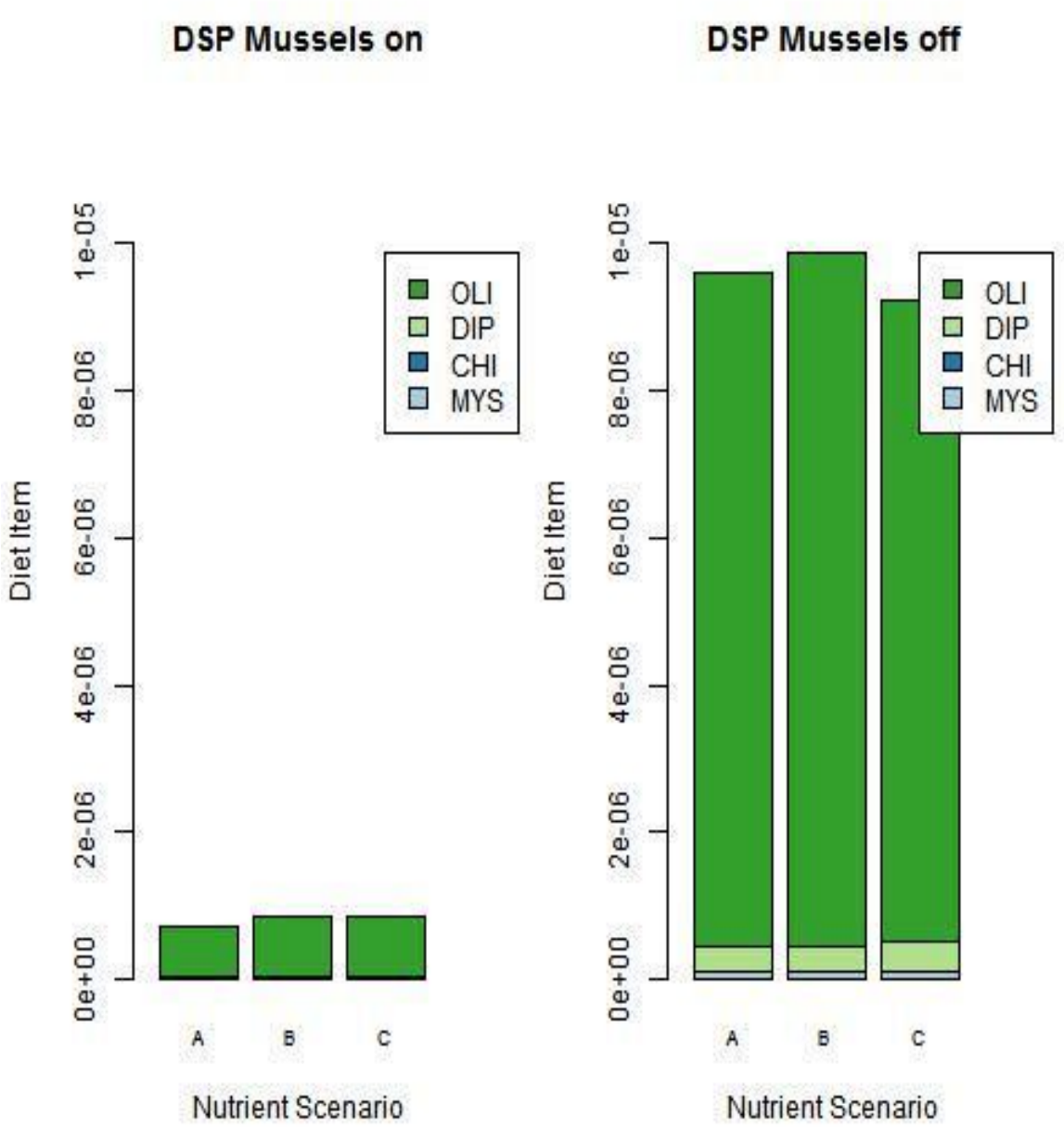

Figure 22. Deepwater Sculpin diet composition in mg N/m^3 s^{-1} averaged for the last 25 years of each 50 year run. A, B, and C are low, baseline, and high nutrient scenarios, respectively. Mussels present scenarios are displayed on the left. Mussels absent scenarios are displayed on the right. See Table 1 for species codes.

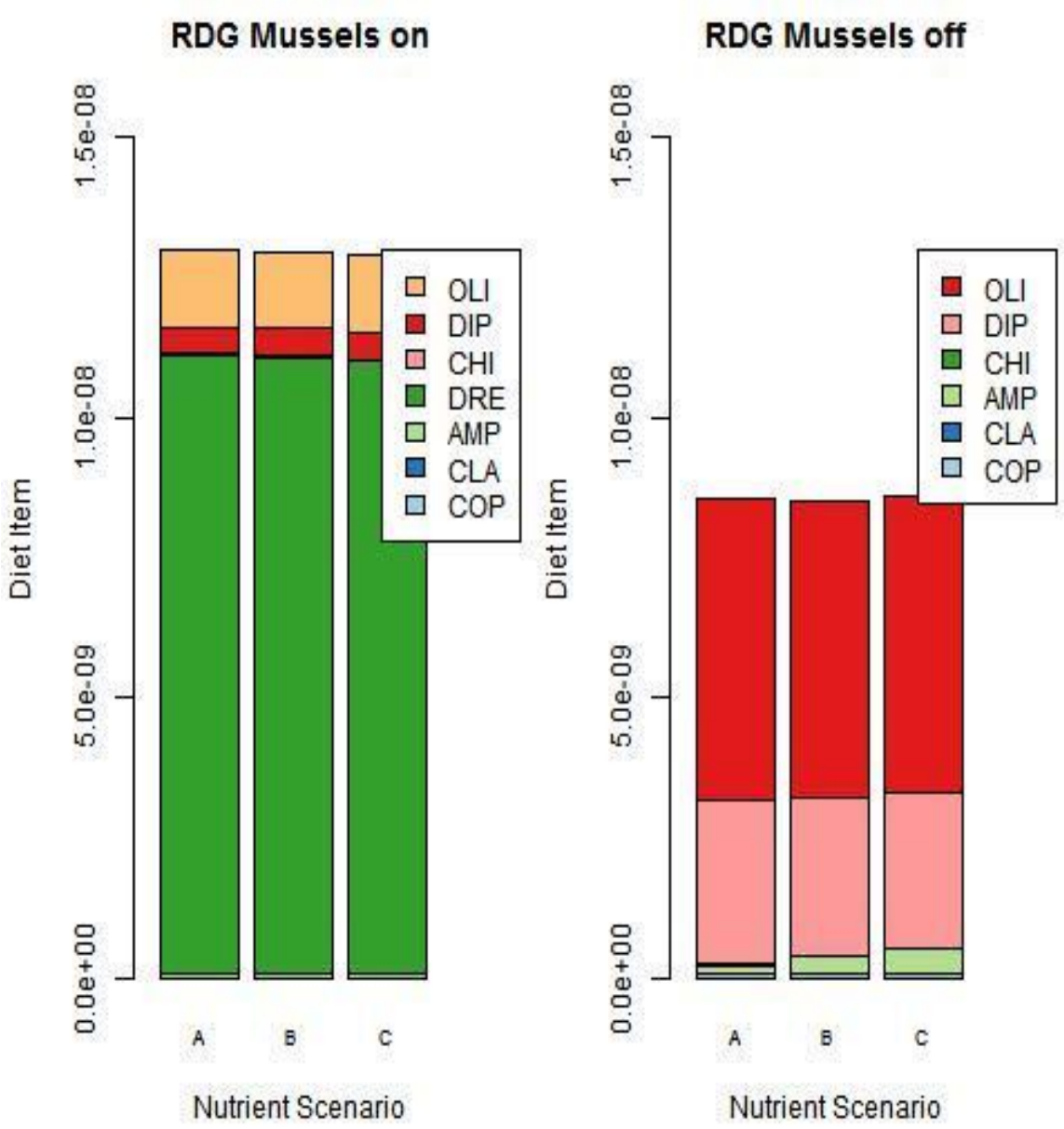

Figure 23. Round Goby diet composition in mg N/m^3 s^{-1} averaged for the last 25 years of each 50 year run. A, B, and C are low, baseline, and high nutrient scenarios, respectively. Mussels present scenarios are displayed on the left. Mussels absent scenarios are displayed on the right. See Table 1 for species codes.

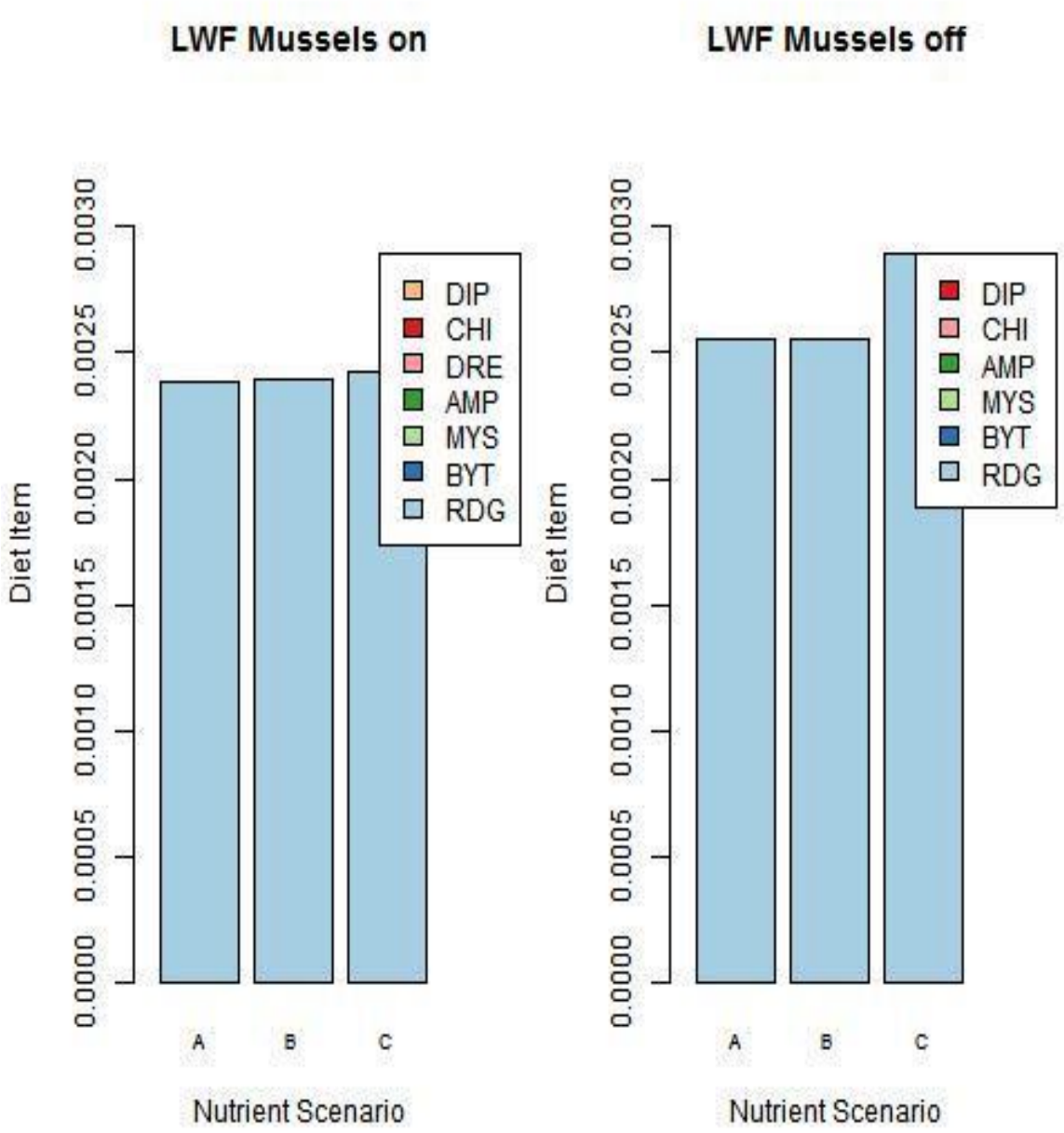

Figure 24. Lake Whitefish diet composition in numbers consumed s^{-1} averaged for the last 25 years of each 50 year run. A, B, and C are low, baseline, and high nutrient scenarios, respectively. Mussels present scenarios are displayed on the left. Mussels absent scenarios are displayed on the right. See Table 1 for species codes.

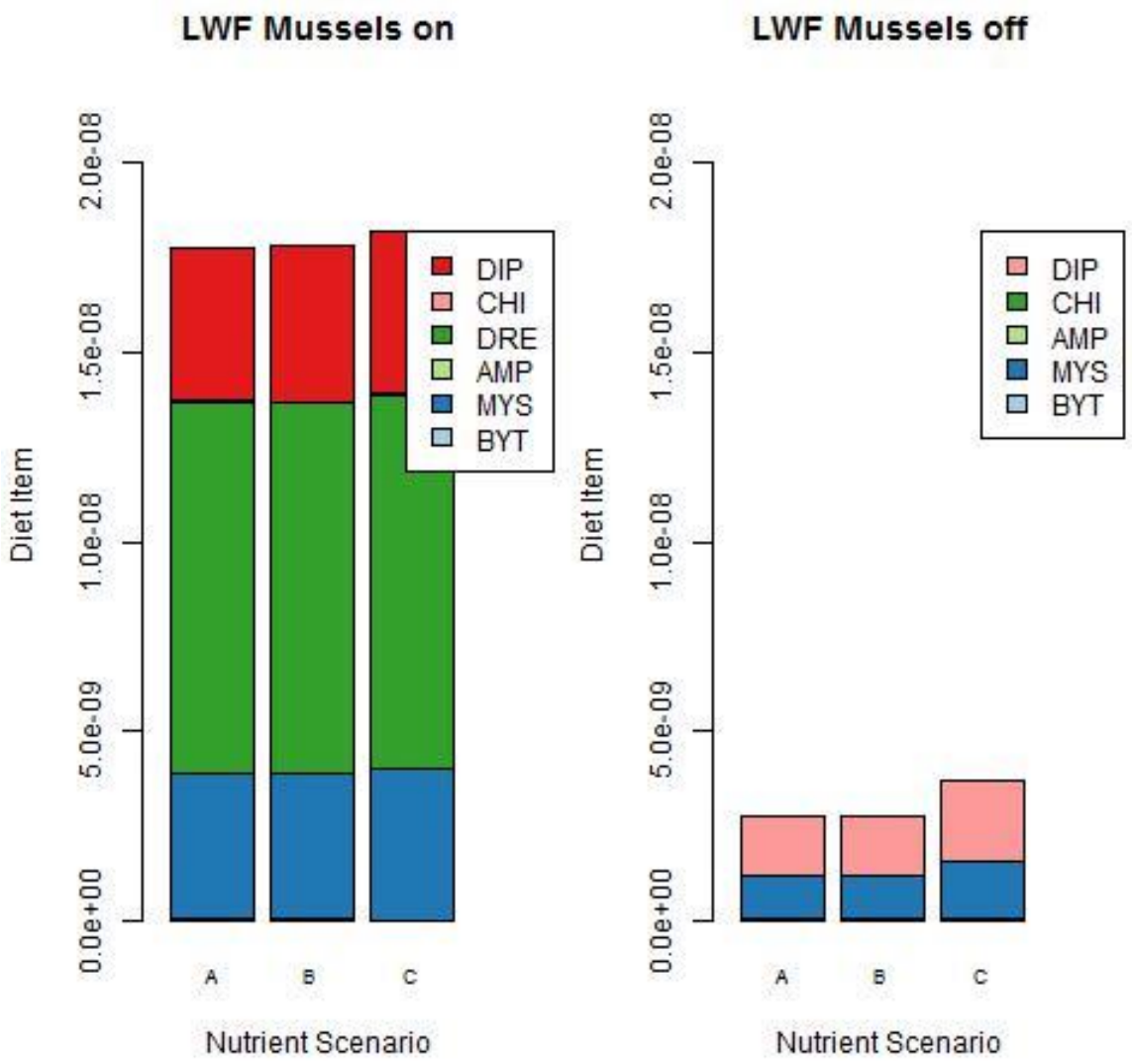

Figure 25. Lake Whitefish invertebrate diet composition in mg N/m3 s-1 averaged for the last 25 years of each 50 year run. A, B, and C are low, baseline, and high nutrient scenarios, respectively. Mussels present scenarios are displayed on the left. Mussels absent scenarios are displayed on the right. See Table 1 for species codes

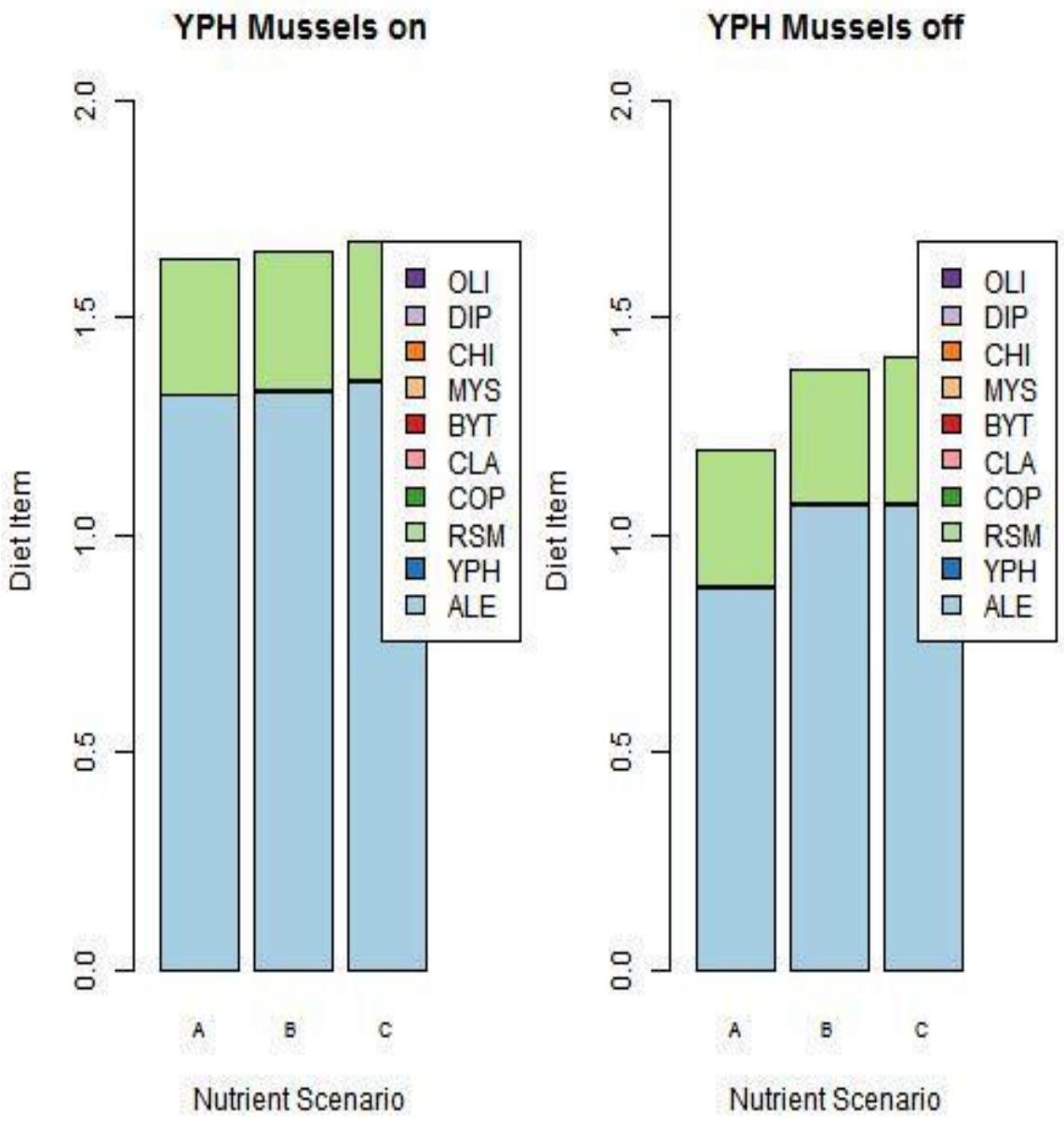

Figure 26 Yellow Perch diet composition in numbers consumed s^{-1} averaged for the last 25 years of each 50 year run. A, B, and C are low, baseline, and high nutrient scenarios, respectively. Mussels present scenarios are displayed on the left. Mussels absent scenarios are displayed on the right. See Table 1 for species codes.

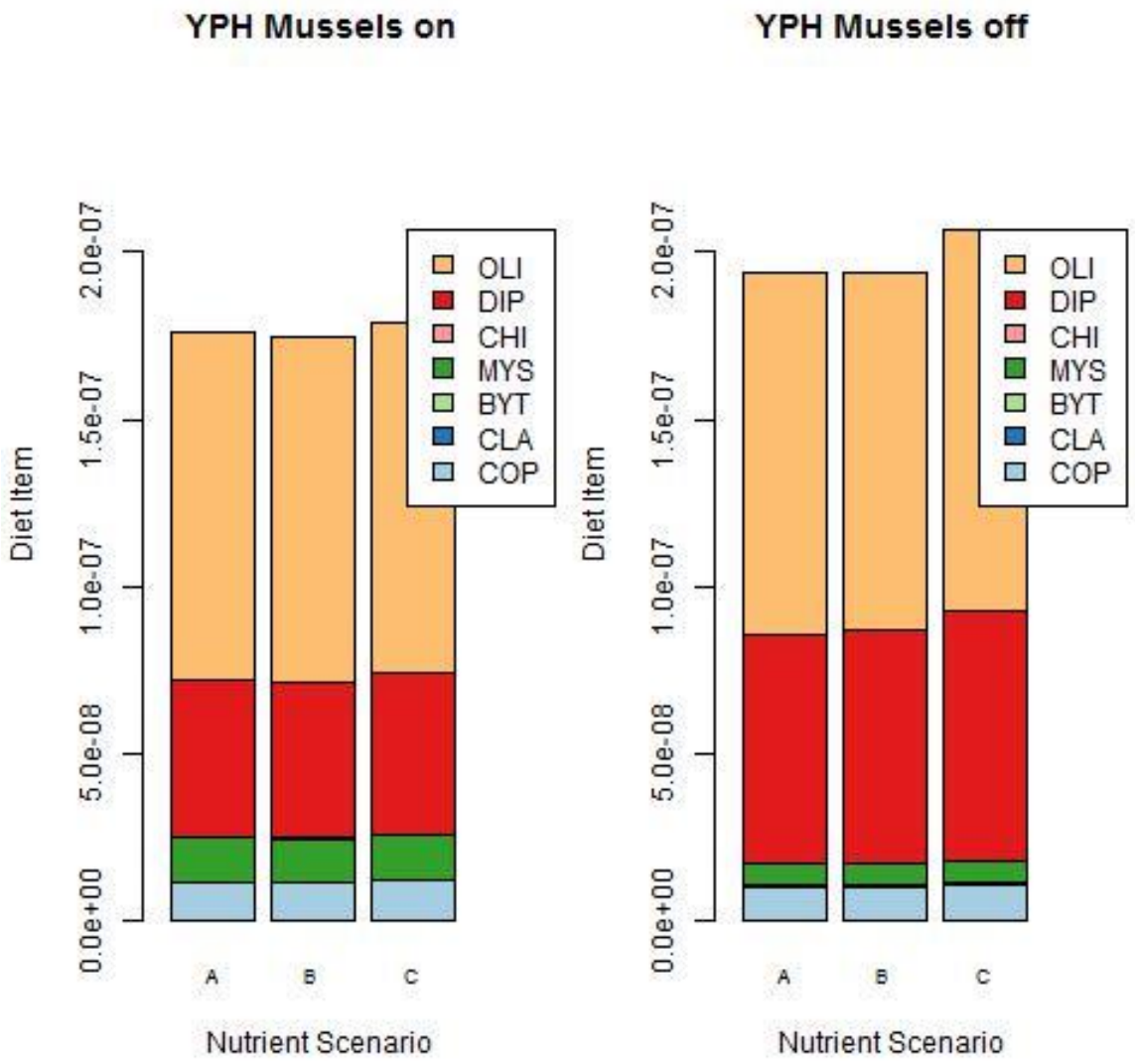

Figure 27. Yellow Perch invertebrate diet composition in mg N/m3 s^{-1} averaged for the last 25 years of each 50 year run. A, B, and C are low, baseline, and high nutrient scenarios, respectively. Mussels present scenarios are displayed on the left. Mussels absent scenarios are displayed on the right. See Table 1 for species codes.

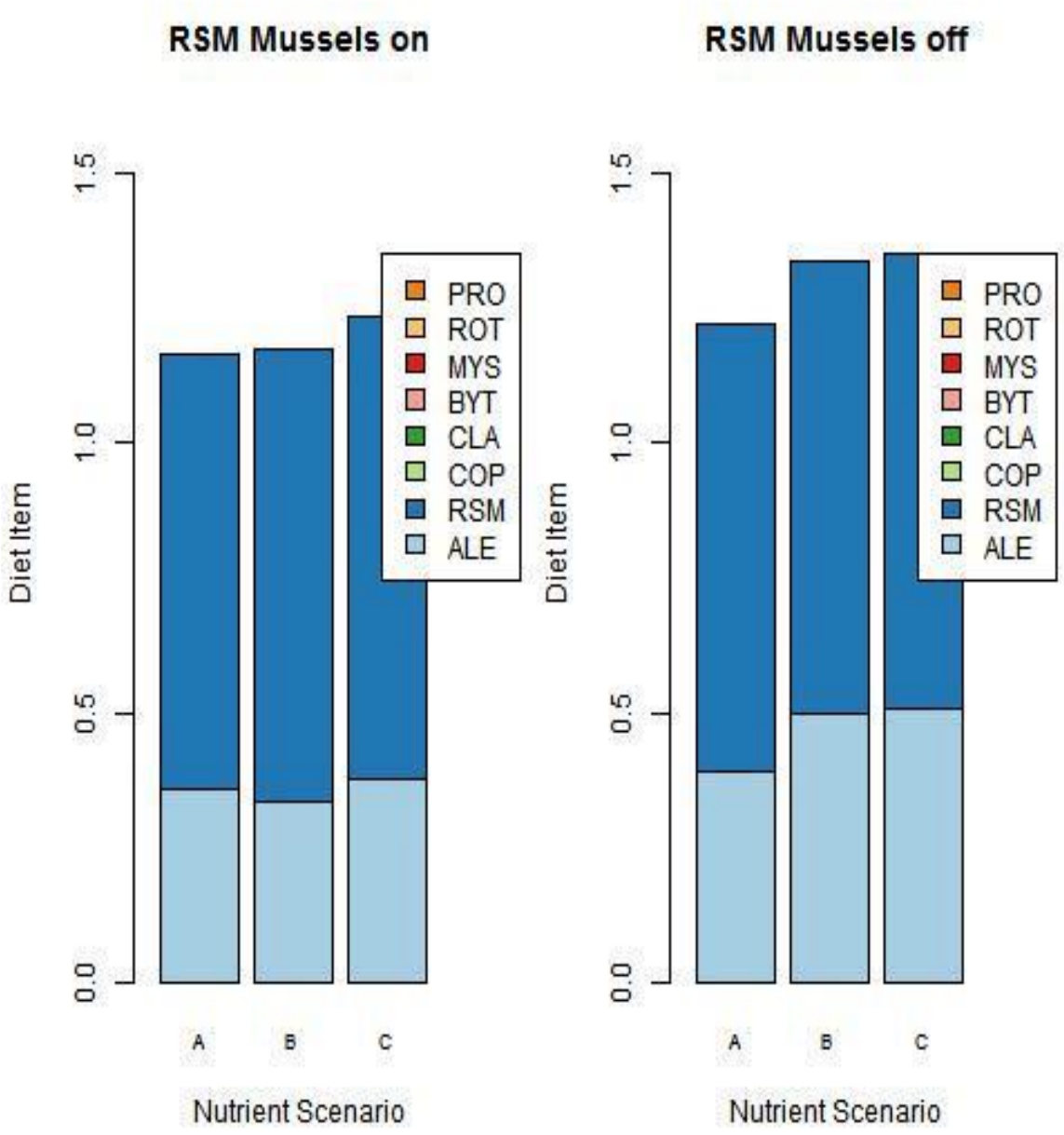

Figure 28. Rainbow Smelt diet composition in numbers consumed s^{-1} averaged for the last 25 years of each 50 year run. A, B, and C are low, baseline, and high nutrient scenarios, respectively. Mussels present scenarios are displayed on the left. Mussels absent scenarios are displayed on the right. See Table 1 for species codes.

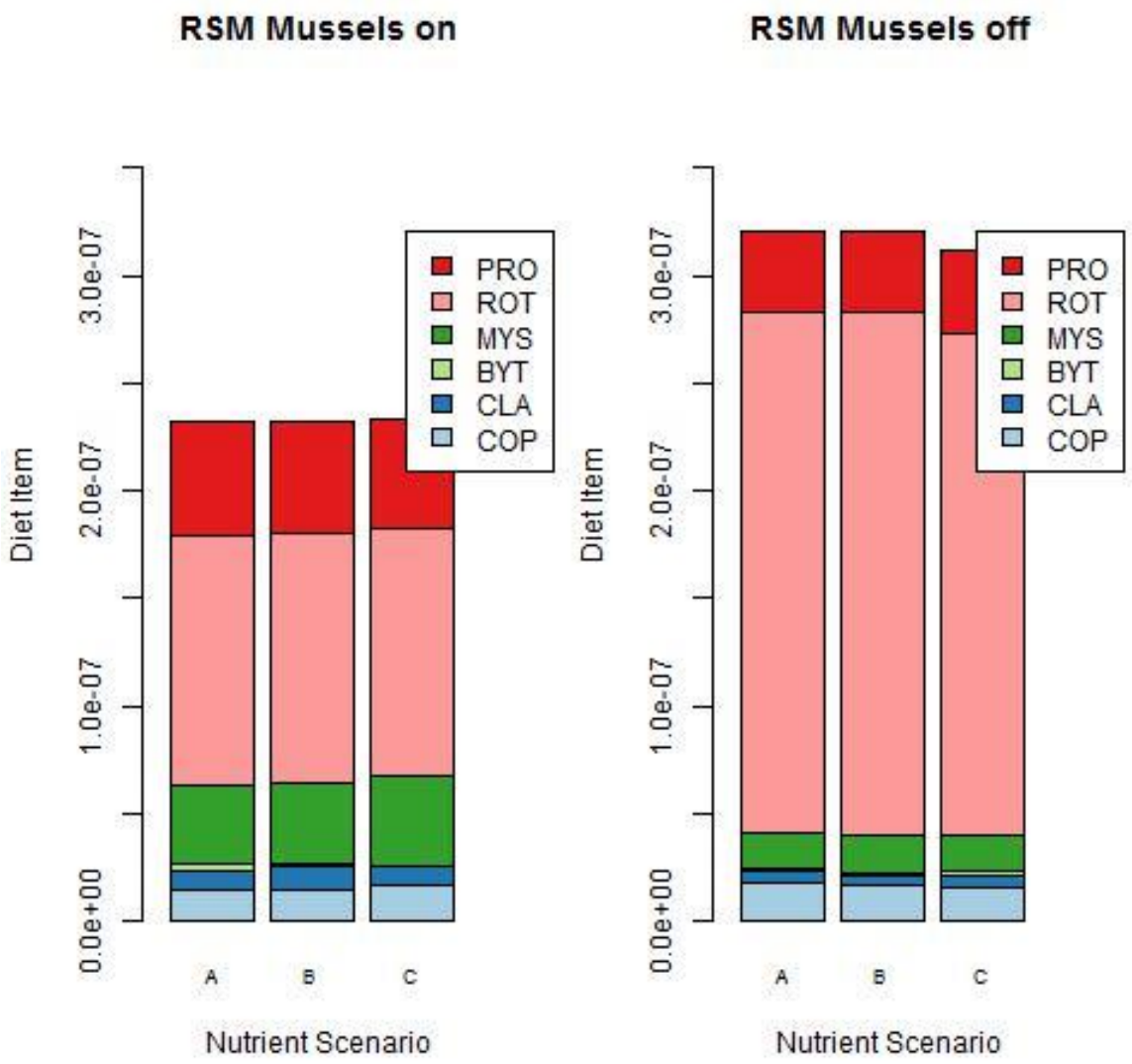

Figure 29. Rainbow Smelt invertebrate diet composition in mg N/m3 s^{-1} averaged for the last 25 years of each 50 year run. A, B, and C are low, baseline, and high nutrient scenarios, respectively. Mussels present scenarios are displayed on the left. Mussels absent scenarios are displayed on the right. See Table 1 for species codes.

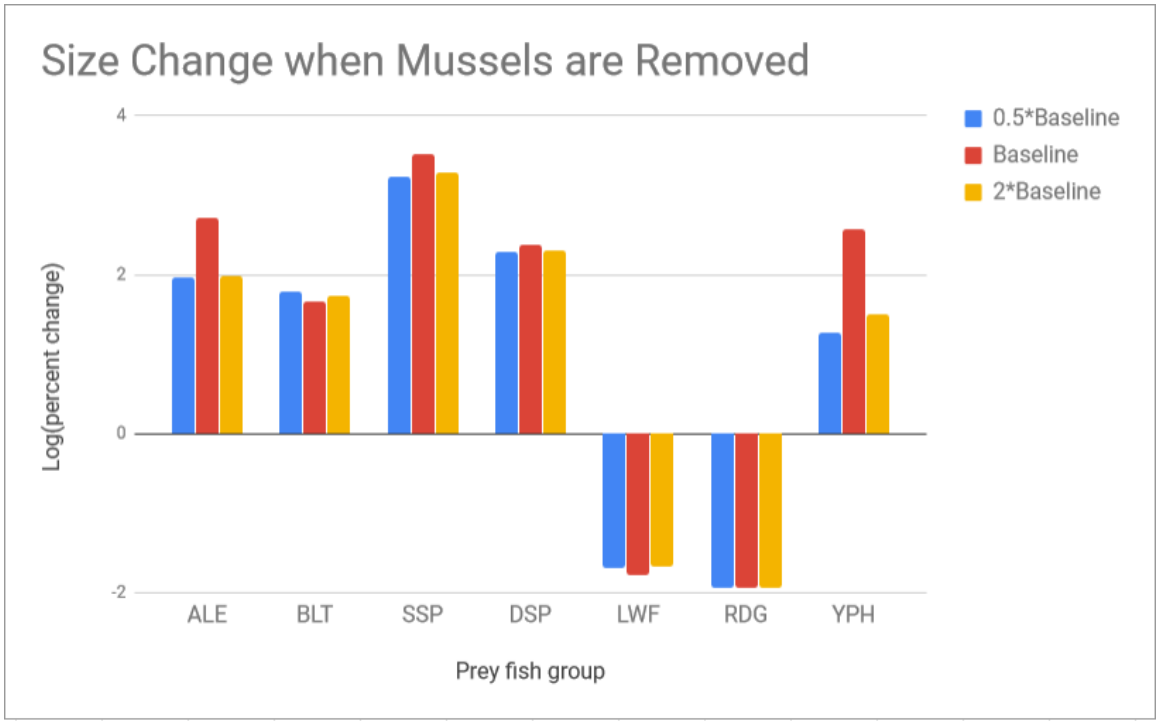

Figure 30. Log_{10}(Percent change) of individual prey fish size biomass between scenarios of mussels present/absent and variable nutrient loads. Individual prey fish biomass of each year class were extracted from LMAM at the last timestep of each run and averaged to find the average biomass of each prey fish group. Average prey fish biomass in each scenario was then used to calculate percent change resulting from removing mussels from the model when nutrient scenario was held constant. A value of 100 indicates a 100 percent increase in average biomass across all year classes under a mussels absent scenario. See Table 1 for species codes.

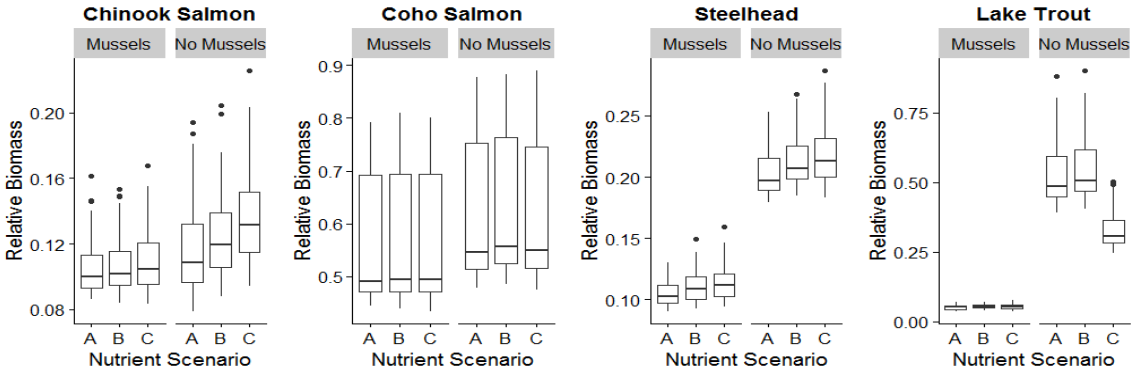

Figure 31. LMAM predictions of piscivore fish biomass under scenarios of dreissena mussel presence/absence and varying nutrient loading scenarios. Refer to Figure 3 for scenario descriptions.

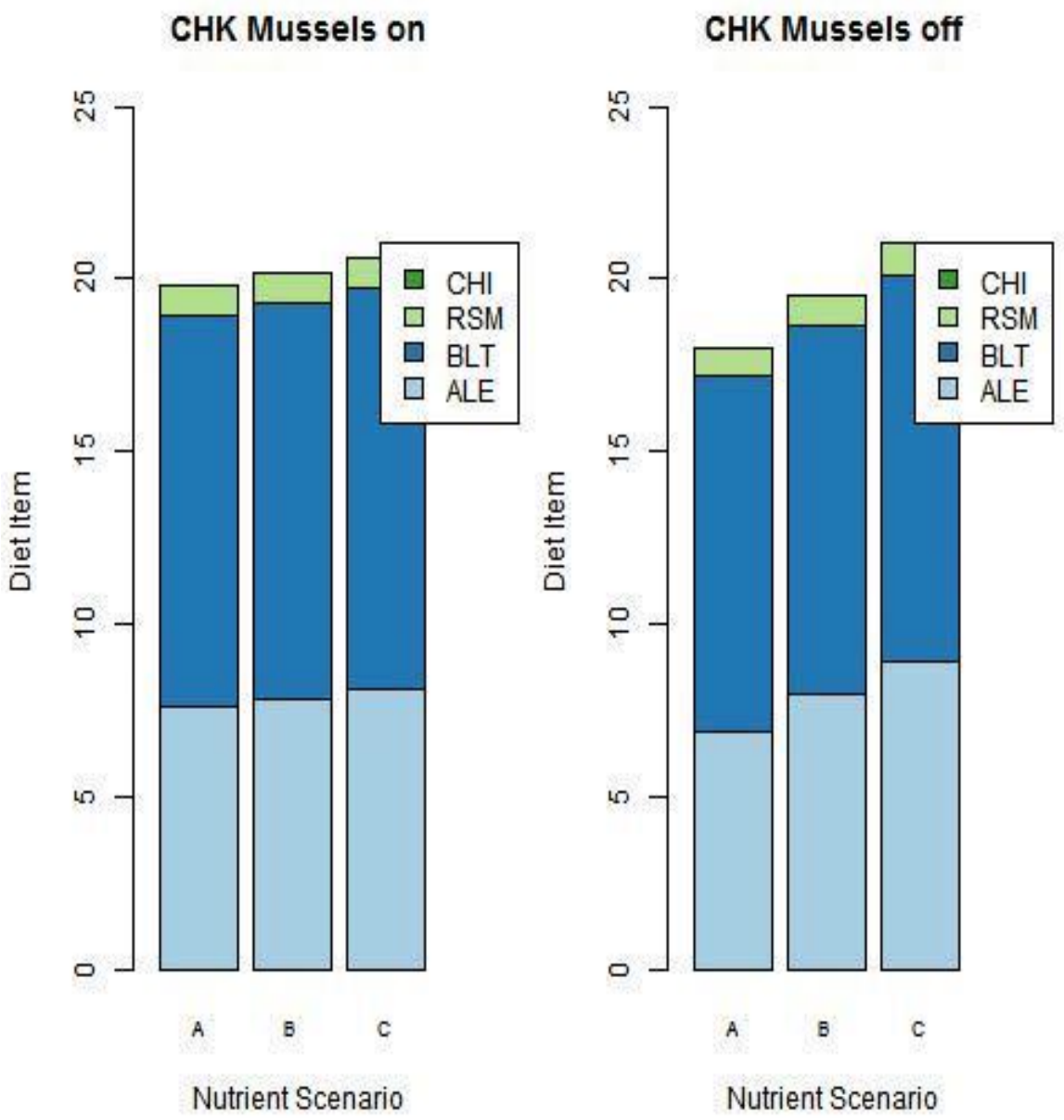

Figure 32. Chinook Salmon diet composition in numbers consumed s^{-1} averaged for the last 25 years of each 50 year run. A, B, and C are low, baseline, and high nutrient scenarios, respectively. Mussels present scenarios are displayed on the left. Mussels absent scenarios are displayed on the right. See Table 1 for species codes.

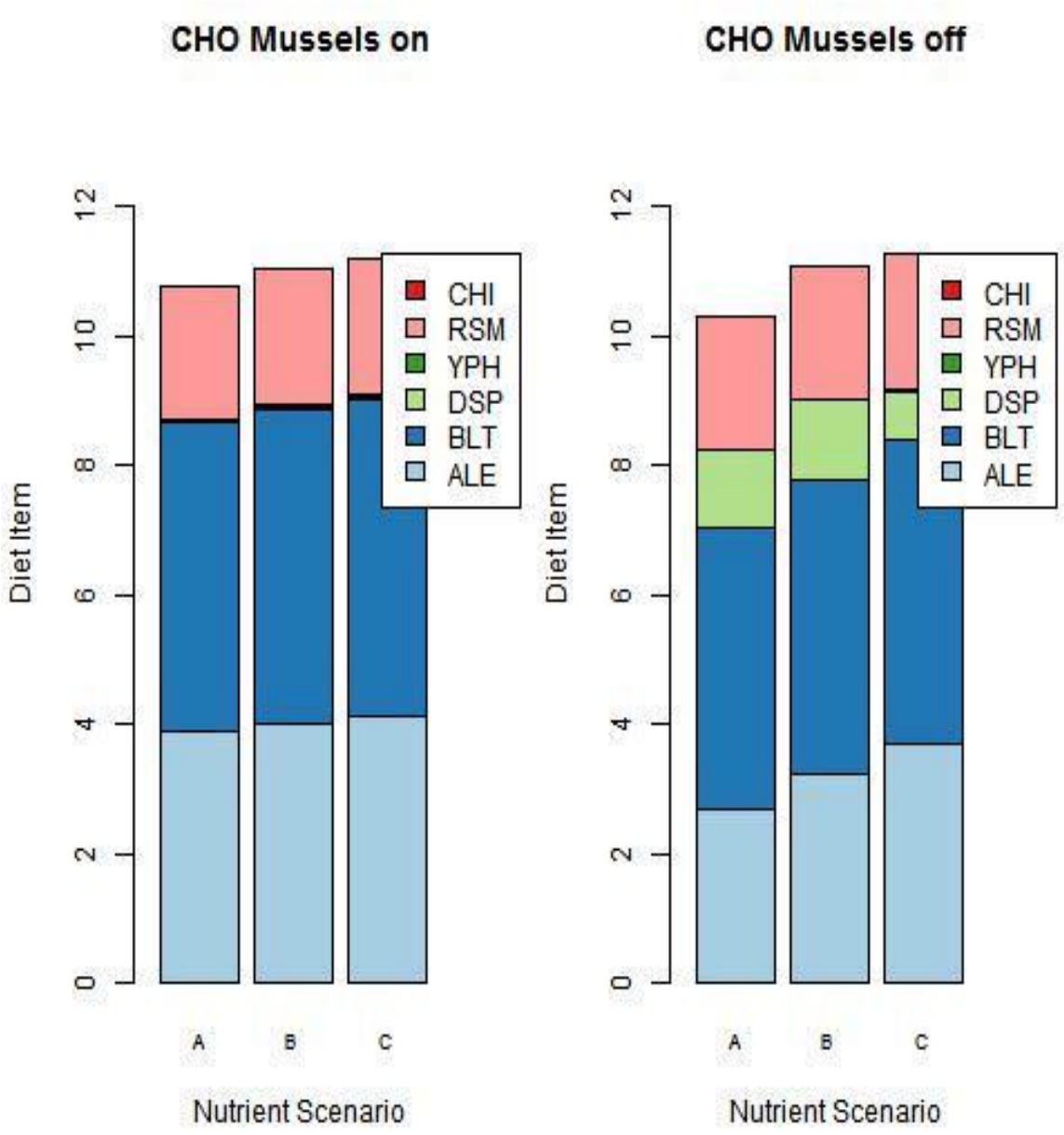

Figure 33. Coho Salmon diet composition in numbers consumed s^{-1} averaged for the last 25 years of each 50 year run. A, B, and C are low, baseline, and high nutrient scenarios, respectively. Mussels present scenarios are displayed on the left. Mussels absent scenarios are displayed on the right. See Table 1 for species codes.

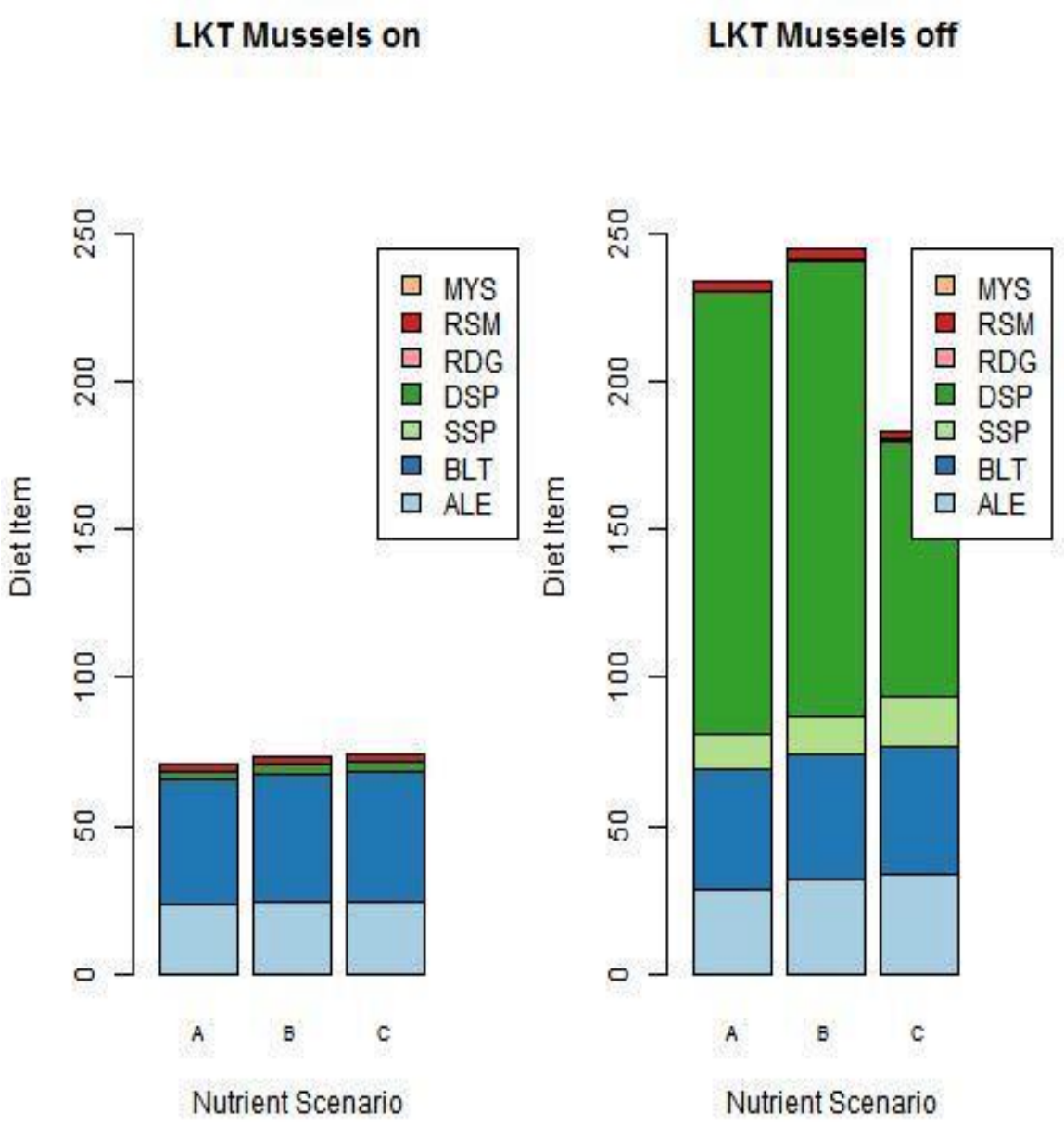

Figure 34. Lake Trout diet composition in numbers consumed s^{-1} averaged for the last 25 years of each 50 year run. A, B, and C are low, baseline, and high nutrient scenarios, respectively. Mussels present scenarios are displayed on the left. Mussels absent scenarios are displayed on the right. See Table 1 for species codes.

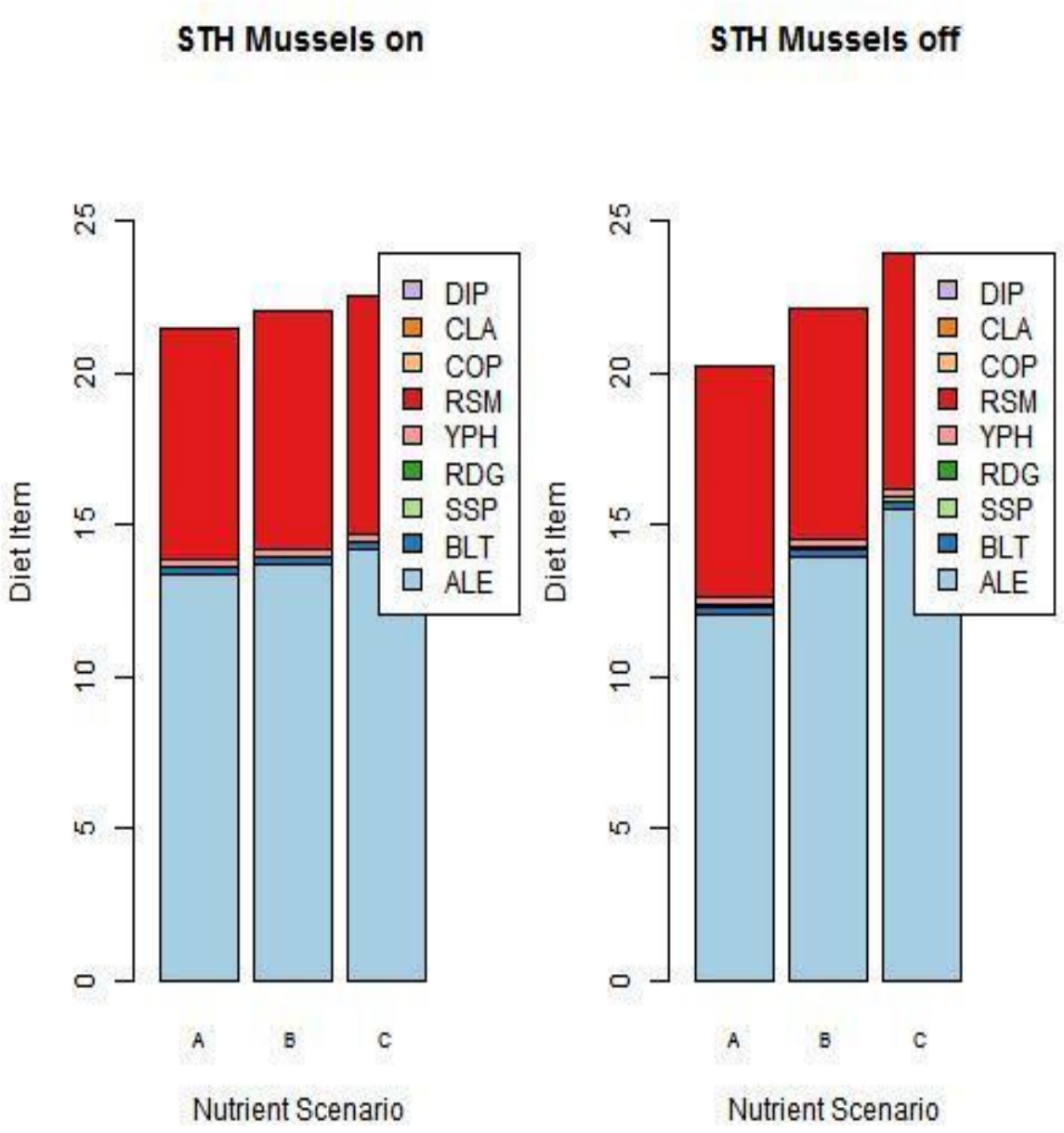

Figure 35. Steelhead diet composition in numbers consumed s^{-1} averaged for the last 25 years of each 50 year run. A, B, and C are low, baseline, and high nutrient scenarios, respectively. Mussels present scenarios are displayed on the left. Mussels absent scenarios are displayed on the right. See Table 1 for species codes.

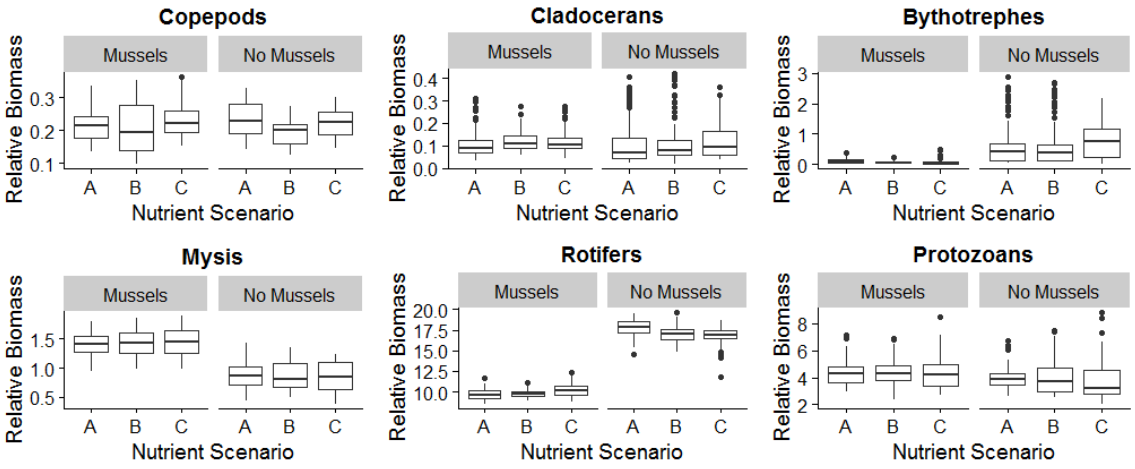

Figure 36. LMAM predictions of pelagic zooplankton biomass under scenarios of dreissena mussel presence/absence and varying nutrient loading scenarios. Refer to Figure 3 for scenario descriptions.

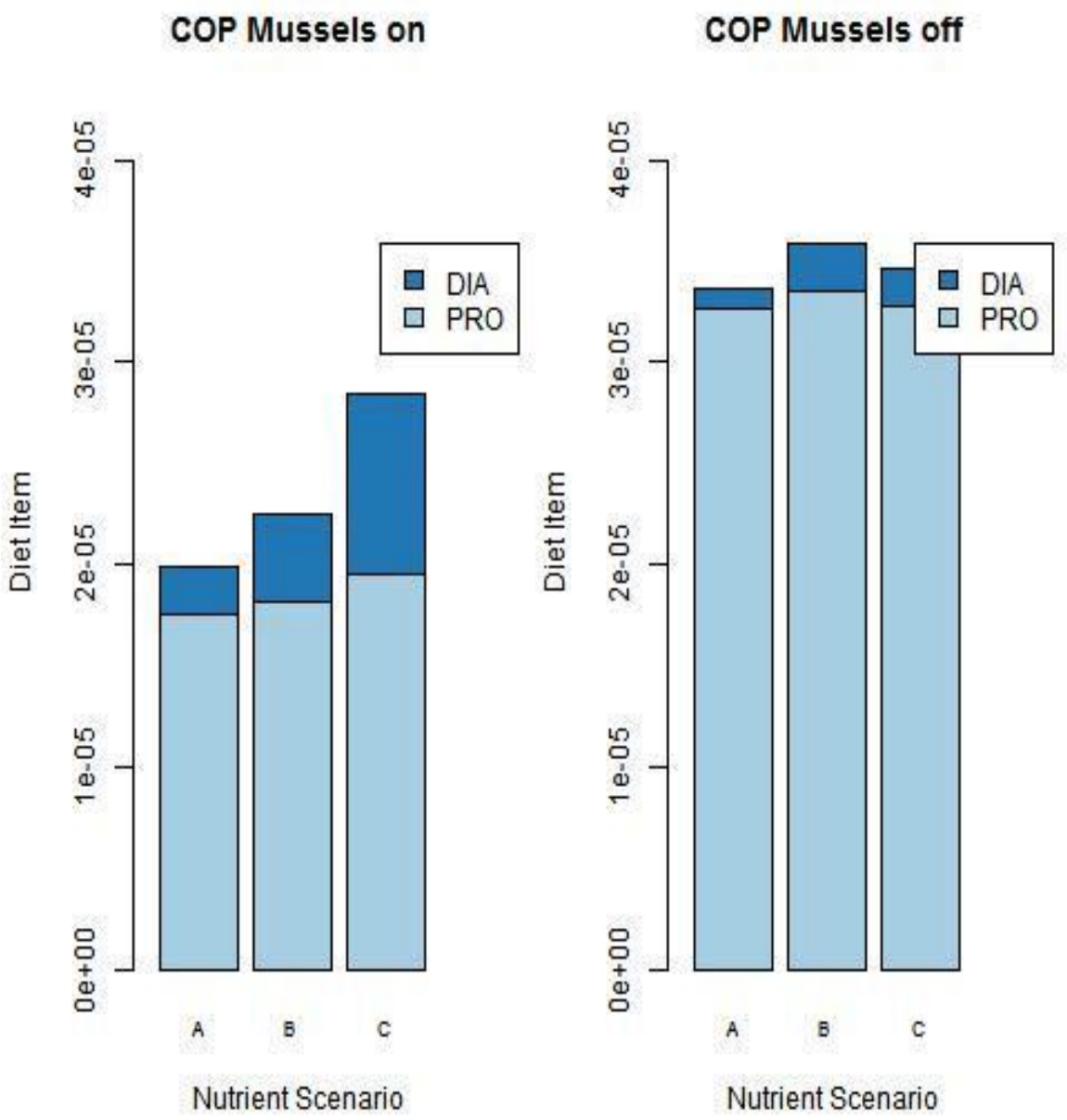

Figure 37. Copepod diet composition in mg N/m^3 s^{-1} averaged for the last 25 years of each 50 year run. A, B, and C are low, baseline, and high nutrient scenarios, respectively. Mussels present scenarios are displayed on the left. Mussels absent scenarios are displayed on the right. See Table 1 for species codes.

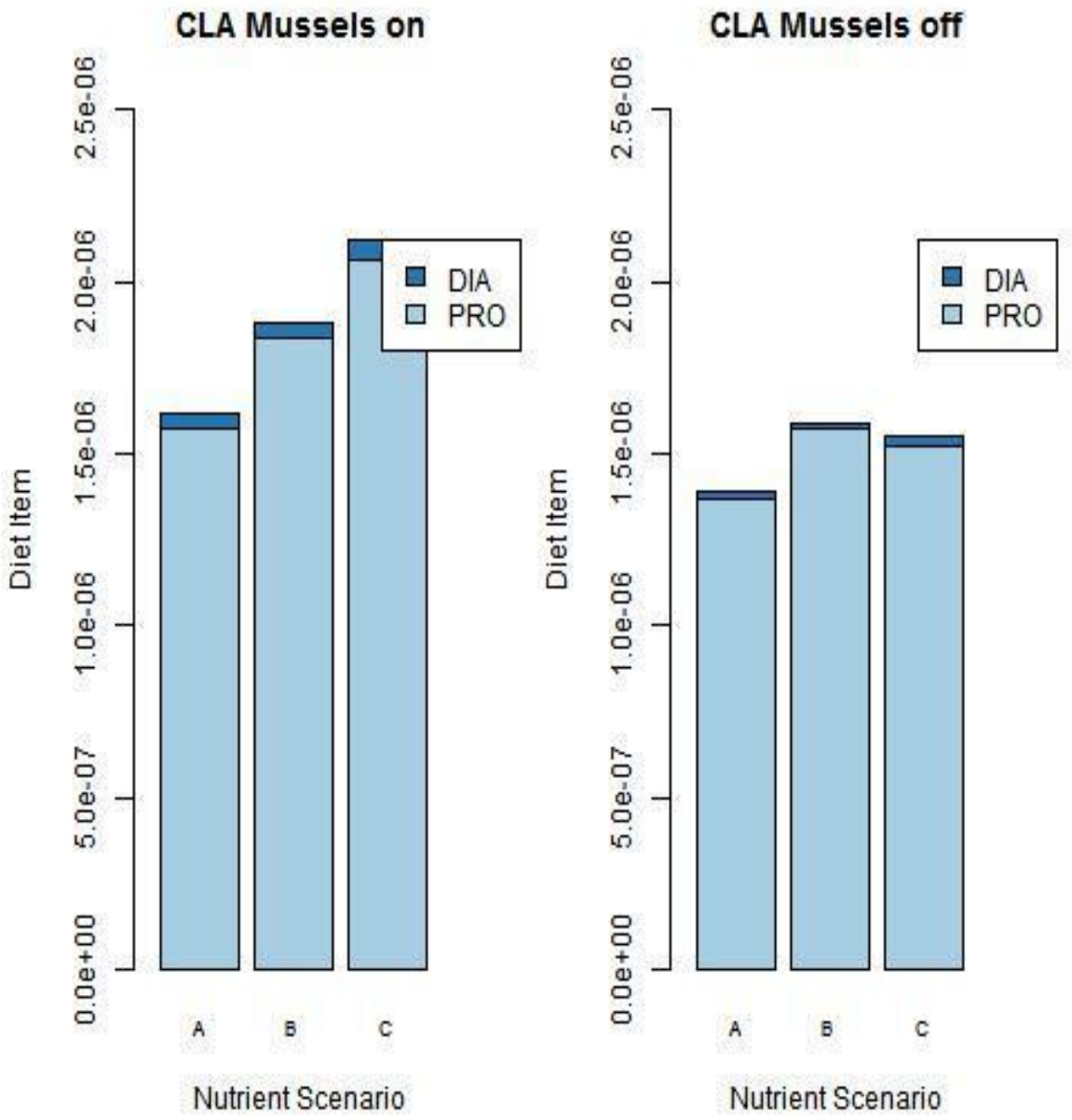

Figure 38. Cladoceran diet composition in mg N/m^3 s^{-1} averaged for the last 25 years of each 50 year run. A, B, and C are low, baseline, and high nutrient scenarios, respectively. Mussels present scenarios are displayed on the left. Mussels absent scenarios are displayed on the right. See Table 1 for species codes.

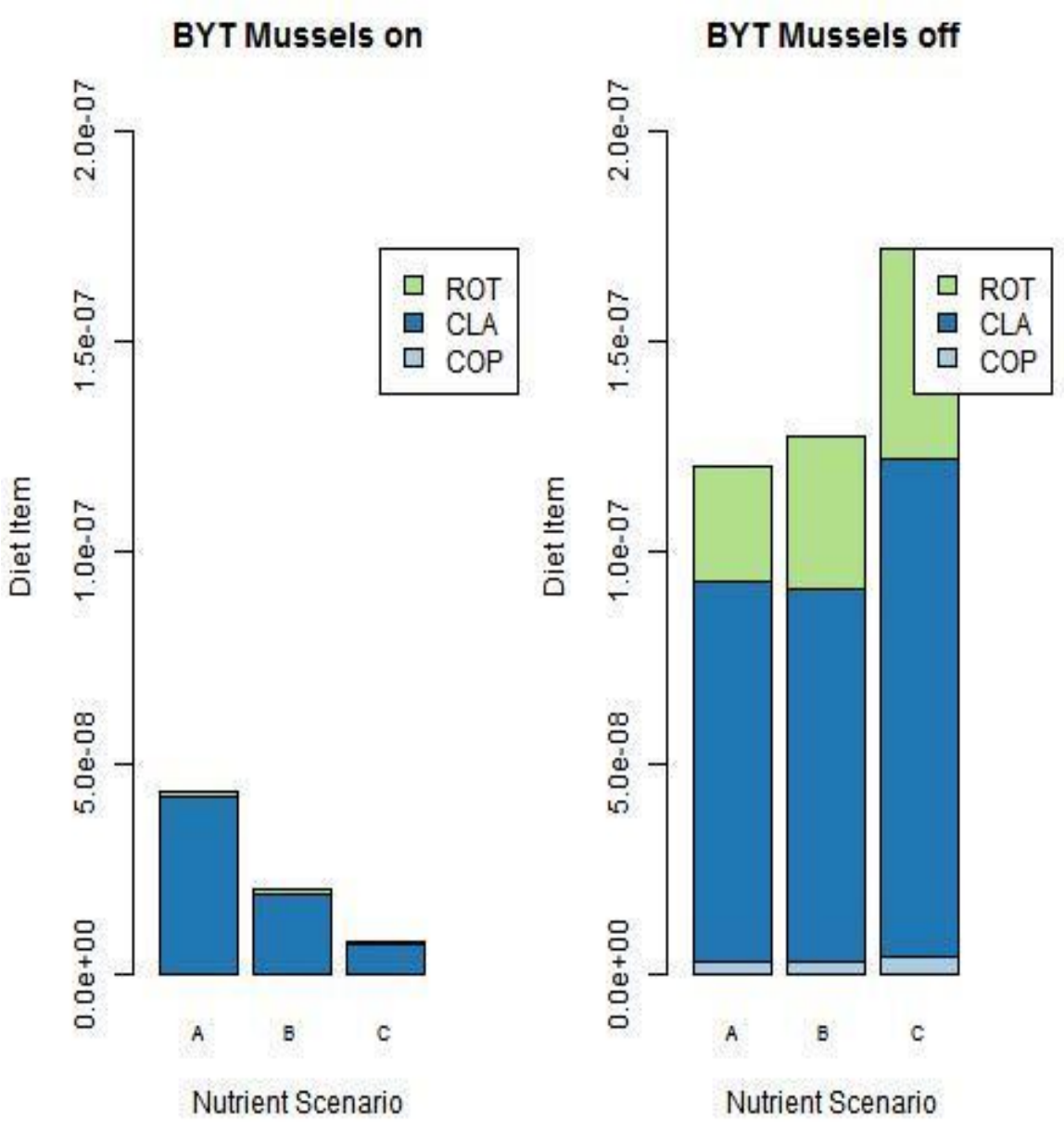

Figure 39. Bythotrephes diet composition in mg N/m^3 s^{-1} averaged for the last 25 years of each 50 year run. A, B, and C are low, baseline, and high nutrient scenarios, respectively. Mussels present scenarios are displayed on the left. Mussels absent scenarios are displayed on the right. See Table 1 for species codes.

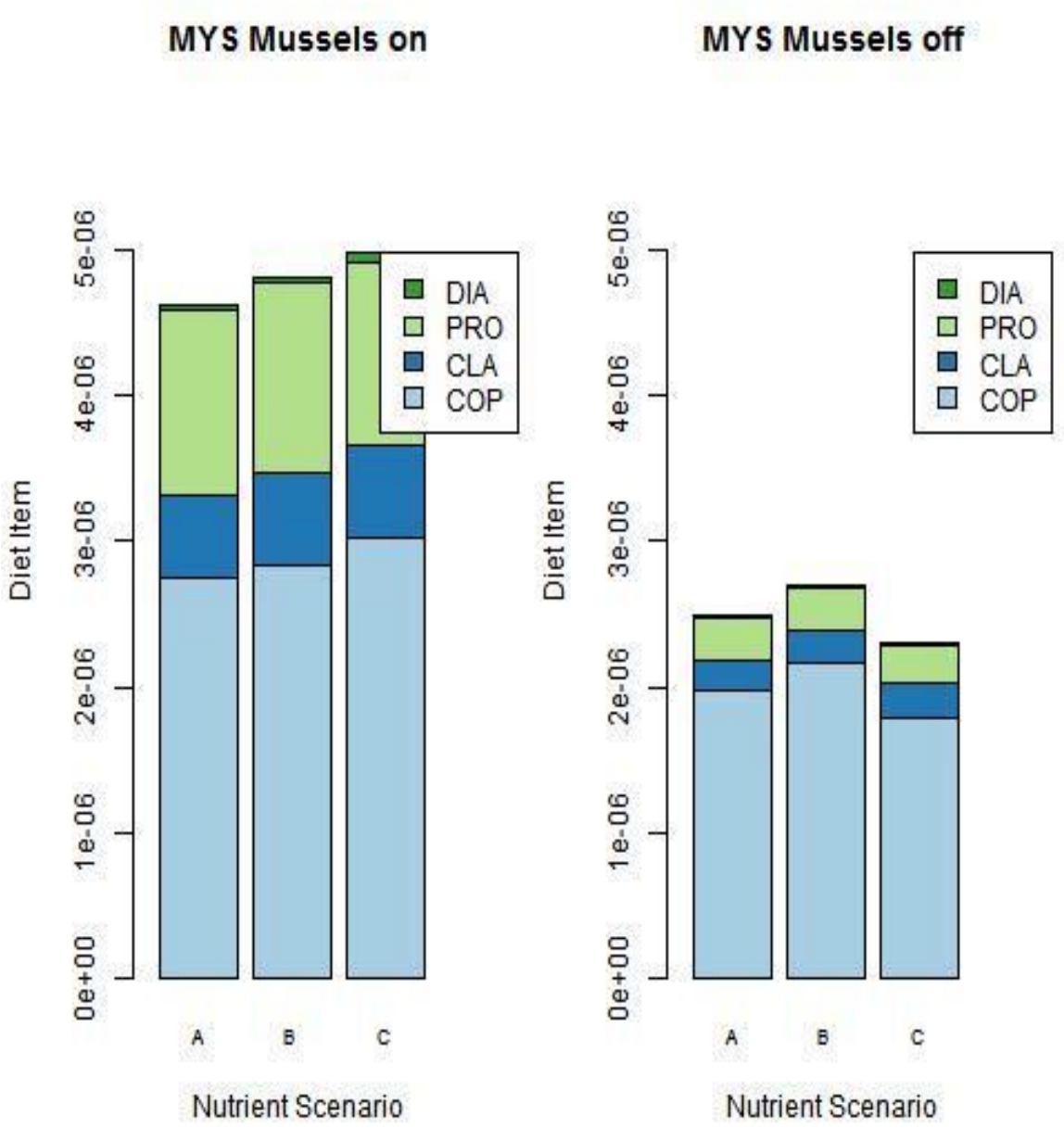

Figure 40. Mysis diet composition in mg N/m^3 s^{-1} averaged for the last 25 years of each 50 year run. A, B, and C are low, baseline, and high nutrient scenarios, respectively. Mussels present scenarios are displayed on the left. Mussels absent scenarios are displayed on the right. See Table 1 for species codes.

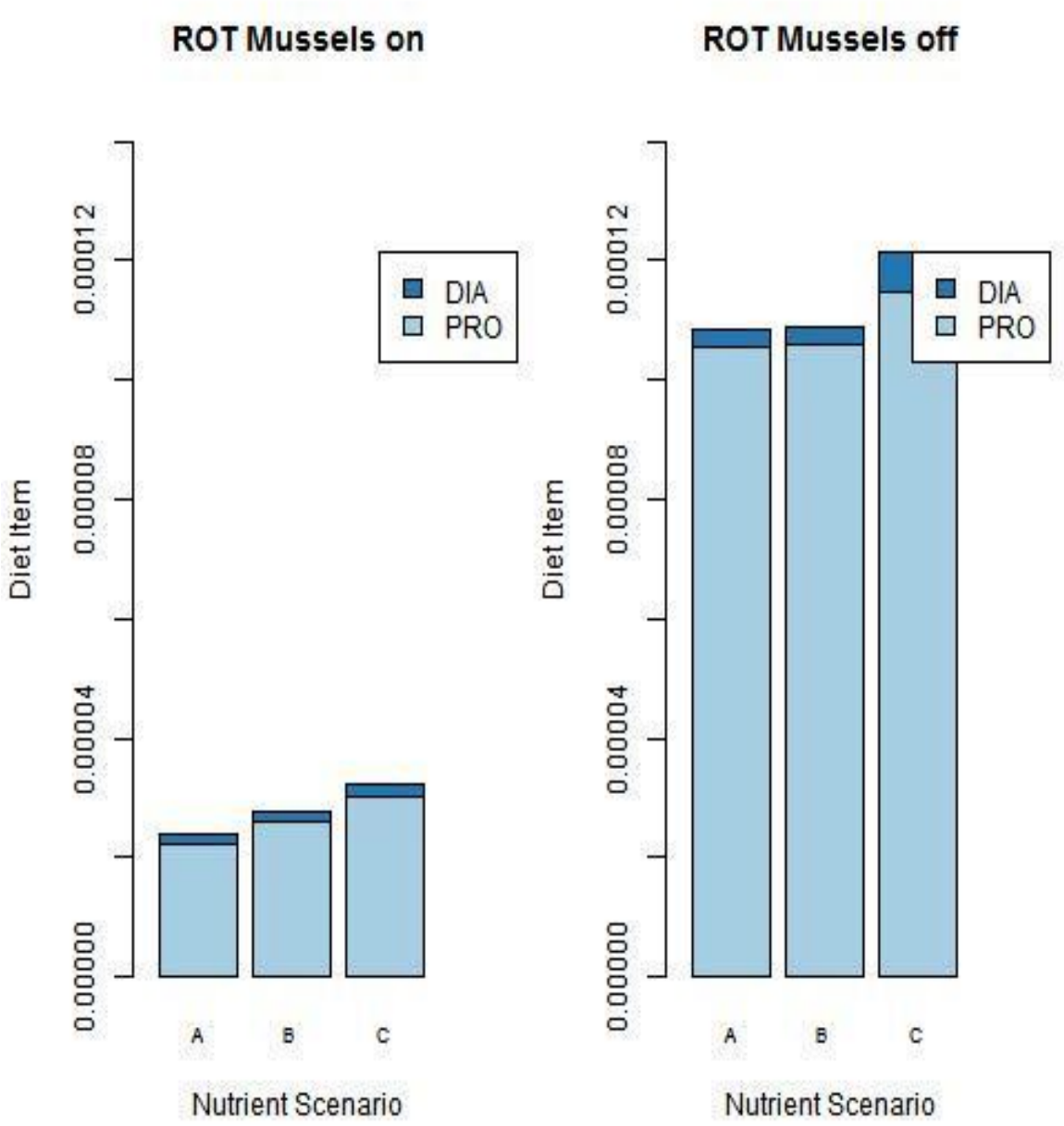

Figure 41. Rotifer diet composition in mg N/m^3 s^{-1} averaged for the last 25 years of each 50 year run. A, B, and C are low, baseline, and high nutrient scenarios, respectively. Mussels present scenarios are displayed on the left. Mussels absent scenarios are displayed on the right. See Table 1 for species codes.

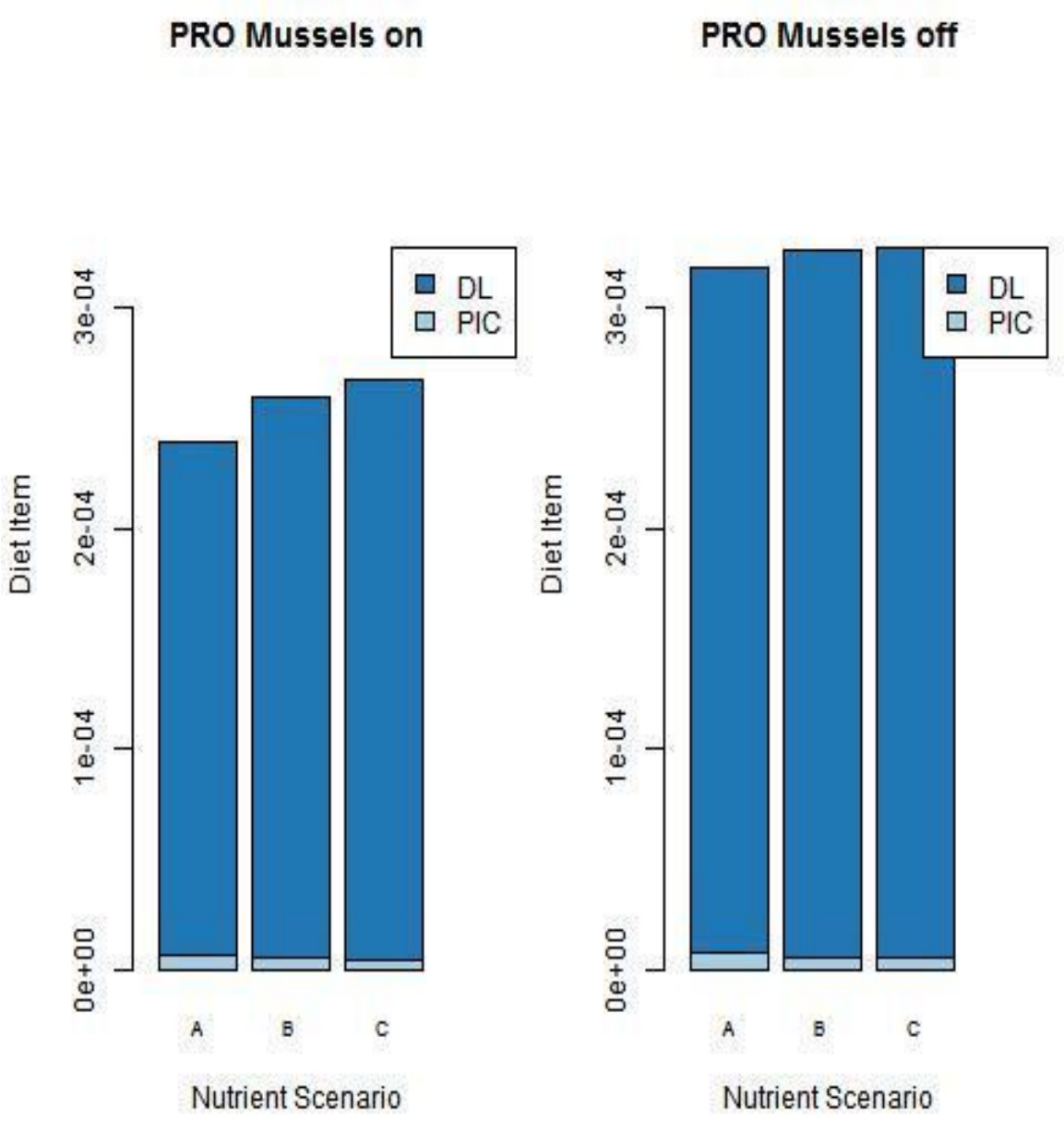

Figure 42. Protozoan diet composition in mg N/m^3 s^{-1} averaged for the last 25 years of each 50 year run. A, B, and C are low, baseline, and high nutrient scenarios, respectively. Mussels present scenarios are displayed on the left. Mussels absent scenarios are displayed on the right. See Table 1 for species codes.

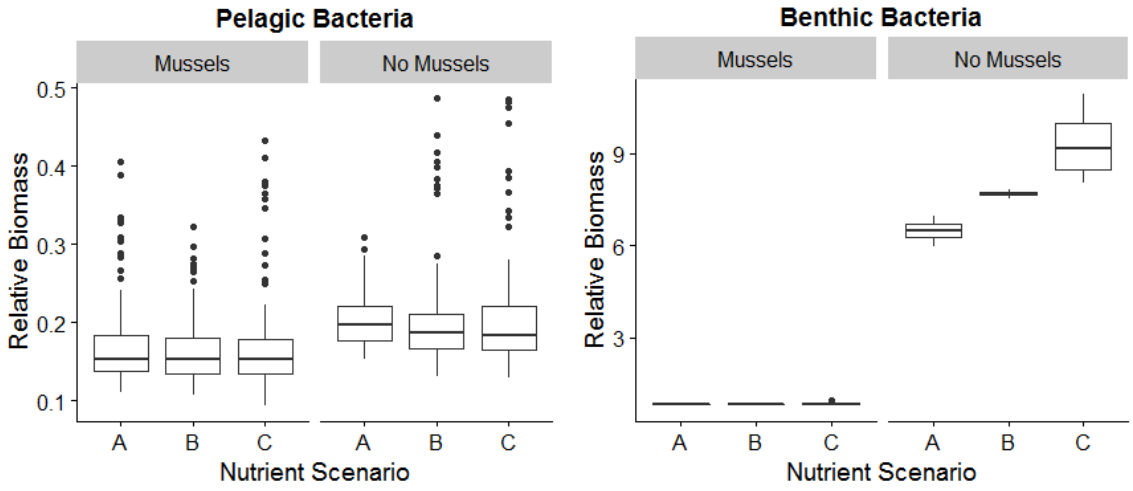

Figure 43. LMAM predictions of pelagic and benthic bacteria biomass under scenarios of dreissena mussel presence/absence and varying nutrient loading scenarios. Refer to Figure 3 for scenario descriptions.

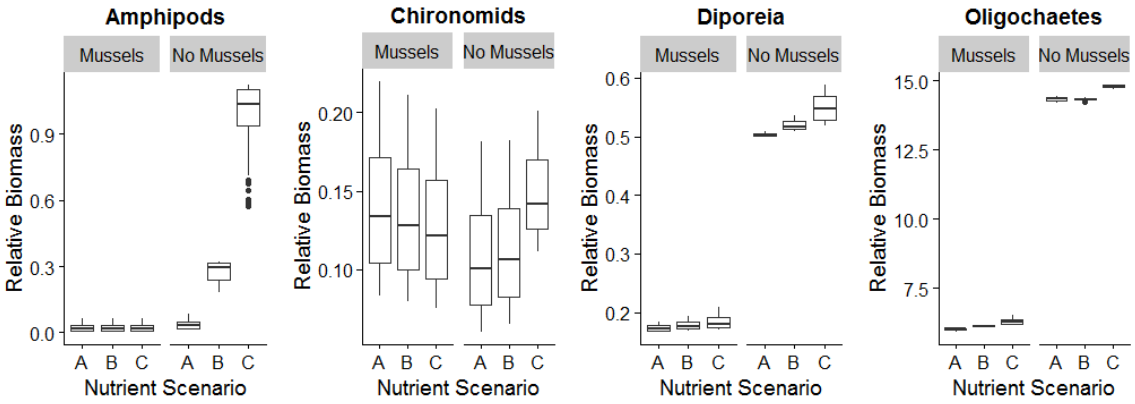

Figure 44. LMAM predictions of benthos biomass under scenarios of dreissena mussel presence/absence and varying nutrient loading scenarios. Refer to Figure 3 for scenario descriptions.

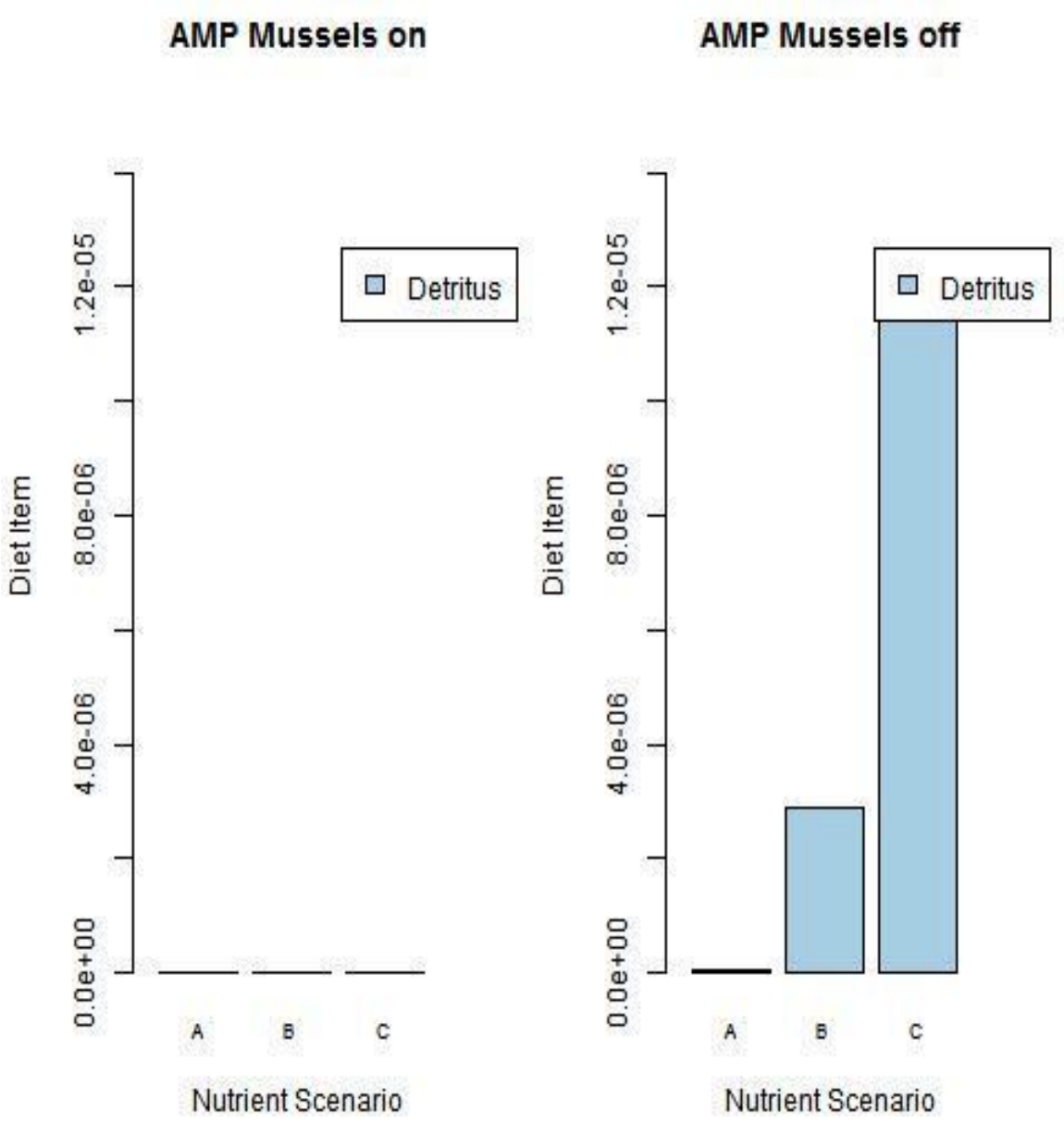

Figure 45. Amphipod diet composition in mg N/m^3 s^{-1} averaged for the last 25 years of each 50 year run. A, B, and C are low, baseline, and high nutrient scenarios, respectively. Mussels present scenarios are displayed on the left. Mussels absent scenarios are displayed on the right. See Table 1 for species codes.

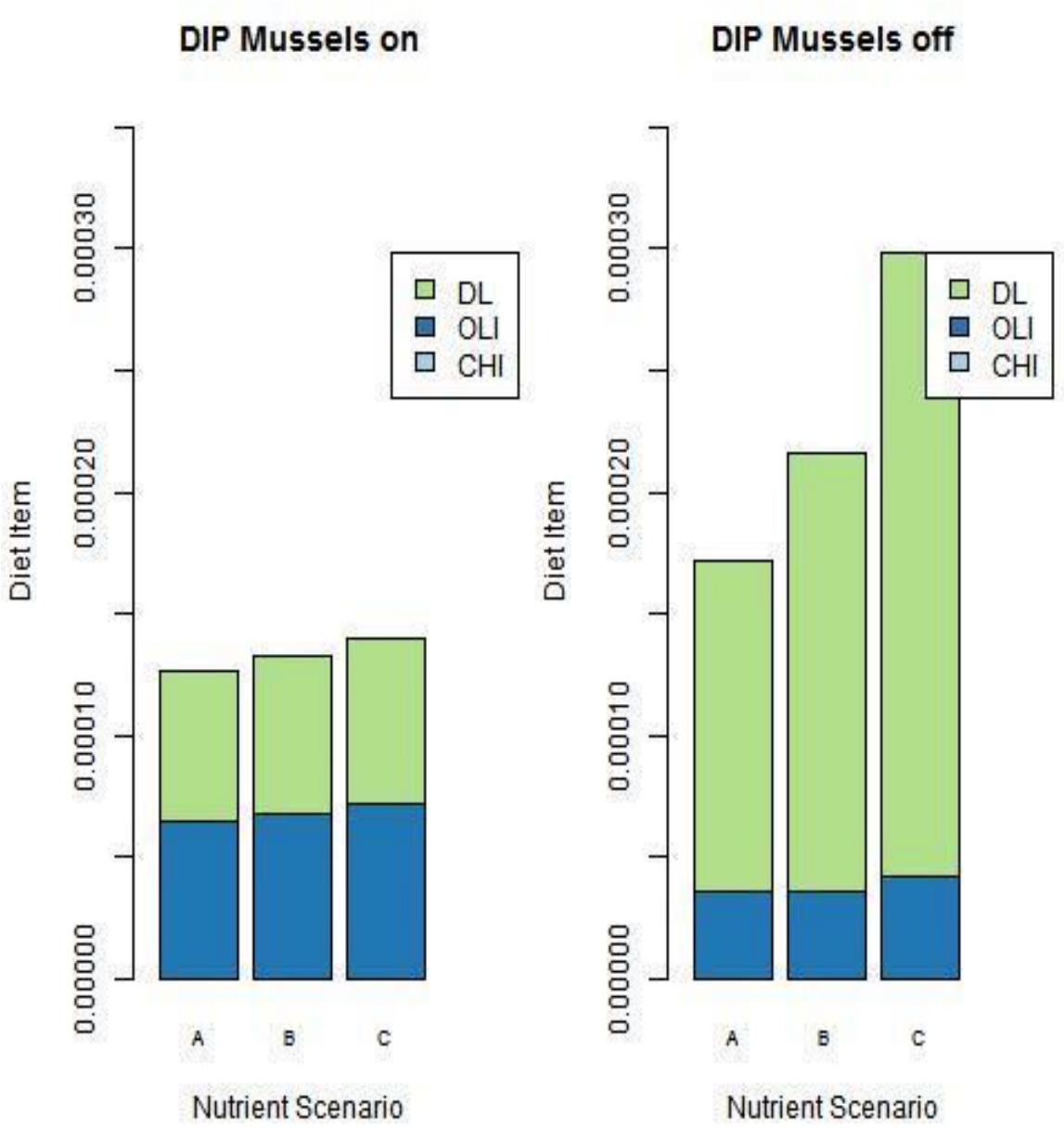

Figure 46. Diporeia diet composition in mg N/m^3 s^{-1} averaged for the last 25 years of each 50 year run. A, B, and C are low, baseline, and high nutrient scenarios, respectively. Mussels present scenarios are displayed on the left. Mussels absent scenarios are displayed on the right. See Table 1 for species codes.

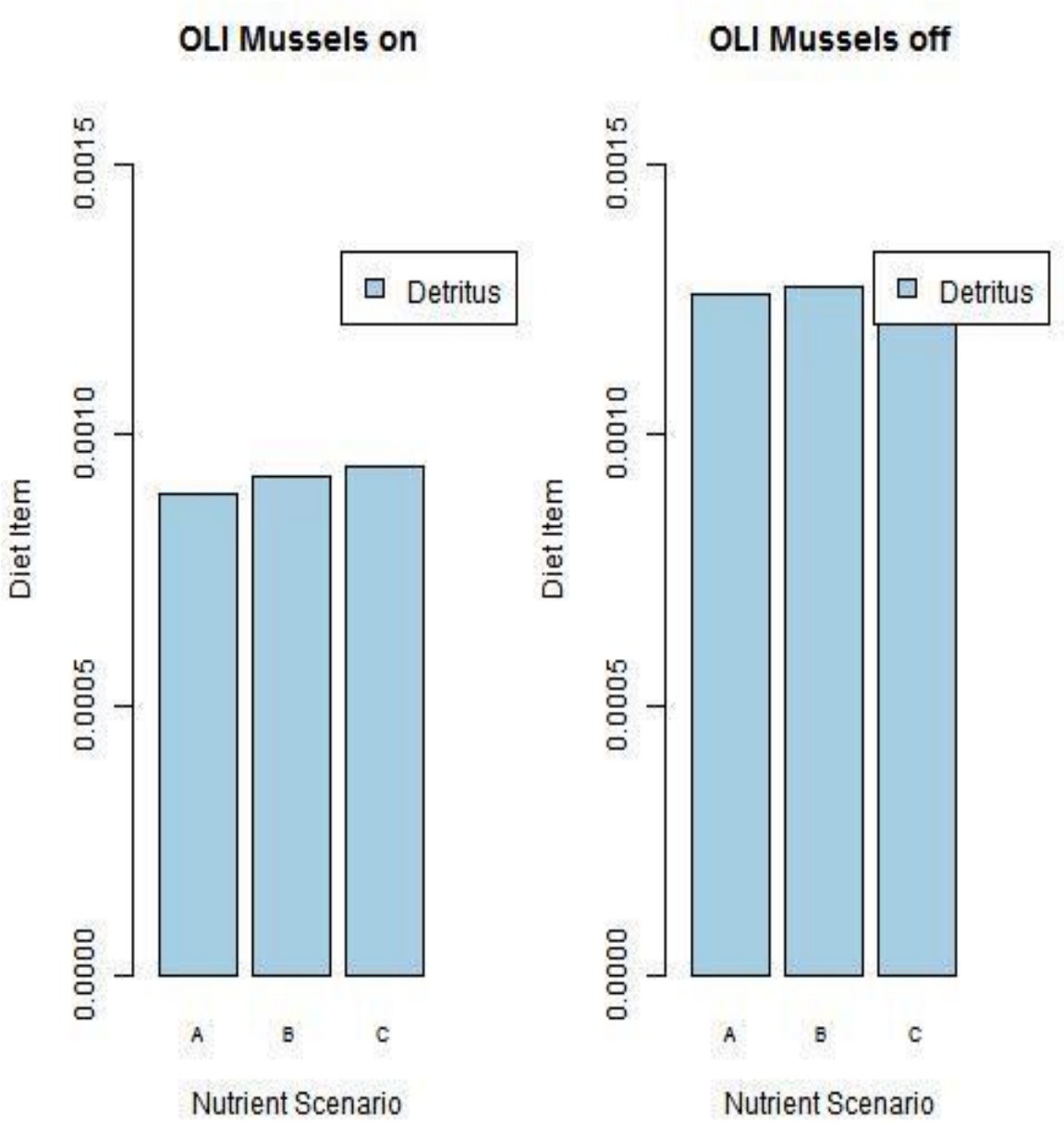

Figure 47. Oligochaete diet composition in mg N/m^3 s^{-1} averaged for the last 25 years of each 50 year run. A, B, and C are low, baseline, and high nutrient scenarios, respectively. Mussels present scenarios are displayed on the left. Mussels absent scenarios are displayed on the right. See Table 1 for species codes.

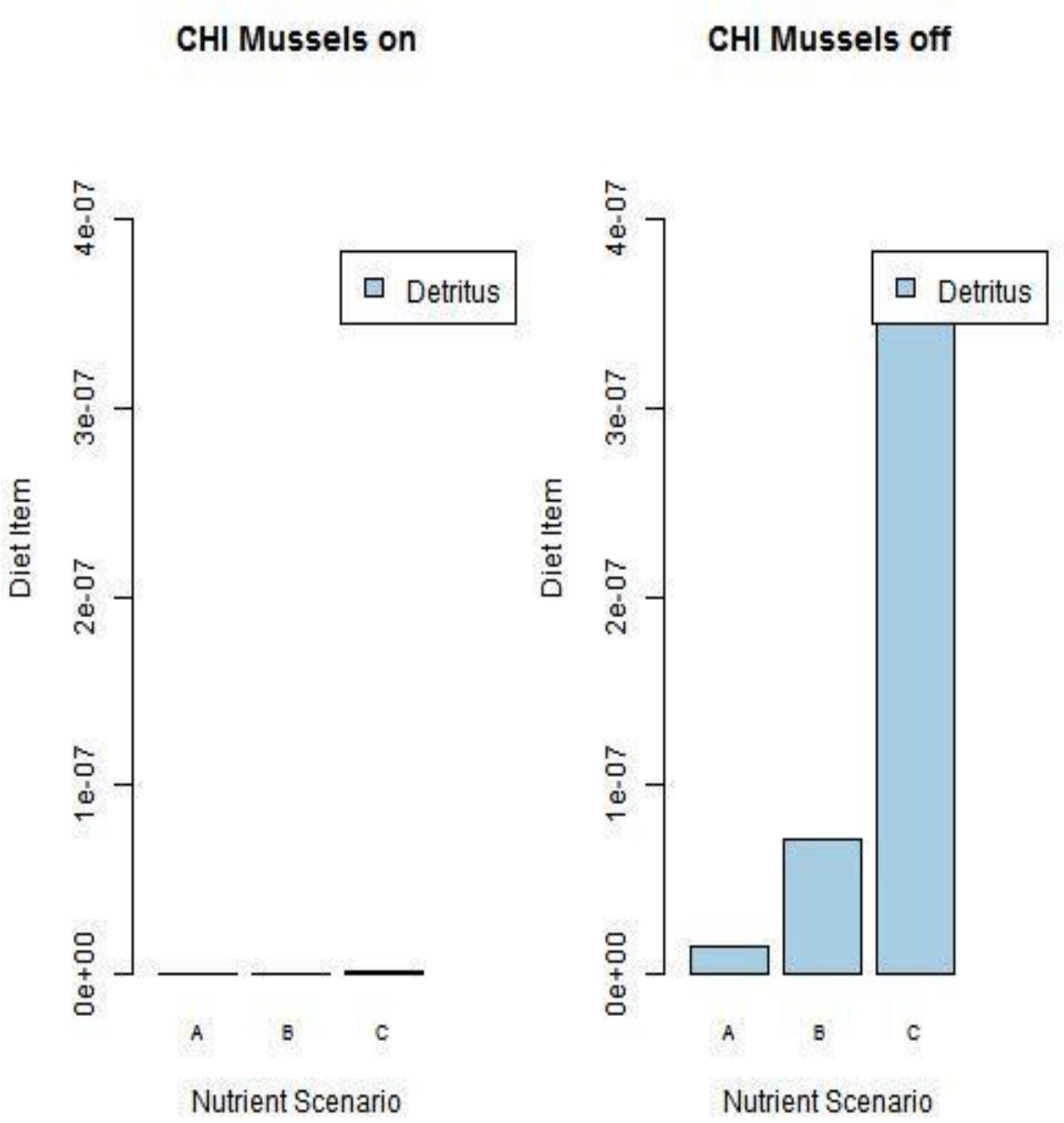

Figure 48. Chironomid diet composition in mg N/m^3 s^{-1} averaged for the last 25 years of each 50 year run. A, B, and C are low, baseline, and high nutrient scenarios, respectively. Mussels present scenarios are displayed on the left. Mussels absent scenarios are displayed on the right. See Table 1 for species codes.

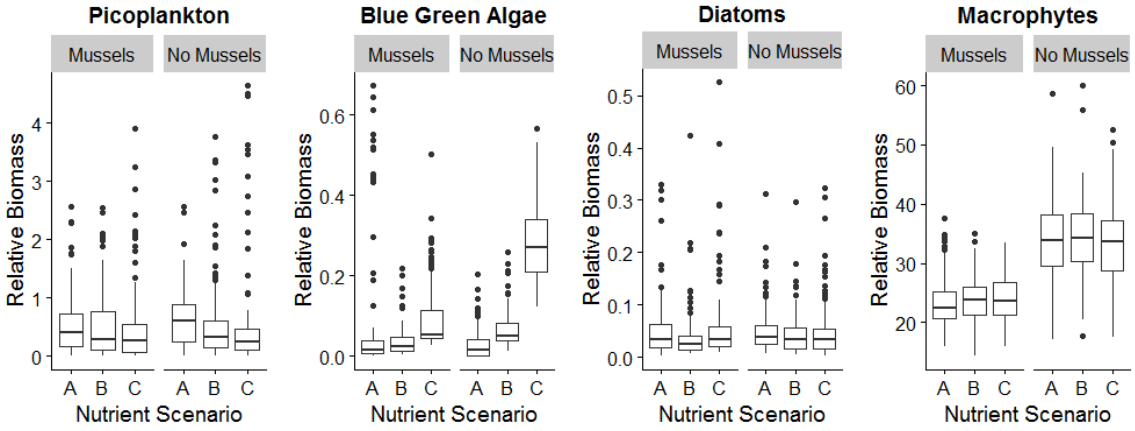

Figure 49. LMAM predictions of phytoplankton biomass under scenarios of dreissena mussel presence/absence and varying nutrient loading scenarios. Refer to Figure 3 for scenario descriptions.

Appendix: Data sources

Bootsma, H. A. 2009. Causes, Consequences and Management of Nuisance *Cladophora.* Project GL-00E06901. Final Report Submitted to the Environmental Protection Agency Great Lakes National Program Office.

Bootsma, H. A., J. T. Waples, and Q. Liao. 2012. Identifying Major Phosphorus Pathways in the Lake Michigan Nearshore Zone. Contract M03029P05. Final Report Submitted to the Milwaukee Metropolitan Sewerage District.

Bunnell, D. B., C. P. Madenjian, and T. E. Croley. 2006. Long-term trends of bloater (Coregonus hoyij) recruitment in Lake Michigan: evidence for the effect of sex ratio. Canadian Journal of Fisheries and Aquatic Sciences **63**:832-844.

Caroffino, D. C., and S. J. Lenart. Technical Fisheries Committee Administrative Report 2011: Status of Lake Trout and Lake Whitefish Populations in the 1836 Treaty-Ceded Waters of Lakes Superior, Huron, and Michigan, with Recommended Yield and effort levels for 2011.

Dawson, H. A., M. L. Jones, K. T. Scribner, and S. A. Gilmore. 2009. An Assessment of Age Determination Methods for Great Lakes Larval Sea Lampreys. North American Journal of Fisheries Management **29**:914-927.

Hanchin, P. A., R. P. O'Neal, R. D. Clark, and R. N. Lock-wood. 2007. The walleye population and fishery of the Muskegon Lake system, Muskegon and Newaygo counties, Michigan in 2002. Michigan Department of Natural Resources, Fisheries Research Report NO. 40, Ann Arbor, MI.

Honeyfield, D. C., A. K. Peters, and M. L. Jones. 2008. Thiamine and Fatty Acid Content of Lake Michigan Chinook Salmon. Journal of Great Lakes Research **34**:581-589.

Kolar, C. S., D. C. Chapman, W. R. Courtenay Jr., C. M. Housel, J. D. Williams, and D. P. Jennings. 2007. Bigheaded carps: a biological synopsis and environmental risk assessment. American Fisheries Society Special Publication 33, Bethesda, Maryland.

Madenjian, C. P., T. J. DeSorcie, and R. M. Stedman. 1998. Maturity schedules of lake trout in Lake Michigan. Journal of Great Lakes Research **24**:404-410.

Madenjian, C. P., D. W. Hondorp, T. J. Desorcie, and J. D. Holuszko. 2005. Sculpin community dynamics in Lake Michigan. Journal of Great Lakes Research **31**:267-276.

Pothoven, S. A., T. F. Nalepa, P. J. Schneeberger, and S. B. Brandt. 2001. Changes in diet and body condition of Lake Whitefish in southern Lake Michigan associated with changes in benthos. North American Journal of Fisheries Management **21**:876-883.

Rand, P. S., D. J. Stewart, P. W. Seelbach, M. L. Jones, and L. R. Wedge. 1993. Modeling Steelhead Population Energetics in Lakes Michigan and Ontario. Transactions of the American Fisheries Society **122**:977-1001.

Rogers, M. W., D. B. Bunnell, C. P. Madenjian, and D. M. Warner. 2014. Lake Michigan offshore ecosystem structure and food web changes from 1987 to 2008. Canadian Journal of Fisheries and Aquatic Sciences **71**:1072-1086.

Rudstam, L. G., P. E. Peppard, T. W. Fratt, R. E. Bruesewitz, D. W. Coble, F. A. Copes, and J. F. Kitchell. 1995. Prey Consumption by the Burbot (*Lota-Lota*) Population in Green Bay, Lake-Michigan, Based on a Bioenergetics Model. Canadian Journal of Fisheries and Aquatic Sciences **52**:1074-1082.

Rutherford, E. S. 1997. Evaluation of natural reproduction, stocking rates, and fishing regulations for steelhead Oncorhynchus mykiss, chinook salmon O. tschawystscha, and coho salmon (O. keta) in Lake Michigan. Final Report Project No. F-35-R-22, study 650, to Federal Aid for Sport Fish Restoration. 29 pp.

Schneider, J. C., P. W. Laarman, and H. Gowing. 2000. Length-weight relationships. Chapter 17 in Schneider, James C. (ed.) 2000. Manual of fisheries survey methods II: with periodic updates. Michigan Department of Natural Resources, Fisheries Special Report 25, Ann Arbor.

Stapanian, M. A., L. D. Witzel, and A. Cook. 2010. Recruitment of burbot (*Lota L.*) in Lake Erie: an empirical modelling approach. Ecology of Freshwater Fish **19**:326-337.
Tomlinson, L. M., M. T. Auer, H. A. Bootsma, and E. M. Owens. 2010. The Great Lakes Cladophora Model: Development, testing, and application to Lake Michigan. Journal of Great Lakes Research **36**:287-297.

Tomlinson, L.M., Auer, M.T., Bootsma, H.A. & Owens, E.M. The Great Lakes Cladophora Model: Development, testing, and application to Lake Michigan. *J. Great Lakes Res.* **36,** 287–297 (2010).

Tsehaye, I., M. L. Jones, J. R. Bence, T. O. Brenden, C. P. Madenjian, and D. M. Warner. 2014. A multispecies statistical age-structured model to assess predator-prey balance: application to an intensively managed Lake Michigan pelagic fish community. Canadian Journal of Fisheries and Aquatic Sciences **71**:627-644.

Wilberg, M. J., J. R. Bence, B. T. Eggold, D. Makauskas, and D. F. Clapp. 2005. Yellow perch dynamics in southwestern Lake Michigan during 1986-2002. North American Journal of Fisheries Management **25**:1130-1152.

Yan, Z., and W. Shi. 1995. Growth and growth models of silver carp and bighead carp in Dahuofang Reservoir. Journal of Fisheries of China **19**:28-34 (in Chinese).